

**Molekularer Mechanismus und strukturelle Implikationen des  
pH-Gatings einwärtsgerichteter  $K^+$ -Kanäle ( $K_{ir}$ )**

**pH-Gating of Inward-Rectifier  $K^+$  Channels ( $K_{ir}$ ):  
Molecular Mechanism and Structural Implications**

Dissertation

der Fakultät für Chemie und Pharmazie  
der Eberhard-Karls-Universität Tübingen  
zur Erlangung des Grades eines Doktors  
der Naturwissenschaften

2000

vorgelegt von

UWE SCHULTE

Tag der mündlichen Prüfung: 13.01.2000

Dekan: Prof. Dr. U. Nagel

1. Berichterstatter: Priv. Doz. Dr. B. Fakler

2. Berichterstatter: Prof. Dr. B. Hamprecht

3. Berichterstatter: Prof. Dr. J.E. Schultz

***"reluctante natura irritus labor est"***

(Lucius Annaeus Seneca d.J.)



## Abbreviations

Throughout the text, the single-letter code for amino acids is used.

Connotation of point mutations: (K80M) = K (lysine) at position 80 replaced by M (methionine)

|                            |   |
|----------------------------|---|
| ABC proteins               | ATP-binding cassette proteins   |
| aBS                        | antenatal Bartter Syndrome  |
| CFTR                       | cystic fibrosis transmembrane conductance regulator, a chloride channel of the ABC protein family         |
| CNG                        | cyclic nucleotide gated channel   |
| cRNA                       | mRNA synthesized <i>in-vitro</i> from complementary DNA   |
| Cu-Phen                    | Cu(II)-1,10-phenanthroline  |
| DEPC                       | diethylpyrocarbonate  |
| DTNB                       | 5,5'-dithio-bis[-2-nitrobenzoic acid]   |
| DTT                        | dithiothreitol  |
| EAG                        | ether-à-go-go-related gene encoded K <sup>+</sup> channel   |
| E <sub>K<sup>+</sup></sub> | equilibrium potential for the ion K <sup>+</sup> according to the Nernst equation                         |
| ENac                       | epithelial Na <sup>+</sup> channel  |
| EPR                        | electron paramagnetic resonance   |
| FmocCl                     | 9-fluorenyl-methoxycarbonyl chloride  |
| GYG                        | glycine-tyrosine-glycine; highly conserved motif termed selectivity filter of K <sup>+</sup> channels     |
| h                          | human   |
| I-V                        | current-voltage relation  |
| K <sub>ATP</sub>           | ATP sensitive K <sup>+</sup> channel  |
| KcsA                       | prokaryotic K <sup>+</sup> channel from <i>Streptomyces lividans</i>                                      |
| K <sub>int</sub>           | solution applied to the cytoplasmic side of an inside-out patch (composition see "Materials and Methods") |
| K <sub>ir</sub>            | inward-rectifier K <sup>+</sup> channel   |

|                   |  |
|-------------------|--|
| KQT               | "long-QT" K <sup>+</sup> channel; "long-QT" refers to a prolonged repolarization period (Q-T interval) of cardiac action potentials measured in electrocardiograms |
| K <sub>v</sub>    | superfamily of voltage-gated K <sup>+</sup> channels   |
| m                 | mouse  |
| MTSES             | (2-sulfonatoethyl)-methanethiosulfonate  |
| NMDG              | N-methyl-d-glucosamine   |
| PGE <sub>2</sub>  | prostaglandin E <sub>2</sub>   |
| pH <sub>i</sub>   | intracellular pH   |
| PIP2              | phosphatidylinositol-4,5-bisphosphate  |
| pK <sub>app</sub> | apparent pK  |
| PVP               | polyvinyl-pyrrolidone  |
| r                 | rat  |
| RKR triad         | structural arrangement, in which two arginine and a lysine residue closely interact  |
| ROMK              | renal outer medulla K <sup>+</sup> channel   |
| SK                | small conductance K <sup>+</sup> channel   |
| Slo               | slopoke-like K <sup>+</sup> channels, also termed BK-type K <sup>+</sup> channels  |
| SPM               | spermine   |
| SSCP              | single-strand conformation polymorphism  |
| TOK               | two P-domain outward-rectifier K <sup>+</sup> channel  |
| TWIK              | two P-domain weak inward-rectifier K <sup>+</sup> channel  |
| V <sub>m</sub>    | membrane potential   |

# Contents

|           |   |           |
|-----------|---|-----------|
| <b>1.</b> | <b>Introduction</b>   | <b>1</b>  |
| 1.1       | Inward-rectifier K <sup>+</sup> channels (K <sub>ir</sub> )                                       | 1         |
| 1.1.1     | Superfamily of P-loop channel proteins  | 1         |
| 1.1.2     | Molecular structure   | 2         |
| 1.1.3     | Physiological functions   | 3         |
| 1.1.4     | Mechanism and determinants of inward-rectification  | 4         |
| 1.1.5     | The family of inward-rectifier K <sup>+</sup> channels  | 5         |
| 1.2       | K <sub>ir</sub> 1.1 channels (ROMK)   | 6         |
| 1.2.1     | <i>romk</i> splice variants   | 6         |
| 1.2.2     | Regulation of channel activity  | 7         |
| 1.2.3     | Physiological role in the kidney  | 8         |
| 1.2.4     | The antenatal Bartter Syndrome (aBS)  | 9         |
| 1.3       | Goal of this study  | 11        |
| <b>2.</b> | <b>Results</b>  | <b>12</b> |
| 2.1       | pH-gating of K <sub>ir</sub> 1.1 is associated with conformational rearrangements                 | 12        |
| 2.1.1     | K <sub>ir</sub> 1.1 channels are gated by intracellular pH  | 12        |
| 2.1.2     | Dependence of K <sub>ir</sub> 1.1 channels on extracellular K <sup>+</sup> is linked to pH-gating | 14        |
| 2.1.3     | State-dependent cysteine modification reveals a conformational change induced by pH-gating        | 17        |
| 2.1.4     | Cysteines 49 and 308 are targets for state-dependent modification                                 | 19        |

|          |   |           |
|----------|---|-----------|
| 2.2      | Identification of lysine 80 (K80) as the sensor for $\text{pH}_i$ in the neutral pH range                                 | 22        |
| 2.2.1    | Current-pH-relation in $\text{K}_{ir}1.1$ and $\text{K}_{ir}4.1$ channels   | 22        |
| 2.2.2    | pH sensitivity of other $\text{K}_{ir}$ channels  | 24        |
| 2.2.3    | Substitution of K80 by non-basic amino acids eliminates pH-gating of $\text{K}_{ir}1.1$ channels                          | 26        |
| 2.2.4    | Chemical modification with amino-specific agents renders $\text{K}_{ir}1.1$ channels $\text{pH}_i$ -insensitive           | 27        |
| 2.2.5    | Introduction of lysine at the pre-M1 site confers pH-gating to other $\text{K}_{ir}$ channels                             | 28        |
| 2.3      | Intrasubunit assembly of K80 with R41 and R311 causes the shift in $\text{pK}_{app}$                                      | 29        |
| 2.3.1    | Substitution of some conserved positively charged amino acids leads to shifts in $\text{pK}_{app}$                        | 29        |
| 2.3.2    | $\text{K}_{ir}1.1(\text{R41Q})$ and $\text{K}_{ir}1.1(\text{R311Q})$ form permanently pH-inactivated channels             | 31        |
| 2.3.3    | Titration of $\text{K}_{ir}4.1(\text{R294Q})$ shows a $\text{pK}_{app}$ close to the standard pK of $\text{NH}_2$ -lysine | 32        |
| 2.3.4    | Evidence for electrostatic interaction of R311 and R41 with the sensor for $\text{pH}_i$                                  | 33        |
| 2.3.5    | The triad of K80, R41 and R311 is formed <i>within</i> an individual $\text{K}_{ir}$ subunit                              | 34        |
| 2.4      | Defective pH-gating as a molecular mechanism for the pathogenesis of aBS  | 37        |
| <b>3</b> | <b>Discussion</b>   | <b>40</b> |
| 3.1      | pH-gating of $\text{K}_{ir}$ channels   | 40        |
| 3.1.1    | Comparison of whole cell and patch experiments with physiological data  | 40        |
| 3.1.2    | The role of K80 as a determinant for pH-gating  | 41        |



|          |  |           |
|----------|--|-----------|
| 3.1.3    | Mechanisms for shifts in $pK_{app}$ as found for titratable residues within proteins | 42        |
| 3.1.4    | Positive cooperativity and stoichiometry of pH-gating                                | 43        |
| 3.1.5    | <i>Intra-</i> versus <i>inter</i> -subunit interaction                               | 45        |
| 3.1.6    | A model for pH-gating of $K_{ir}1.1$ channels  | 46        |
| 3.2      | Structural implications for gating of $K_{ir}$ channels                              | 47        |
| 3.2.1    | Conformational changes in $K_{ir}1.1$ induced by protonation                         | 47        |
| 3.2.2    | Comparison of pH-gating with gating mechanisms in other $K_{ir}$ channels            | 49        |
| 3.3      | Physiological importance   | 50        |
| 3.3.1    | Redox sensitivity of $K_{ir}1.1$ channels  | 50        |
| 3.3.2    | $K^+$ secretion in the kidney  | 51        |
| 3.3.3    | Differential diagnosis and possible treatment of aBS                                 | 52        |
| 3.4      | Research perspectives  | 53        |
| <b>4</b> | <b>Materials and Methods</b>   | <b>55</b> |
| 4.1      | Equipment and materials  | 55        |
| 4.1.1    | Laboratory equipment   | 55        |
| 4.1.2    | Materials  | 57        |
| 4.1.3    | Chemicals and reagents   | 57        |
| 4.2      | Heterologous expression in <i>Xenopus</i> oocytes                                    | 59        |
| 4.2.1    | cRNA synthesis   | 59        |
| 4.2.2    | Preparation and injection of oocytes   | 60        |
| 4.2.3    | Culture media  | 60        |

|          |  |           |
|----------|--|-----------|
| 4.2.4    | K <sub>ir</sub> 1.1 mutations identified in aBS patients | 61        |
| 4.3      | Immunocytochemistry                                      | 61        |
| 4.4      | Whole-cell recording                                     | 62        |
| 4.4.1    | Two-electrode voltage-clamp                              | 62        |
| 4.4.2    | Recording of intracellular pH                            | 63        |
| 4.4.3    | Voltage protocols and data acquisition                   | 63        |
| 4.5      | Patch-clamp experiments                                  | 63        |
| 4.5.1    | Giant inside-out patch-clamp technique                   | 63        |
| 4.5.2    | Chemical modification of cysteine                        | 64        |
| 4.5.3    | Chemical modification of lysine                          | 65        |
| 4.5.4    | Voltage protocols and data evaluation                    | 65        |
| <b>5</b> | <b>References</b>  | <b>66</b> |
| <b>6</b> | <b>Summary</b>   | <b>75</b> |

# 1. Introduction

## 1.1 Inward-rectifier K<sup>+</sup> channels

### 1.1.1 Superfamily of P-loop channel proteins

Ion channels are integral membrane proteins that are used in all types of cells for transport of ions across plasma membranes. In the early ages of electrophysiology these channels have been characterized by their ion selectivity, conductance and time dependent activation and deactivation properties (termed gating). With the molecular cloning of many genes coding for ion selective channels during the last 15 years, a classification has been based on the primary structure of the channel proteins (Wei et al., 1996):

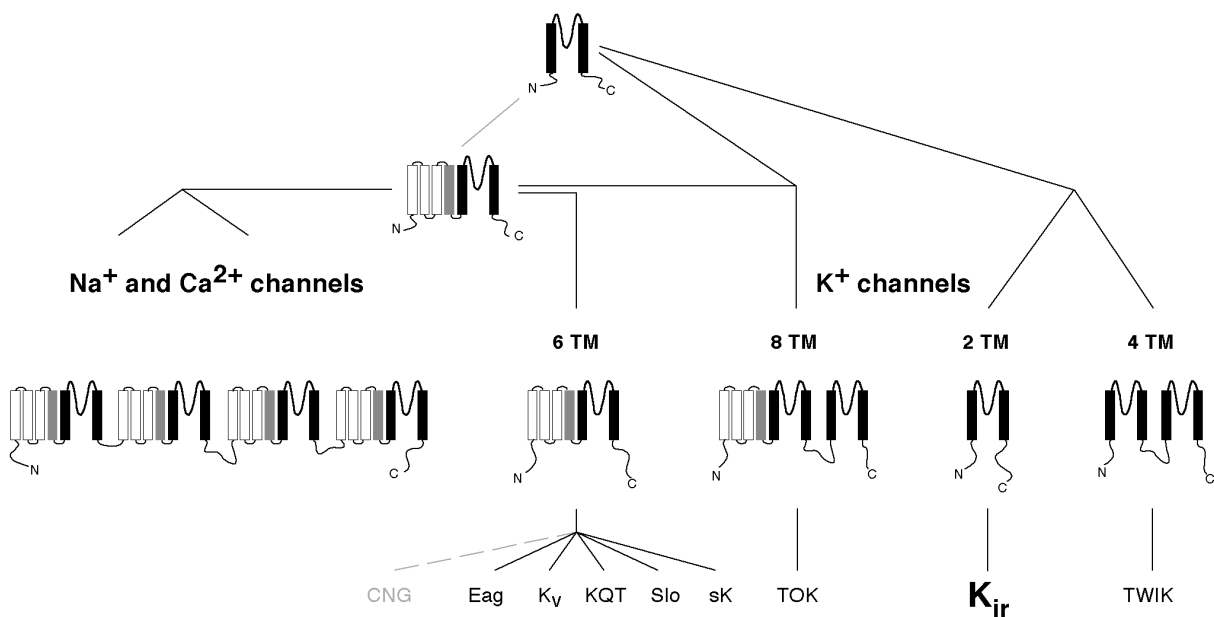


**Fig. 1.** Superfamily of mammalian P-loop channel proteins forming cation selective channels. Transmembrane domains black: conserved core M1 (S5) and M2 (S6); grey: S4-helix (voltage sensor in voltage-gated channels); white: S1, S2, S3. N- and C-termini are located intracellularly.

Ion channel families (grouped according to the number of transmembrane domains TM): CNG (cyclic nucleotide-gated channels), EAG (ether-à-go-go-related channels), K<sub>v</sub> (voltage-gated K<sup>+</sup> channels), KQT (long-QT K<sup>+</sup> channels), Slo (BK-type K<sup>+</sup> channels), sK (small conductance K<sup>+</sup> channels), TOK (two P-domain outward-rectifier K<sup>+</sup> channels), K<sub>ir</sub> (inward-rectifier K<sup>+</sup> channels) and TWIK (two P-domain weak inward-rectifier K<sup>+</sup> channels).

Na<sup>+</sup>-, K<sup>+</sup>- and Ca<sup>2+</sup>-channels are structurally related and seem to have originated from a common ancestor early in evolution. The conserved core region consists of two membrane spanning domains (commonly designated M1 and M2) flanking a pore-forming loop. This P-loop (or H5-region) is highly conserved and defines the superfamily of P-loop channel proteins. Later on, the structural motif of M1-P-M2 has been extended by four additional trans-membrane segments (S1-S5-P-S6), and subsequent fusion and diversification of these genes created the variety of cation selective ion channel subunits known so far. As illustrated in Fig. 1, inward-rectifier K<sup>+</sup> channels (K<sub>ir</sub>) are the smallest proteins in this superfamily. Their simple membrane topology resembles the ancestral channel architecture (see Fig. 1, top) which is also found in bacterial homologs (Schrempf et al., 1995).

### 1.1.2 Molecular structure

The membrane topology and secondary structure of K<sub>ir</sub> channels has been predicted from hydropathy plots of the primary sequence and investigated by detailed mutagenesis. Two hydrophobic segments M1 and M2 form membrane spanning domains and flank a stretch of amino acids that is highly homologous to the H5- or P-region. N- and C-termini are thought to be located in the cytoplasm, although a partial association with the membrane can not be excluded. There is experimental evidence that parts of the C-terminus contribute to the intracellular vestibule of the pore (Tagliatela et al., 1994; Baukowitz et al., 1999).

Recently, the crystal structure of the core region of KcsA, a K<sup>+</sup> channel from the bacterium *Streptomyces lividans* with structural homology to K<sub>ir</sub> channels, has been resolved with a resolution of 3.2 Å (Doyle et al., 1998). The results are in good agreement with structural predictions and provide a basis for understanding ion selectivity and permeation. The N-terminal part of the P-loop is  $\alpha$ -helical and forms the shallow outer vestibule of the channel. Ion selectivity is determined by a narrow binding site in the pore termed selectivity filter which is formed by the backbone carbonyls of the GYG consensus motif. The long and narrow inner vestibule is formed by residues of the second transmembrane helix (M2) and contains binding sites for K<sup>+</sup> and small blocking ions. M1 also lines the pore but is tilted around M2. However, the structure of intracellular domains (N- and C-terminus) remains unknown.

In analogy to voltage gated K<sup>+</sup> channels (MacKinnon, 1991), K<sub>ir</sub> channels are assembled from four subunits. This was shown by a functional approach (Glowatzki et al., 1995) as well as biochemically (Yang et al., 1995b). Most K<sub>ir</sub> subunits form functional homotetramers, some require co-assembly with other K<sub>ir</sub> subunits in order to form functional channels (Fakler et al., 1996a). Formation of heteromeric channels seems to underly several K<sub>ir</sub> conductances of physiological importance. For example K<sub>ir</sub>3.1/K<sub>ir</sub>3.4 heterotetrameric channels closely resemble the native atrial I<sub>K,ACh</sub> (Krapivinsky et al., 1995b).

### 1.1.3 Physiological functions

Inward-rectifier potassium channels maintain the membrane potential ( $V_m$ ) near the  $K^+$  reversal potential ( $E_{K^+}$ ), in excitable and non-excitable cells. These channels mediate a high  $K^+$  conductance at  $E_{K^+}$  and at voltages slightly positive to  $E_{K^+}$ , which decreases when the membrane is further depolarized (Hille, 1992). Thus inward-rectifier  $K^+$  channels have a highly stabilizing effect on  $V_m$  around  $E_{K^+}$  but allow depolarization of the cell. The range of membrane potential over which inward-rectifier  $K^+$  channels stabilize  $V_m$  basically depends on their voltage-dependence of rectification which may be "strong" or "mild" (Hille, 1992). Strong inward-rectifier  $K^+$  channels have been described in a wide variety of cells including skeletal muscle (Leech and Stanfield, 1981), cardiac muscle cells (Kurachi, 1985; Vandenberg, 1987; Matsuda, 1991), starfish egg cells (Hagiwara et al., 1976), endothelial cells (Silver and DeCoursey, 1990) and osteoclasts (Kelly et al., 1992). In the current-voltage relation (I-V) of strong inward-rectifier channels the outward current exhibits a maximum at potentials close to  $E_{K^+}$  which is followed by a region of negative slope conductance at more positive potentials (see Fig. 2 below). This outward current maximum is physiologically important since it determines a "trigger threshold" of excitation: whenever a depolarizing current exceeds the maximal outward current, the inward-rectifier  $K^+$  channels close down and  $V_m$  is free to change (Hille, 1992).

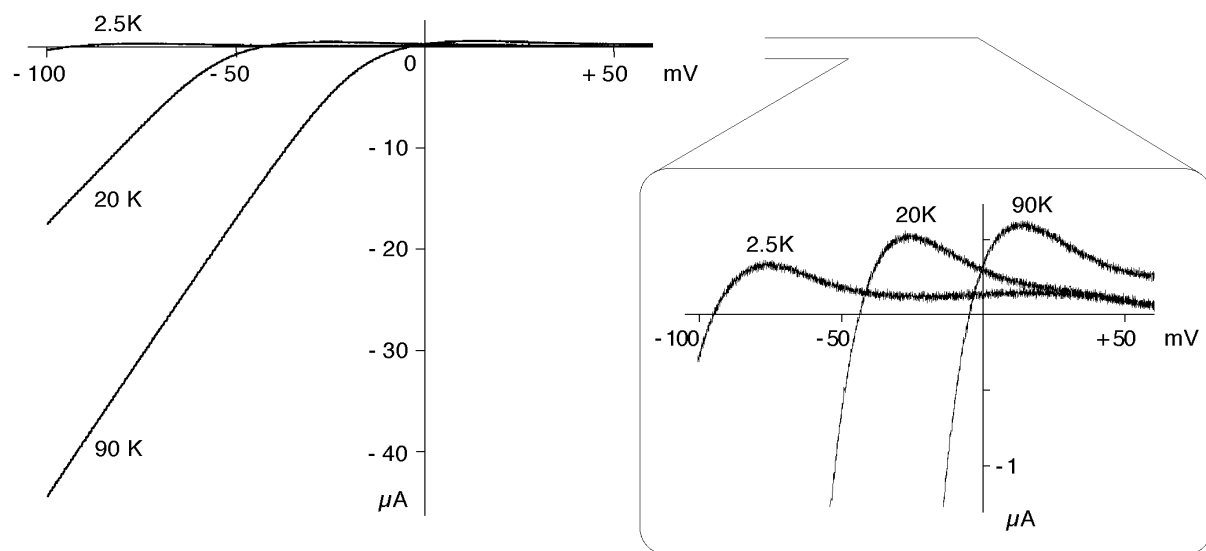


**Fig. 2.** Strong inward-rectification of  $K^+$  currents recorded from *Xenopus* oocytes injected with  $K_{ir}2.1$  cRNA in a two-electrode-voltage-clamp experiment. Note the shift in reversal potential  $E_{K^+}$  and slope conductance for 2.5, 20 and 90 mM extracellular  $K^+$ . Inset: enlarged current scale, showing the change in conductance around the reversal potential.

In contrast to that, weak inward-rectifiers conduct significant outward currents over the whole physiological voltage range (for an example see Fig. 12). This has two consequences: they suppress electrical excitation and they are able to effectively secrete  $K^+$  from cells. Inhibition of

electrical excitation is an important mechanism to protect muscle cells during metabolic exhaustion or to regulate insulin secretion in pancreatic  $\beta$ -cells (Ashcroft, 1988). A decrease of intracellular ATP levels activates  $K_{ir}$  channels of the  $K_{ATP}$ -type (see section 3.1.5) and the resulting hyperpolarisation reduces the energy demand of the cell. In the kidney,  $K^+$  secretion by epithelial cells is crucial for  $K^+$  homeostasis and NaCl reabsorption (Lang and Rehwald, 1992; Wang et al., 1992; Wang, 1995). Active transport processes provide the concentration gradient for  $K^+$  efflux through weak inward-rectifier  $K^+$  channels (see section 1.2.3).

#### 1.1.4 Mechanism and determinants of inward-rectification

The hallmark property of  $K_{ir}$  channels is their inward-rectification of  $K^+$ -currents which depends on both, membrane voltage ( $V_m$ ) and  $K^+$  equilibrium potential  $E_{K^+}$  (Hille, 1992). These parameters determine the driving force for  $K^+$  ( $V_d = V_m - E_{K^+}$ ), which directs  $K^+$  flow. As the molecular mechanism underlying the phenomenon of inward-rectification, block of  $K_{ir}$  channels by intracellular  $Mg^{2+}$  and the polyamines spermine and spermidine has been identified (Vandenberg, 1987; Fakler et al., 1994b, 1995; Ficker et al., 1994; Lopatin et al., 1994). The pore-block by these intracellular cations is characterized by a voltage-dependence which may be strong ('strong rectifiers') or weak ('weak rectifiers') and which is determined by the quantity of  $V_m - E_{K^+}$  rather than by  $E_m$  alone (Hagiwara et al., 1976; Leech and Stanfield, 1981; Cohen et al., 1989; Hille, 1992). Since the latter was primarily found for changes in extracellular  $K^+$  concentration ( $[K^+]_{ex}$ ) inward-rectification is more correctly said to depend on  $[K^+]_{ex}$  and  $V_m$  but not on the intracellular  $K^+$  concentration ( $[K^+]_{in}$ ). To account for this fact, an extracellular binding site for  $K^+$  ions on  $K_{ir}$  channels was hypothesized (Hille, 1992).

Comparison of the primary sequence of strongly and weakly rectifying  $K_{ir}$  channels identified two structural determinants involved in inward-rectification. These are negatively charged residues, one in the second transmembrane segment (M2-site) (Fakler et al., 1994b; Lu and MacKinnon, 1994; Stanfield et al., 1994; Wible et al., 1994), the other in the cytoplasmic C-terminal domain (C-terminal-site) (Taglialatela et al., 1995; Yang et al., 1995a). Inward-rectifiers of the  $K_{ir2}$  subfamily that exhibit both the M2- and C-terminal-site display complex kinetics of spermine block (Lopatin et al., 1995; Fakler and Ruppersberg, 1996). In contrast, those carrying only the M2-site show monoexponential blocking behavior and their steady state block is described by a single Boltzmann function (Fakler et al., 1994b; Glowatzki et al., 1995). Voltage-dependence of block is usually quantified in terms of the change in membrane voltage necessary for an e-fold increase in block. This parameter is assumed to correlate with the number of blocking charges times the percentage of the transmembrane electric field which these charges move through in the blocking reaction (electrical distance according to Woodhull (1973)).

In agreement with these determinants, all  $K_{ir}$  channels known to date can be classified as either strong or weak rectifiers, except for  $K_{ir}6.2$ . Channels formed from this subunit are unique in that polyamine-mediated rectification is not fixed but changes with intracellular pH in the physiological range (Baukrowitz et al., 1999). Inward-rectification is prominent at basic pH, while at acidic pH rectification is very weak. Mutagenesis uncovered a titratable C-terminal histidine residue (H216) in  $K_{ir}6.2$  as the structural determinant and electrostatic interaction between this residue and spermine as the molecular mechanism underlying pH-dependent inward-rectification.

### 1.1.5 The family of inward-rectifier $K^+$ channels

In 1993, the first cDNA clones encoding inward-rectifier  $K^+$  channels - termed ROMK ( $K_{ir}1.1$ , from kidney (Ho et al., 1993)) and IRK1 ( $K_{ir}2.1$ , from a mouse macrophage library (Kubo et al., 1993)) - were successfully isolated by expression cloning. Until today, cloning based on sequence homology resulted in discovery of more than a dozen of  $K_{ir}$  genes (Fig. 3). They all code for proteins of 361-502 amino acids length with the characteristic membrane topology described in section 1.1.2. The short intracellular N-terminus comprises about 80 amino acids in all  $K_{ir}$  subunits whereas the C-terminus varies in length between 201 and 315 amino acids.

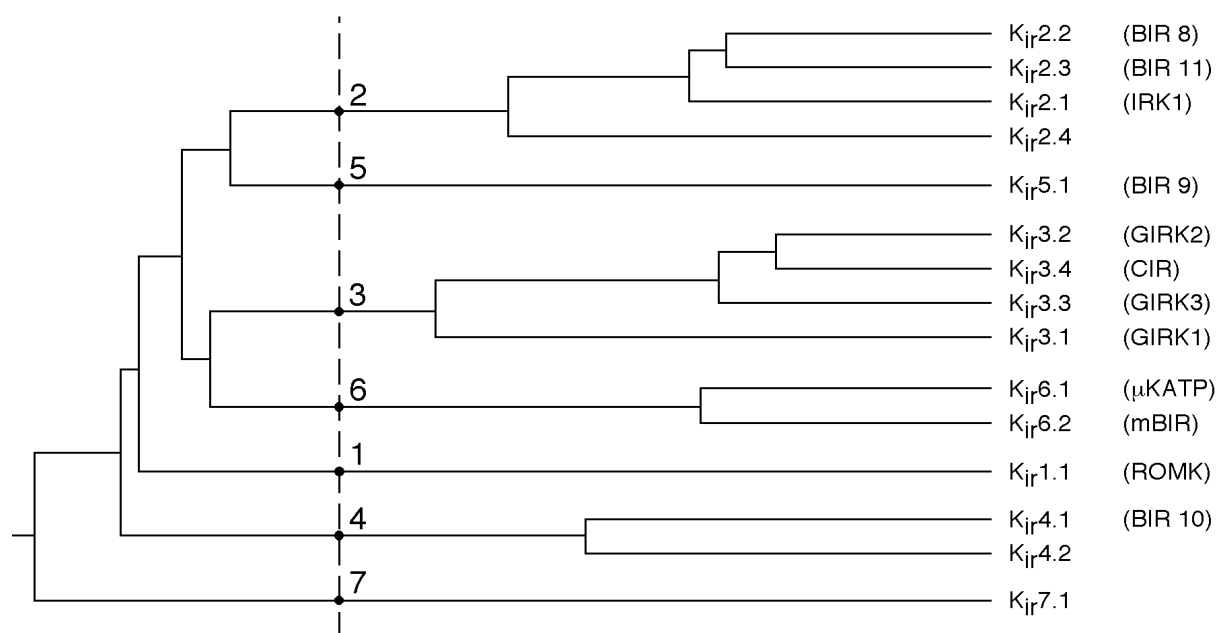


**Fig. 3.** The family of mammalian inward-rectifier  $K^+$  channels ( $K_{ir}$ ). Primary sequences of the  $K_{ir}$  subunits indicated were aligned using the Clustal method (Hein, 1989) with the PAM250 residue weight table. Distances in the tree are based on the homology index calculated by the program. The dashed line defines seven different  $K_{ir}$  subfamilies. The generic nomenclature is given together with the original names published (in parentheses).

A first classification based on primary sequence homology (Doupnik et al., 1995) proposed 6 different subfamilies. Although this nomenclature is widely accepted, it poorly reflects functional homologies. Other reviews proposed four  $K_{ir}$  subgroups (including new genes) based on both functional and structural properties (Fakler and Ruppersberg, 1996; Nichols and Lopatin, 1997).

The weak inward-rectifier  $K_{ir}1.1$  (ROMK1) displays high sensitivity to changes in intracellular pH and is primarily expressed in kidney and uterus (Ho et al., 1993).  $K_{ir}6$  ( $\mu K_{ATP}$ , (Inagaki et al., 1995b) and mBIR (Inagaki et al., 1995a)), another subfamily of weak inward-rectifiers, forms ATP-sensitive channels ( $K_{ATP}$ ) by assembly with sulfonylurea receptors (SUR1 (Aguilar-Bryan et al., 1995), SUR2A (Inagaki et al., 1996) or SUR2B (Isomoto et al., 1996)), members of the superfamily of ATP-binding cassette proteins. They are expressed in a wide variety of tissues including pancreatic  $\beta$ -cells, cardiac myocytes, skeletal muscle and brain. The  $K_{ir}4$  subfamily comprises two strong inward-rectifiers expressed in brain (BIR10 (Bond et al., 1994) and kidney ( $K_{ir}4.2$  (Shuck et al., 1997)). Members of the  $K_{ir}3$  subfamily are strong rectifiers primarily expressed in brain and heart (Dascal et al., 1993; Ashford et al., 1994; Lesage et al., 1994). A hallmark property is their activation by direct binding of  $\beta$ -subunits ("G-protein coupling" (Huang et al., 1995; Krapivinsky et al., 1995a). Subfamily  $K_{ir}2$  comprises strong inward-rectifiers with complex blocking characteristics expressed in a variety of cells ( $K_{ir}2.1$  (Kubo et al., 1993),  $K_{ir}2.2$  (Takahashi et al., 1994),  $K_{ir}2.3$  (Bond et al., 1994) and  $K_{ir}2.4$  (Krapivinsky et al., 1998)). The other subfamilies are poorly characterized since  $K_{ir}5.1$  (BIR9 (Bond et al., 1994)) does not express homomeric channels and  $K_{ir}7.1$  has only recently been cloned (Partiseti et al., 1998).

## 1.2 $K_{ir}1.1$ channels (ROMK)

### 1.2.1 *romk* splice variants

$K_{ir}1.1$  was originally cloned from a rat kidney cDNA library as the first member of the  $K_{ir}$  family. Genomic analysis revealed, that human and rat *romk* genes contain 6 exons, which are spliced alternatively to yield the three isoforms (Shuck et al., 1994; Yano et al., 1994; Boim et al., 1995; Kondo et al., 1996) as depicted in Fig. 4. Since exon 6 (core) encodes the major part of the channel protein, splicing results primarily in variable length of the N-terminus. rROMK2 ( $K_{ir}1.1b$ ) is shortened by 19 amino acids, and rROMK3 ( $K_{ir}1.1c$ ) is extended by 7 amino acids compared to rROMK1 ( $K_{ir}1.1a$ ).



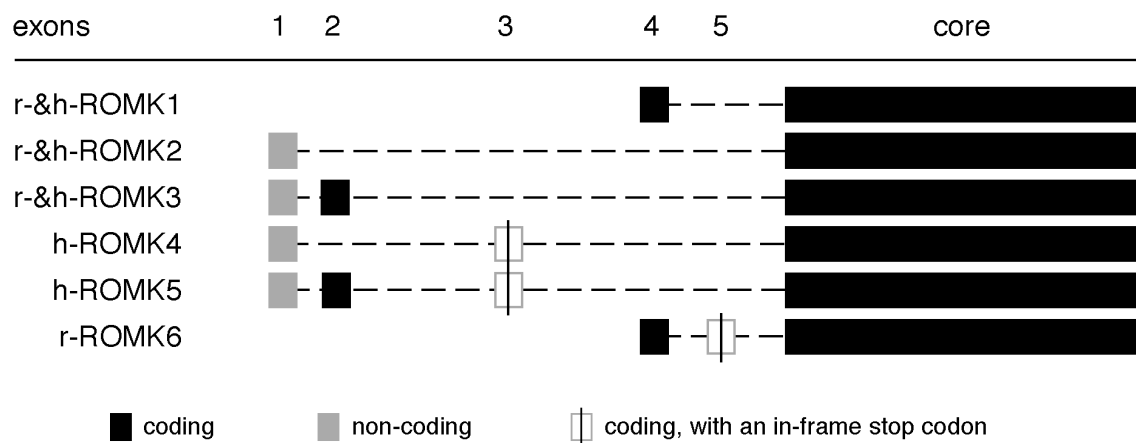


**Fig. 4.** Alternative splicing of the *romk* gene (adapted from Kondo et al. (1996)) yielding 6 different ROMK mRNAs. Exons 2 and 4 code for different N-termini in ROMK3 ( $K_{ir}1.1c$ ) and ROMK1 ( $K_{ir}1.1a$ ), respectively. Exons 1, 3 and 5 do not contribute to the primary structure of ROMK subunits. Exon 6 (core) encodes ROMK2 ( $K_{ir}1.1b$ ) and the major part of the other  $K_{ir}1.1$  splice variants.

ROMK1 as well as the other splice variants are differentially expressed in renal tubular cells (Boim et al., 1995; Lee and Hebert, 1995), except rROMK6 mRNA which is found in several other tissues (Kondo et al., 1996). Up to date, no functional differences could be observed between  $K_{ir}1.1$  isoforms when expressed in *Xenopus* oocytes. Thus, all  $K_{ir}1.1$  experiments in this study were carried out with the r $K_{ir}1.1a$  splice variant unless stated otherwise.

### 1.2.2 Regulation of channel activity

Tsai and colleagues showed that  $K_{ir}1.1$  channels are particularly sensitive to changes in intracellular pH (Tsai et al., 1995).  $pH_i$  did not affect the single channel amplitude, instead a decrease in channel open probability was observed upon acidification (Fakler et al., 1996, Choe et al., 1997, McNicholas et al., 1998). The steady-state current- $pH_i$  relation showed a  $pH_i$  value for half maximal activation ( $pK_{app}$ ) of 6.9 and a Hill coefficient of around 3 indicating cooperativity of the gating process. Binding of  $K^+$  ions to an extracellular site has been shown to be essential for  $K_{ir}1.1$  channel activity but not for that of other  $K_{ir}$  channels (Doi et al., 1996). The halfmaximal  $K^+$  concentration determined in whole-cell experiments was around 4.5 mM but shifted to higher values when the intracellular pH was decreased.

Binding of the negatively charged phospholipid PIP2 appears to be a general property of  $K_{ir}$  channels (Hilgemann and Ball, 1996; Huang et al., 1998), and has also been reported for  $K_{ir}1.1$ . Fusion proteins constructed from the  $K_{ir}1.1$  C-terminus bound PIP2 *in-vitro*, and the presence of PIP2 was shown to be necessary for  $K_{ir}1.1$  channel activity (Huang et al., 1998). Finally, regulatory phosphorylation by PKA has been demonstrated for  $K_{ir}1.1$  channels in renal epithelial cells (McNicholas et al., 1994) and biochemically verified in detail (Xu et al., 1996).

### 1.2.3 Physiological role in the kidney

Intracellular  $K^+$  (approximately 145 mM) represents the major portion of total body  $K^+$ . The  $K^+$  concentration in extracellular fluids ranges from 3.5-5 mM. To maintain a constant serum  $K^+$  level, 95% of dietary  $K^+$  absorbed from the intestine is excreted through the kidney and the remaining portion is eliminated via the colon (Thier, 1986; Stanton, 1989). Under pathophysiological conditions like chronic renal failure, colonic excretion is increased and can contribute significantly to  $K^+$  homeostasis (Martin et al., 1986).

$K^+$  secretion in the kidney is a very complex process depending on flow rate, luminal  $K^+$ ,  $Na^+$  and  $Cl^-$  concentrations, hormones and the acid-base status (Stanton, 1989; Wang, 1995; Giebisch, 1998).

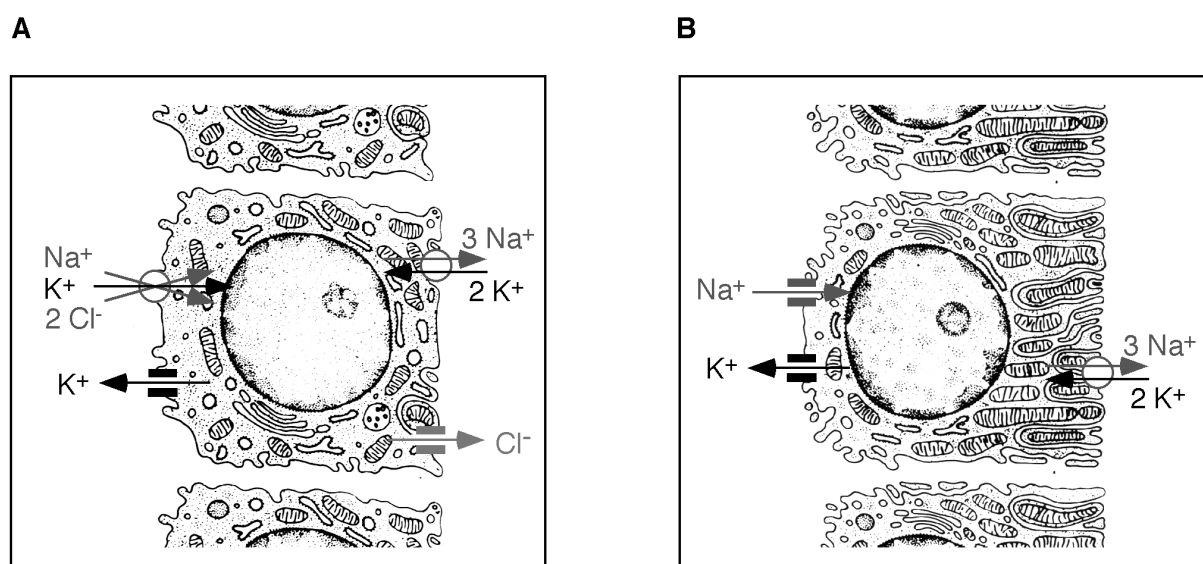


**Fig. 5.** (A) Salt reabsorption in tubular cells of the ascending loop of Henle; left (luminal side): apical membrane with  $Na^+/K^+/2Cl^-$  cotransporter and  $K_{ir}1.1$  channels; right: basolateral membrane with  $Na^+/K^+$ -ATPase and cAMP-dependent  $Cl^-$  channels. (B)  $K^+$  secretion in principal cells in distal tubule and cortical collecting duct; left (luminal side): apical membrane with  $K_{ir}1.1$  channels and epithelial  $Na^+$  channels (ENaC); right: basolateral membrane with  $Na^+/K^+$ -ATPase. Arrows indicate the direction of ion flux under physiological conditions.

In the ascending loop of Henle,  $K^+$  participates in the reabsorption of  $NaCl$  from the primary urine as illustrated in Fig. 5 A. Luminal  $Na^+$ ,  $K^+$  and  $Cl^-$  enters the tubular cells via the furosemide-sensitive  $Na^+/K^+/2Cl^-$  cotransporter. This process depends on  $K^+$  efflux through apical  $K^+$  channels ( $K_{ir}1.1$ ), which allow recycling of luminal  $K^+$  (Hebert, 1998).  $Na^+$  and  $Cl^-$  are eliminated from the cells by cAMP-dependent  $Cl^-$  channels and  $Na^+/K^+$ -ATPase in the basolateral membrane (Giebisch, 1998; Köckerling et al., 1998).

K<sup>+</sup> secretion (Fig. 5 B) is mediated by principal cells in the distal tubulus and cortical collecting duct (Wang, 1995; Köckerling et al., 1998). Na<sup>+</sup> influx through amiloride-sensitive epithelial Na<sup>+</sup> channels (ENaC) in the apical membrane is rate limiting for K<sup>+</sup> excretion. The driving force for Na<sup>+</sup> influx is generated by the action of basolateral Na<sup>+</sup>/K<sup>+</sup>-ATPase which also provides the necessary K<sup>+</sup> gradient. Both Na<sup>+</sup> reabsorption and K<sup>+</sup> secretion are stimulated by aldosterone. This hormone was shown to increase the apical Na<sup>+</sup> conductance within hours and to upregulate expression of ENaC and Na<sup>+</sup>/K<sup>+</sup>-ATPase (O'Neil, 1990). Intercalated cells (not shown), which constitute the second type of epithelial cells in these nephron segments, partially reabsorb urinary K<sup>+</sup> via H<sup>+</sup>/K<sup>+</sup>-ATPase (Graber and Pastoriza-Munoz, 1993; Giebisch, 1998).

K<sup>+</sup> secretion in the distal tubules is mediated by intermediate conductance (35 pS) weak inward-rectifier K<sup>+</sup> channels (Wang et al., 1990, 1992). Their activity has been shown to be linked to basolateral Na<sup>+</sup>/K<sup>+</sup>ATPase by a pathway involving ion exchange, Ca<sup>2+</sup> and PKC (Wang et al., 1993). In addition to regulation by protein kinases (Wang and Giebisch, 1991b) they have been shown to be particularly sensitive to changes in intracellular pH (pH<sub>i</sub>) (Wang et al., 1990; Wang and Giebisch, 1991a). Intracellular acidification in the physiological range reversibly reduced channel open probability (Wang et al., 1990). An inward-rectifier K<sup>+</sup> channel (31 pS) with a similar sensitivity to pH<sub>i</sub> has been characterized in luminal membranes of the thick ascending limb of Henle's loop (Bleich et al., 1990).

These functional properties together with immunocytochemical data (Xu et al., 1997) confirmed, that K<sub>ir</sub>1.1 channels underly the K<sup>+</sup> conductances involved in renal salt reabsorption and K<sup>+</sup> secretion.

#### 1.2.4 The antenatal Bartter Syndrome (aBS)

Hereditary tubular disorders leading to excessive salt wasting are rare diseases with an incidence of approximately 1 : 50000 newborns. The first patients have been described by Bartter (Bartter et al., 1962) with symptoms of renal salt loss, hyperreninaemia, hyperaldosteronism and hypokalemic alkalosis. In the following years, cases showing variants of this syndrome were reported by several groups (Gitelman et al., 1966; Fanconi et al., 1971; Seyberth et al., 1985). Currently, three types with biochemical and physiological characteristics that are similar to those resulting from long-term application of certain diuretics can be distinguished (Seyberth et al., 1997; Köckerling et al., 1998):

- antenatal Bartter Syndrome (aBS), more correctly termed Hyper-Prostaglandin E-Syndrome (HPS; (Konrad et al., 1999)) or FSLT (furosemide-like salt-losing tubulopathy)
- Gitelman-Syndrome; synonyms: Hypocalciuric Bartter Syndrome or TSLT (thiazide-like salt-losing tubulopathy)
- Pseudohypoaldosteronism Type 1 or ASLT (amiloride-like salt-losing tubulopathy)

This classification was confirmed by identification of the genes underlying these defects. Mutations in the gene coding for the thiazide-sensitive  $\text{Na}^+/\text{Cl}^-$ -cotransporter were found in patients with TSLT (Simon et al., 1996a). ASLT can be caused by mutations in the ENaC channel subunits  $\alpha$ ,  $\beta$ ,  $\gamma$  (Chang et al., 1996). The most severe form, aBS, is genetically heterogeneous: Mutations of either the furosemide-sensitive  $\text{Na}^+/\text{K}^+/\text{2Cl}^-$ -cotransporter or *romk* have been identified in aBS patients (Simon et al., 1996b, c).

aBS is inherited as an autosomal recessive disorder. Mutations of *romk* appear to be rare, since the gene shows little allelic variation in the healthy population and most identified mutations are unique for single patients. Typically, affected children are compound heterozygous, i.e. they harbour a different mutation on either *romk* gene. Point mutations linked to aBS are apparently distributed over the whole coding region of the gene.

The molecular mechanisms leading to impairment or loss of  $\text{K}_{\text{ir}}1.1$  channel function are yet unknown. A major pathophysiological consequence seems to be the impairment of NaCl reabsorption in the ascending loop of Henle which depends on  $\text{K}^+$  recycling through  $\text{K}_{\text{ir}}1.1$  channels ((Hebert, 1998), see also Fig. 5 A). The resulting loss of salt and fluid leads to polyhydramnios and premature birth (Seyberth et al., 1997). Polyuria remains life-threatening in young children if they are not treated by substitution with fluid, NaCl and KCl.  $\text{PGE}_2$  is markedly elevated and plays an important role in the pathogenesis as it aggravates salt and fluid loss. Renin and aldosterone levels are also increased, but are insufficient to counteract the loss of NaCl, as  $\text{Na}^+$  reabsorption by principal cells in the distal tubulus depends on the presence of functional  $\text{K}_{\text{ir}}1.1$  channels in the apical membrane (Fig. 5 B). Other secondary symptoms are hypercalciuria, which may lead to nephrocalcinosis, and alkalosis possibly resulting from excessive  $\text{H}^+/\text{K}^+$  exchange in the collecting duct to reduce  $\text{K}^+$  loss (Seyberth et al., 1985, 1997; Köckerling et al., 1998).

### 1.3 Goal of this study

The main goal of this work was to resolve the molecular mechanism underlying pH-dependent gating of  $K_{ir}1.1$ . It included

- characterization of conformational changes associated with gating,
- investigation of interactions of pH-gating with other factors,
- identification of molecular determinants involved in  $pH_i$  sensing,
- investigation of stoichiometry and cooperativity of pH-gating and
- verification of general implications for structure and function of other  $K_{ir}$  proteins.

As a result, a structural model of the pH-dependent gating mechanism was established and tested with respect to its applicability to the pathophysiology of aBS.

## 2. Results

### 2.1 pH-gating of $K_{ir}1.1$ is associated with conformational rearrangements

#### 2.1.1 $K_{ir}1.1$ channels are gated by intracellular pH

Sensitivity to intracellular acidification has been demonstrated for both  $K^+$  secretion channels in the kidney and cloned  $K_{ir}1.1$  (ROMK) channels (Ohno-Shosaku et al., 1990; Wang et al., 1990; Tsai et al., 1995). The pH-dependent gating of  $K_{ir}1.1$  channels was more closely investigated in giant inside-out patches from *Xenopus* oocytes. Solutions containing 120 mM  $K^+$  buffered with HEPES ( $K_{int}$ ) at pH values indicated were applied to the cytoplasmic side of the membrane patches. During the experiment every 800 ms the membrane potential of -80 mV was intermittently stepped to +50 mV for 50 ms. These experimental conditions were used for all patch experiments unless stated otherwise.

Intracellular acidification (from  $pH_i$  8.0 to 6.0) led to complete channel closure within a few seconds, while alkalinization resulted in channel reactivation (Fig. 6). Under steady-state conditions, pH-gating showed half-maximal inhibition ( $pK_{app}$ ) at  $pH_i$  6.8 with a Hill coefficient of around 3 (Figs. 19 and 20).

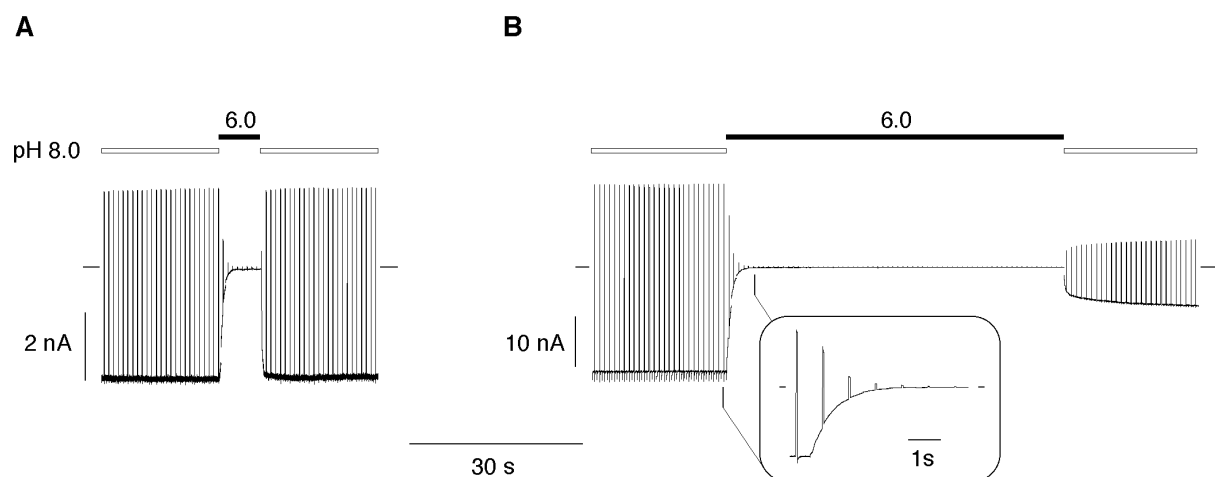


**Fig. 6.** (A), (B)  $pH_i$ -induced inactivation of  $K_{ir}1.1$  currents in excised inside-out patches. Voltage step protocol and pipette solution as described in the text, application of solutions as indicated by bars (filled white: pH 8.0; black: pH 6.0). Inset: kinetics of pH-induced inactivation at an enlarged time scale. Note that the current amplitude at pH 8.0 remained constant, i.e. there was no "channel rundown".

The effect of intracellular pH on  $K_{ir}1.1$  single channel behaviour was studied in small inside-out-patches. In the recording in Fig. 7 currents through single  $K_{ir}1.1$  channels are resolved.

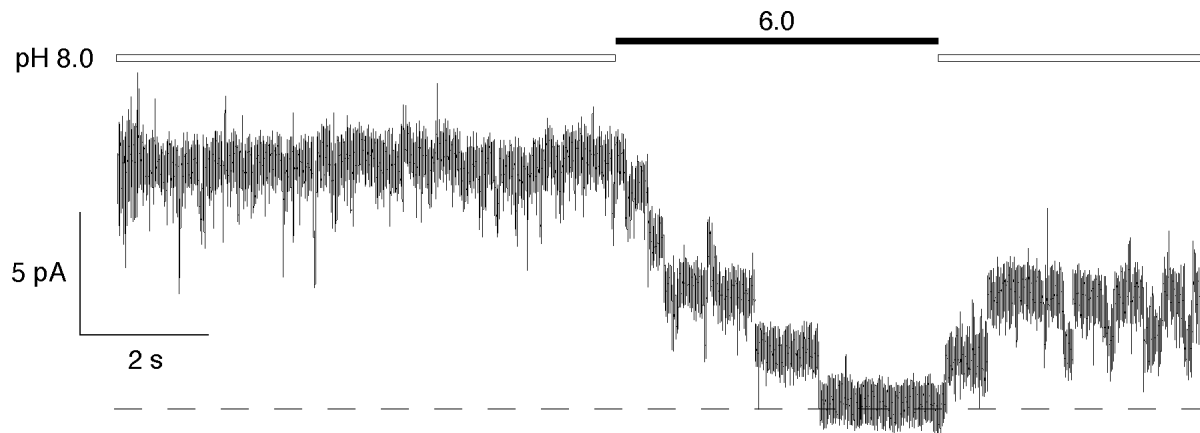


**Fig. 7.** Dependence of  $K_{ir}1.1$  single channel amplitude on  $pH_i$ . Current recording at high gain from an excised inside-out patch containing 4 active channels at a holding potential of  $-80$  mV. The dashed line marks the current baseline (closing of the last active channel). Data were sampled at 10 kHz and filtered with 0.3 kHz. The patch pipette was filled with  $K_{pipette}$  and intracellular solutions ( $K_{int}$ ) were applied as indicated by bars.

The single channel amplitude ( $32.2 \pm 2.1$  pS,  $n=4$ ) was not affected by acidification. Instead, the decrease of the macroscopic current amplitude at  $pH_i$  6.0 was due to a reduced channel open probability. In further control experiments, pH-induced inactivation was found to be independent of transmembrane voltage. The results were the same when a voltage protocol was used with a membrane potential of  $+50$  mV intermittently stepped to  $-80$  mV for 50 ms every 800 ms (data not shown). When the extracellular pH was varied from 8.0 to 6.0 no effect on  $K_{ir}1.1$  currents was observed (data not shown). In summary,  $K_{ir}1.1$  channels are gated specifically by intracellular protons in the physiological range without involvement of soluble cofactors.

After short periods of acidification recovery from pH-inactivation was complete, i.e. all channels reopened (Fig. 6 A). With longer periods of inactivation by low pH only a fraction of channels could be recovered (Fig. 6 B). This time-dependent loss of channel activity after pH-induced inactivation was reminiscent of ‘channel run-down’, a phenomenon well-known for  $K_{ir}$  channels. Therefore, MgATP (Fakler et al., 1994a; McNicholas et al., 1994) and the anionic phospholipid PIP2 (Hilgemann and Ball, 1996; Huang et al., 1998) both reported to counteract ‘run-down’, were tested.

As shown in Fig. 8 A, B neither reagent was able to restore channel activity lost after pH-induced inactivation. However, addition of dithiothreitol (DTT, 100  $\mu$ M) or reduced glutathione (GSH, 5 mM) to the pH 8.0 solution resulted in complete recovery even after prolonged acidification (Fig. 8 C, D). This suggested that oxidation occurred during acidification, which subsequently prevented channel recovery from pH-induced inactivation.

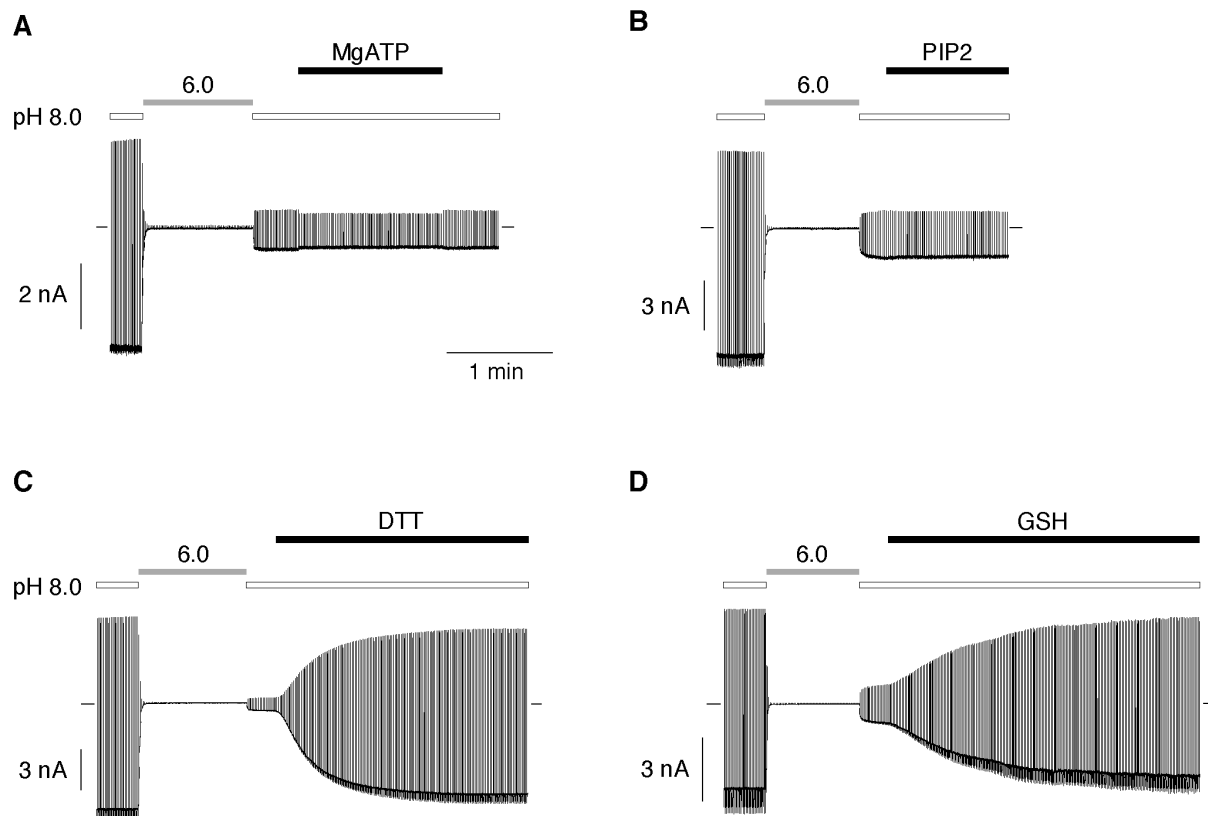


**Fig. 8.** Recovery of  $K_{ir}1.1$  currents from pH-induced inactivation in excised inside-out patches. (A) with MgATP (e.g., free concentrations of 1 mM  $Mg^{2+}$  and 1 mM MgATP, see "Materials and Methods"); (B) with 0.1 mM PIP2; (C) 0.1 mM dithiothreitol (DTT); and (D) 5 mM glutathione (GSH). Voltage protocol as before, application of solutions and scalings as indicated.

### 2.1.2 Dependence of $K_{ir}1.1$ channels on extracellular $K^+$ is linked to pH-gating

The activity of  $K_{ir}1.1$  channels does not only depend on  $pH_i$  but also on the concentration of extracellular  $K^+$ , referred to as ' $K^+$ -regulation' (Doi et al., 1996), and both factors interact allosterically. In whole-cell experiments, outward currents in  $K^+$ -free extracellular solution inactivated slowly and were completely restored in solution containing 90 mM  $K^+$  (see also Fig. 12). The inactivation time constant increased by 50fold when the intracellular pH was lowered from  $pH_i$  7.5 to 6.7. The activation time constant (switching to an extracellular solution containing 90 mM  $K^+$ ) was independent from  $pH_i$ .

The interaction of extracellular  $K^+$  with pH-gating of  $K_{ir}1.1$  was subsequently investigated in giant inside-out patches. pH-induced inactivation of  $K_{ir}1.1$  was completely reversible as long as solutions on either side of the membrane contained high concentrations of  $K^+$  (120 mM) and DTT at the intracellular side (Fig. 8). As a variation from these conditions,  $K^+$  in the pipette was replaced by  $Na^+$  in the two experiments shown in Fig. 9.



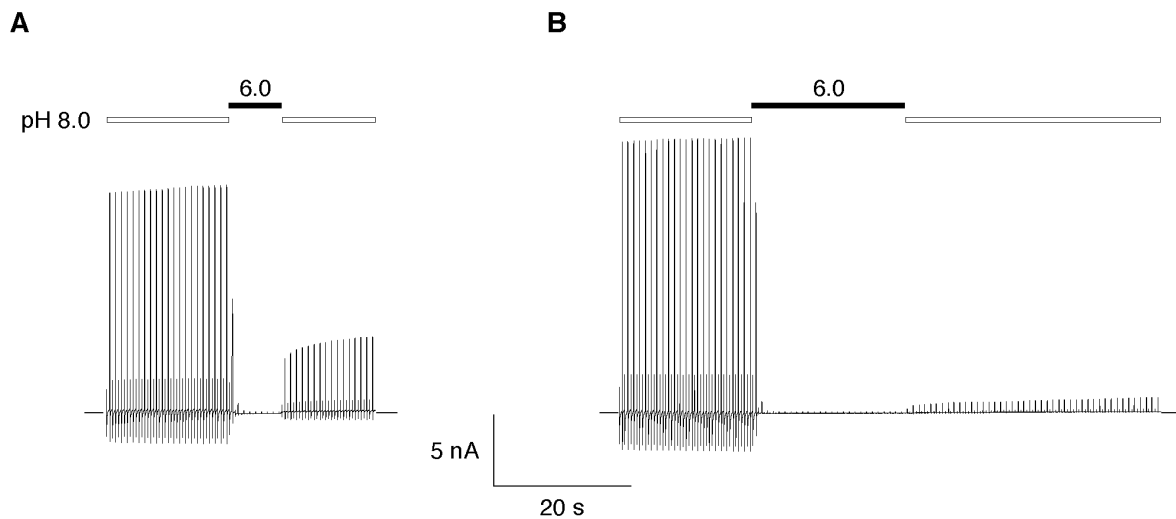


**Fig. 9.** (A), (B) Recovery of  $K_{ir}1.1$  currents from pH-induced inactivation in the absence of extracellular  $K^+$  (excised inside-out patch). Pipettes were filled with  $K^+$ -free solution ( $Na_{pipette}$ ). Voltage protocol as before. The transient inward currents most likely result from local accumulation of  $K^+$  at the extracellular space after the depolarising pulse. All intracellular solutions contained 0.1 mM DTT.

Outward currents were stable at alkaline pH, but after pH-induced inactivation only a small fraction of channels recovered depending on the time spent in the closed state. This result could be explained in two ways: pH-gating changes the conformation of a  $K^+$  binding site in the extracellular portion of the channel in a way, that  $K^+$  is tightly bound in the open state but dissociates when the channel is closed. Alternatively,  $K^+$  passing the pore could bind to an extracellular site stabilizing the channels' open state, and channel closure would prevent access of intracellular  $K^+$  to this site. In the latter case  $K_{ir}1.1$  channel activity would be expected to depend on the presence of intracellular  $K^+$  when extracellular  $K^+$  is absent.

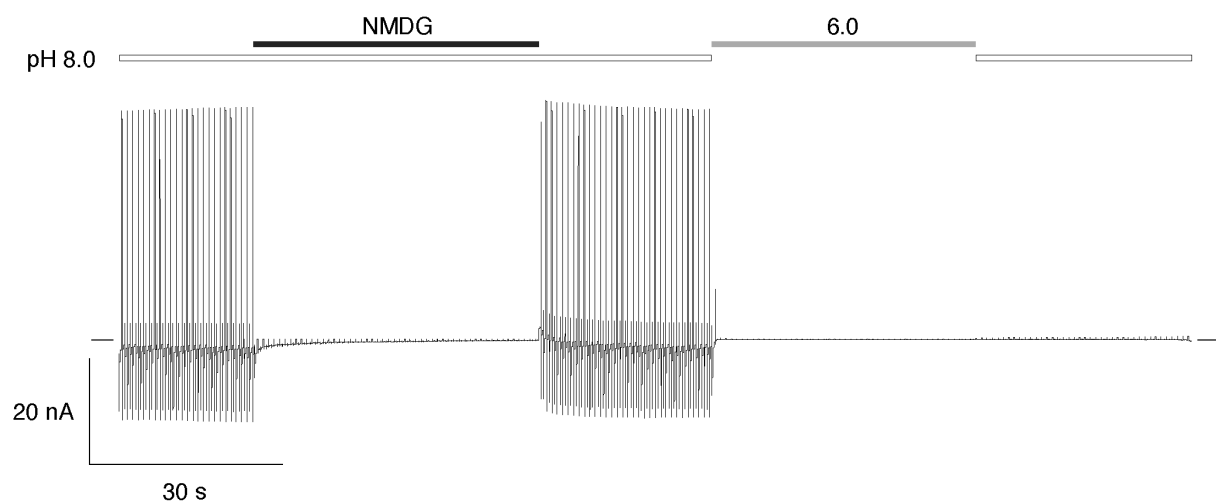


**Fig. 10.** Recovery of  $K_{ir}1.1$  currents from complete removal of  $K^+$  at pH 8.0 (excised inside-out patch). Intracellular  $K^+$  was temporarily replaced by equimolar NMDG (non-permeant cations, 120 mM). Application of  $K_{int}$  pH 6.0 as control. All other experimental conditions as in Fig. 9.

The effect of complete  $K^+$  deprivation was investigated in another experiment with  $K^+$ -free pipette solution (Fig. 10). When intracellular  $K^+$  was removed (application of 120 mM NMDG) no current could be observed. However, outward currents were completely and rapidly restored in  $K_{int}$  pH 8.0. Obviously, open channels (at pH 8.0) are either independent of  $K^+$  or have a high affinity for  $K^+$ , i.e. dissociation of  $K^+$  is very slow (time constant > minutes). Subsequent application of  $K_{int}$  pH 6.0 for the same period of time led to an almost complete, irreversible loss of channel activity. Thus, dissociation of  $K^+$  in the pH-inactivated state must be considerably faster (the time constant can be estimated to be in the range of seconds).

$K_{ir}$ .1.1 currents could also be activated by extracellular  $Cs^+$  which does not permeate the channel (Doi et al., 1996). This suggested that the interaction site is located extracellular to the selectivity filter. Indeed, dependence on extracellular  $K^+$  was lost in a chimeric construct where the P-loop of  $K_{ir}$ .1.1 had been replaced by a homologous sequence of  $K^+$ -independent  $K_{ir}$ .2.1 ( $K_{ir}$ .1.1- $K_{ir}$ .2.1p), Fig. 11). These channels were still gated by intracellular pH, i.e. currents inactivated completely at pH 6.0, but recovered upon alkalization in the absence of extracellular  $K^+$ .

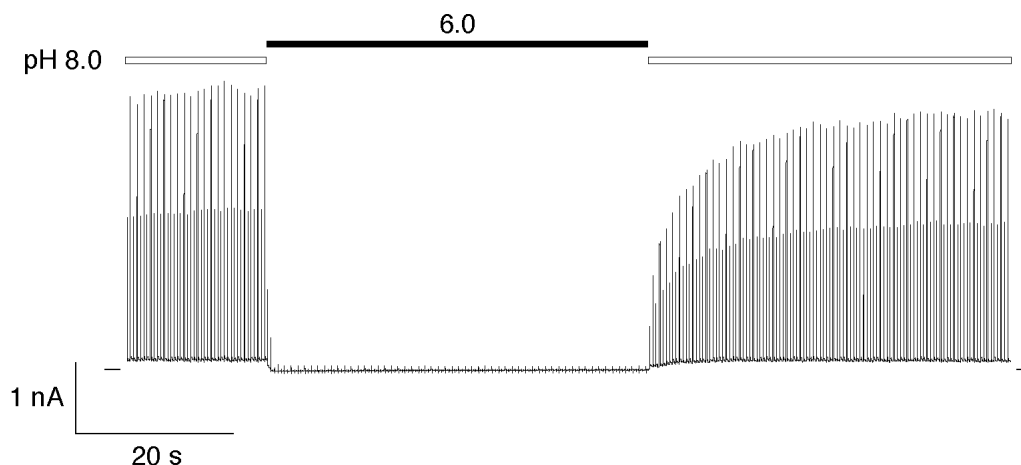


**Fig. 11.** Recovery of  $K_{ir}$ .1.1( $K_{ir}$ .2.1p) currents from pH-inactivation in the absence of extracellular  $K^+$  (excised inside-out patch). Experimental conditions as in Fig. 9.

However, when pH-gating was removed by an intracellular point mutation ( $K_{ir}$ .1.1(K80M), see section 2.2.3), dependence on extracellular  $K^+$  was also abolished. This is demonstrated in whole-cell experiments which allow the exchange of extracellular solution. After one hour of preincubation in  $K^+$ -deprived extracellular solution,  $K_{ir}$ .1.1 currents had decreased close to background levels but slowly activated when switched to a solution containing 90 mM  $K^+$  (Fig. 12 A). For the mutant  $K_{ir}$ .1.1(K80M) (Fig. 12 B), outward currents remained constant in  $K^+$ -free solution and there was no additional increase in channel activity after switching to a high  $K^+$  solution.

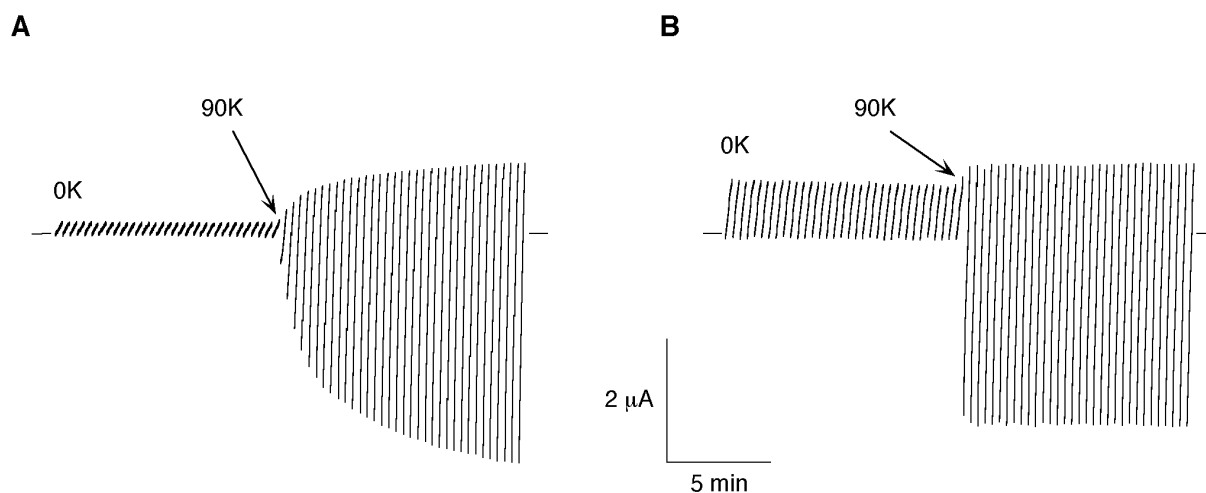


**Fig. 12.** Dependence of (A)  $K_{ir1.1}$  currents and (B)  $K_{ir1.1}(K80M)$  currents on the presence of extracellular  $K^+$  recorded from whole oocytes. Two-electrode voltage-clamp protocol as described in "Materials and Methods". Note the outward currents (B) reflecting the weak inward-rectification of  $K_{ir1.1}$  channels. 0K:  $K^+$ -free bath solution, 90K: bath solution containing 90 mM  $K^+$ .

Taken together, pH-induced inactivation is a prerequisite for the dissociation of extracellular  $K^+$  from the channel. This implies that pH-gating leads to conformational changes in the extracellular P-loop.

### 2.1.3 State-dependent cysteine modification reveals a conformational change induced by pH-gating

Sensitivity of  $K_{ir1.1}$  channels to redox reactions was investigated with reagents that differentially react with sulfhydryl-groups. Oxidizing agents like Cu(II)-1,10-phenanthroline, which induce formation of disulfide bonds between cysteine residues (Kobashi, 1968), largely reduced the fraction of channels that spontaneously recovered upon realkalinization. Addition of DTT to the pH<sub>i</sub> 8.0 solution still resulted in complete recovery from pH-induced inactivation (Schulte et al., 1998). However, when reagents were applied that can also oxidize single cysteine residues (in the following referred to as "modification") such as MTSES (Akabas, 1992) or DTNB (Riddles et al., 1979), DTT failed to recover channels from pH-induced inactivation (Fig. 13; experiment with MTSES not shown). The residual recovery of currents observed upon realkalinization in these experiments most likely represented unmodified channels since no recovery was seen when application of DTNB/pH 6.0 was extended to periods longer than 2 min (experiment not shown).

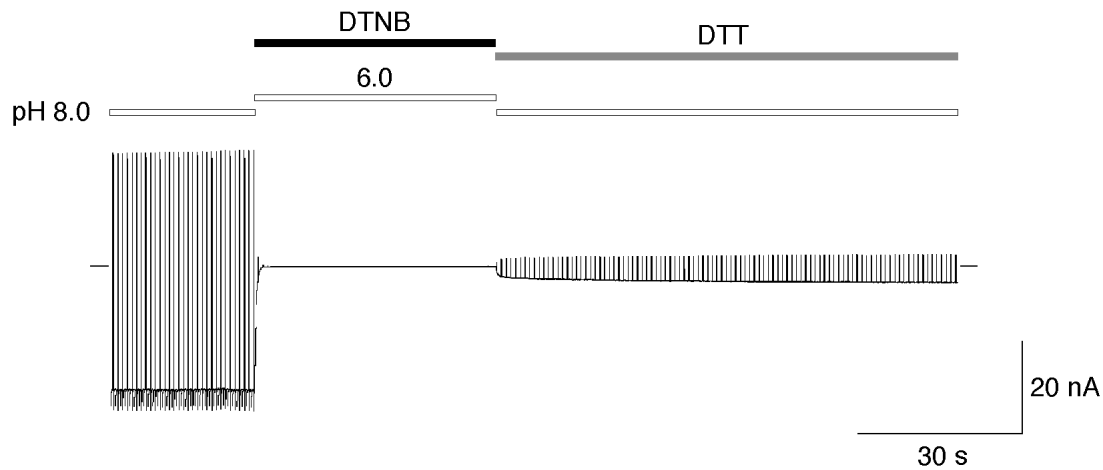


**Fig. 13.** Modification of  $K_{ir}1.1$  channels with DTNB in excised inside-out patches. Application of 0.1 mM DTNB at pH 6.0 and 0.1 mM DTT at pH 8.0 as indicated by bars. Voltage pulse protocol as in Fig. 11.

These experiments demonstrate that formation of disulfide bonds in  $K_{ir}1.1$  channels is reversible, while modification by DTNB or MTSES irreversibly locks pH-inactivated channels in a closed state. In order to more closely characterize modification by DTNB and its relation to pH-dependent gating, experiments were performed where DTNB was applied at  $pH_i$  8.0 either before or after pH-induced inactivation, i.e. when channels were either in the open or pH-inactivated (closed) state.

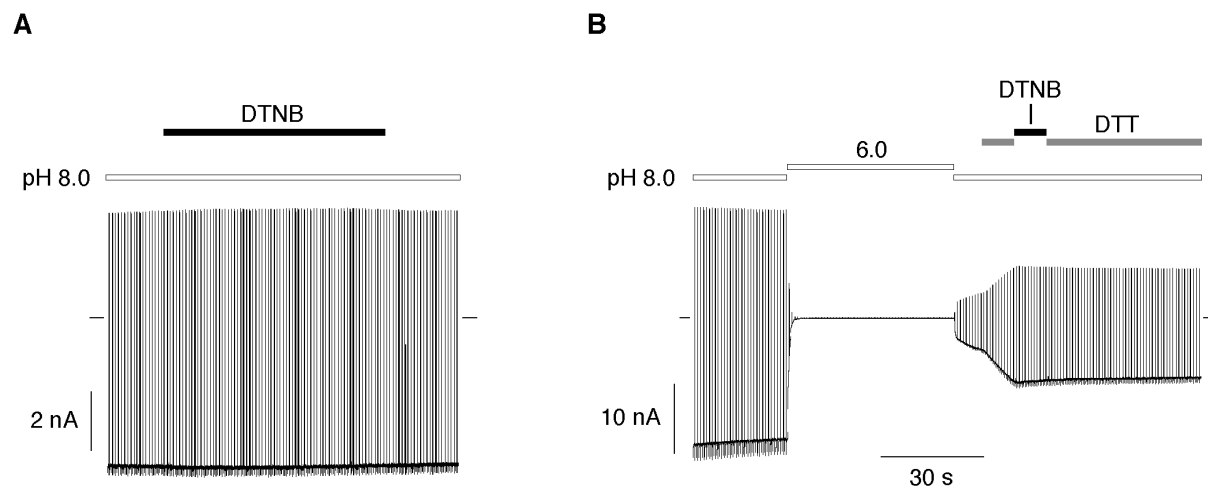


**Fig. 14.** DTNB-modification of open (A) and closed (B)  $K_{ir}1.1$  channels at pH 8.0 in excised inside-out patches. Application of 0.1 mM DTNB at pH 8.0 and 0.1 mM DTT at pH 8.0 as indicated by the bars. Note that already a short time of DTNB-application prevented any further recovery of  $K_{ir}1.1$  channels in 0.1 mM DTT (B).

As shown in Fig. 14, DTNB did not affect open channels at  $pH_i$  8.0, nor did preapplication of DTNB change subsequent pH-gating (experiment not shown). In contrast, when DTNB was applied during DTT-induced recovery from pH-inactivation, recovery was promptly stopped

and did not continue in DTNB-free solution subsequently applied. Thus, under identical conditions, channels were only susceptible to chemical modification when they were pH-inactivated (i.e. in a closed state) prior to DTNB-application.

This coupling of chemical modification to a pH-inactivated state was confirmed by experiments with the mutant  $K_{ir}1.1(K80M)$  in which pH-gating is abolished (see section 2.2.3). As shown in Fig. 15, no effect of DTNB was observed, neither at basic nor at acidic pH<sub>i</sub>.

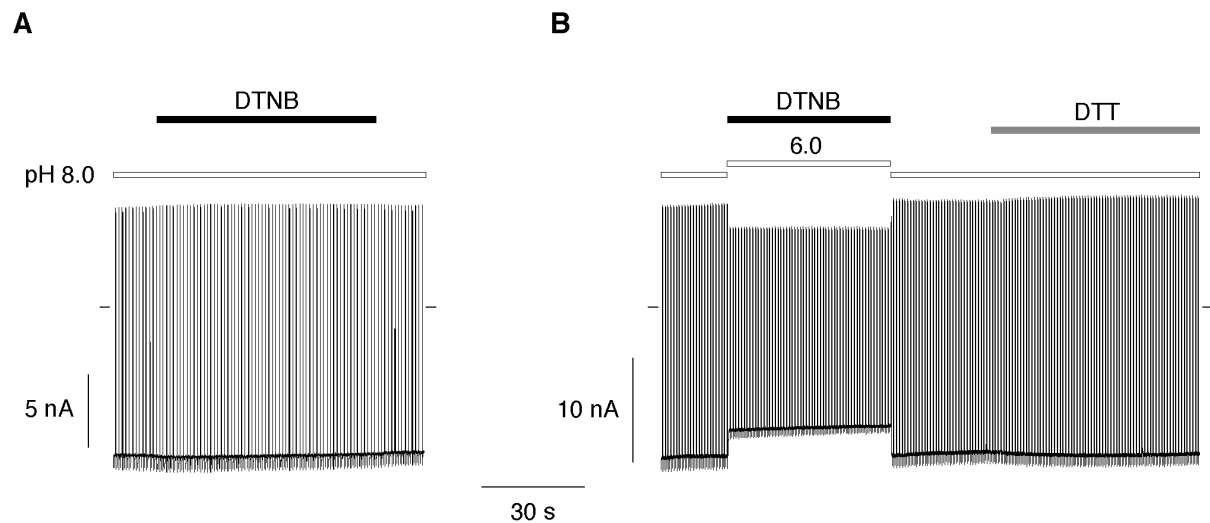


**Fig. 15.** Modification of  $K_{ir}1.1(K80M)$  channels with DTNB at (A) pH 8.0 and (B) pH 6.0 in excised inside-out patches. Application of 0.1 mM DTNB pH 8.0 or pH 6.0 and 0.1 mM DTT pH 8.0 as indicated by the bars.

Taken together,  $K_{ir}1.1$  channels are targeted by DTNB in a state-dependent manner, i.e. channels are modified in the pH-inactivated closed state, but not in the conducting open state.

#### 2.1.4 Cysteines 49 and 308 are targets for state-dependent modification

State-dependence together with the fact that DTNB specifically modifies cysteine residues was exploited to investigate which domains of the  $K_{ir}1.1$  protein move during pH-dependent gating. For this purpose all cysteines in the  $K_{ir}1.1$  sequence were replaced by alanine (A) or serine (S) (Fig. 16). Mutations in the N- and C-termini outside the ‘core-region’ (hydrophobic trans-membrane domains and the P-region) resulted in functional channels gated by intracellular pH, while no currents were observed upon expression of the two mutants carrying C A/S exchanges in the P-region ( $K_{ir}1.1(C121A,S)$  and  $K_{ir}1.1(C153A,S)$ ).

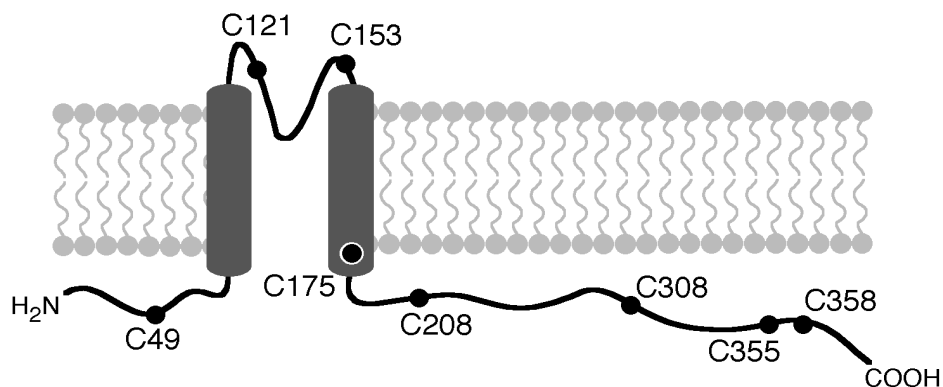


**Fig. 16.** Distribution of cysteine residues in the  $K_{ir}1.1$  subunit. C121 and C153 are present in all  $K_{ir}$  subunits; C49, C208 and C308 are conserved in most  $K_{ir}$  subunits; C175, C355 and C358 are only found in  $K_{ir}1.1$ .

The redox properties of functional mutants were tested with a standardized protocol. Recovery from pH-inactivation in the presence of DTT was measured after a 50 s application of pH<sub>i</sub> 6.0 solution either with or without (control) DTNB. Relative changes of current amplitudes were calculated as described in "Materials and Methods" for a quantitative comparison.

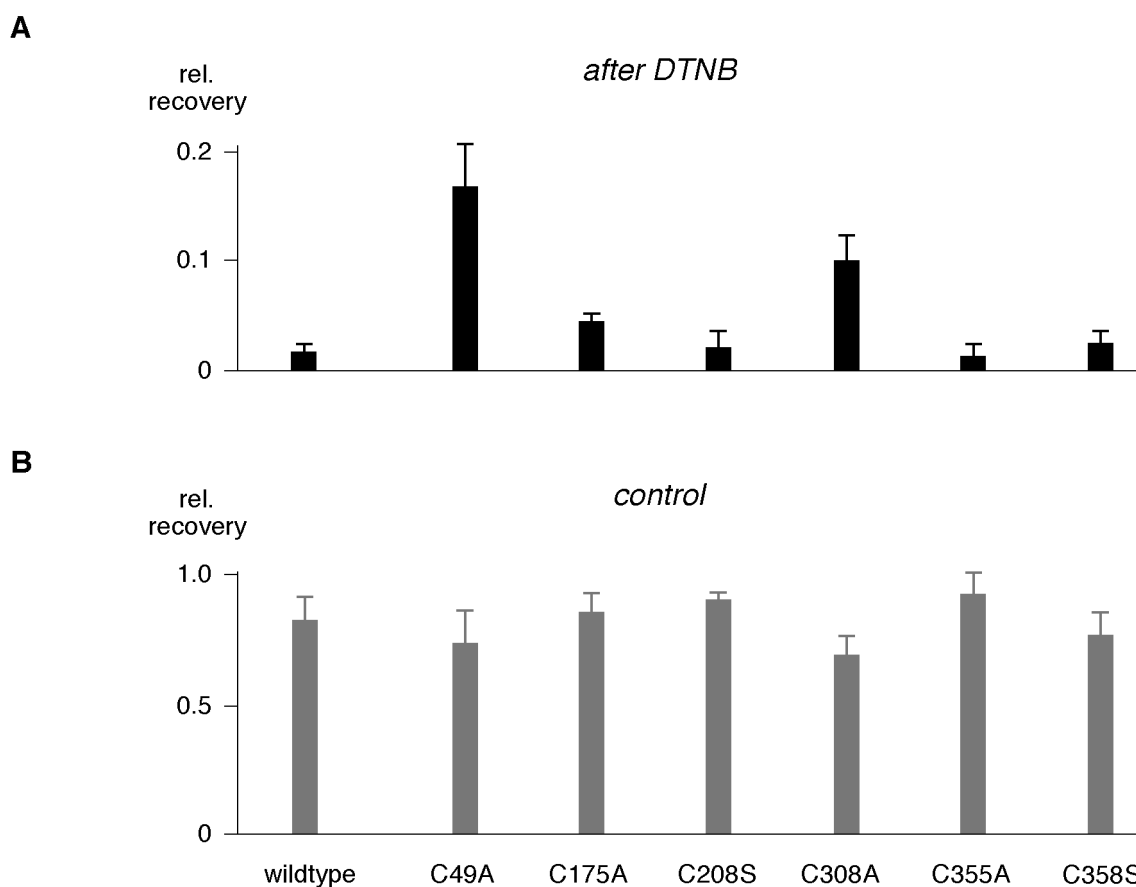


**Fig. 17.** Relative recovery of  $K_{ir}1.1$  currents with DTT in excised inside-out patches after application of (A) pH 6.0 + 0.1 mM DTNB and (B) pH 6.0 alone (control) for 50 s each. Experimental conditions as in Fig. 13. There were no significant differences, no matter whether C A or C S mutants were tested. Calculations from n 3 experiments see "Materials and Methods".

All mutant channels recovered in a way very similar to that of  $K_{ir}1.1$  wildtype channels under control conditions, and modification by DTNB was not abolished by any of the single C A/S exchanges (Fig. 17). However, the fractional recovery from inactivation after DTNB-modification observed in  $K_{ir}1.1(C49A)$  and  $K_{ir}1.1(C308A)$  was significantly larger than that for  $K_{ir}1.1$  wildtype or any of the other mutants. A possible explanation was that DTNB-modification may occur at more than one site. To test for this, a double mutant  $K_{ir}1.1(C49,308A)$  was constructed and investigated under the same conditions.

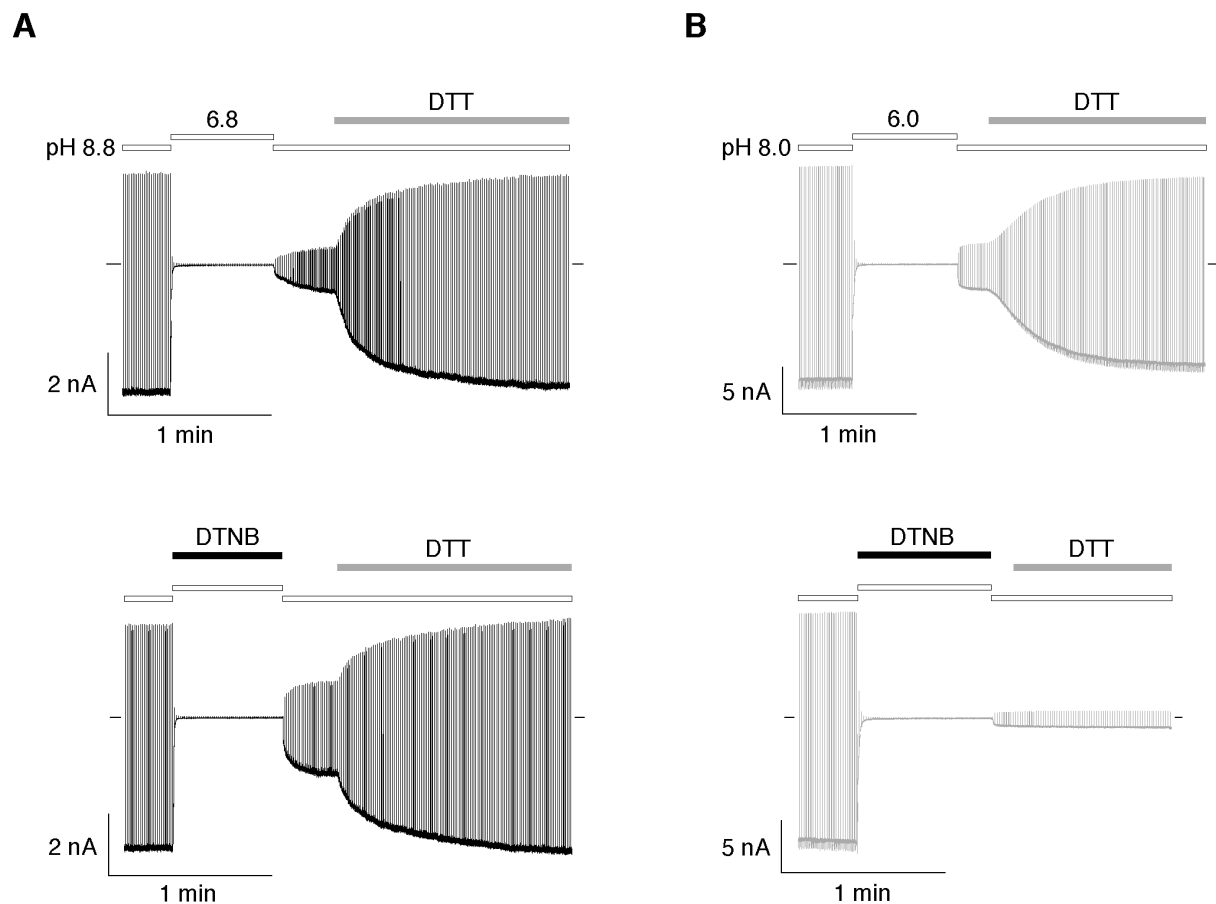


**Fig. 18.** (A)  $K_{ir}1.1(C49,308A)$  current recovery after application of pH 6.8 (upper panel) and pH 6.8 + 0.1 mM DTNB (lower panel) in excised inside-out patches. (B) For comparison,  $K_{ir}1.1$  current recovery after application of pH 6.0 (upper panel) and pH 6.0 + DTNB (lower panel). All other experimental conditions as before.

Like in the case of  $K_{ir}1.1$  and the single cysteine mutants only a fraction of channels recovered spontaneously from pH-induced inactivation (Fig. 18 A and B, upper panels). But in contrast to  $K_{ir}1.1$  wildtype channels, recovery from pH-inactivation in the presence of DTT was complete for the double mutant, independent of whether DTNB had been added to the pH 6.0 solution or not (compare lower panels in Fig. 18 A and B).

These results show, that the cysteine residues modified by sulfhydryl-reagents in a state-dependent manner are C49 in the N-terminus and C308 in the C-terminus of the  $K_{ir}1.1$  protein.

It may be concluded that pH-dependent gating in these channels is accompanied by structural rearrangements in both intracellular N- and C-termini. A noteworthy finding in this context was that  $K_{ir}1.1(C49,308A)$  also displayed an alkaline shift in  $pK_{app}$  (see "Discussion").

## 2.2 Identification of lysine 80 (K80) as the sensor for $pH_i$ in the neutral pH range

### 2.2.1 Current- $pH_i$ -relation in $K_{ir}1.1$ and $K_{ir}4.1$ channels

For a quantitative analysis of pH sensitivity, concentration-responses of  $K_{ir}1.1$  currents were measured in giant inside-out patches. Intracellular pH was varied between pH 8.0 (maximum current = reference pH) and pH 6.0 (no channel activity) with increments of 0.4 pH units.

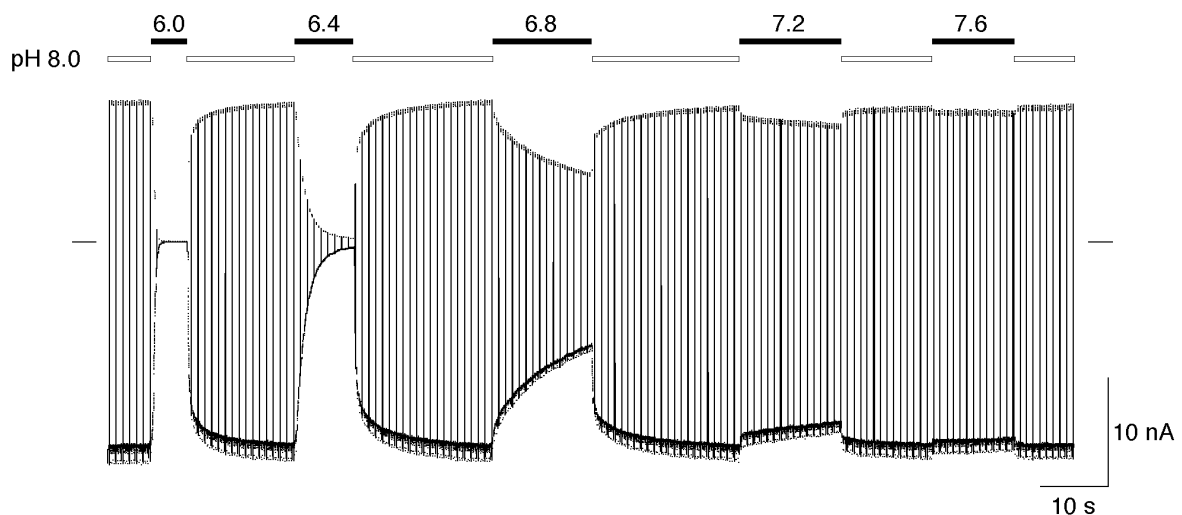


**Fig. 19.** pH titration of  $K_{ir}1.1$  currents in an excised inside-out patch. All intracellular solutions contained 0.1 mM DTT and were applied at the  $pH_i$  values indicated by the bars. Note the pH-dependence of current inactivation kinetics.

The current amplitude was stable at alkaline pH and decreased reversibly upon acidification in a concentration-dependent manner (Fig. 19). The steady-state inhibition of the current was determined from monoexponential fits to the current decrease at a given  $pH_i$  and normalized with respect to the corresponding control current at  $pH_i$  8.0. The resulting concentration-response curve showed half-maximal inhibition at  $pH_i$  (also referred to as  $pK_{app}$ ) 6.8, with a Hill coefficient around 3 indicating cooperativity of the process (Fig. 20).  $K_{ir}1.1a$  and  $K_{ir}1.1b$  channels (data not shown) were indistinguishable with respect to pH-dependence and biophysical properties.



Negatively charged phospholipids have been shown to interact with several  $K_{ir}$  channels (Hilgemann and Ball, 1996; Huang et al., 1998) and to change gating properties of  $K_{ATP}$  channels (Baukrowitz et al., 1998; Shyng and Nichols, 1998). Therefore,  $K_{ir1.1}$  pH concentration-response curves were measured before and after application of PIP2 to the cytoplasmic side of the patch membrane. As illustrated in Fig. 20, PIP2 had no significant effect on pH sensitivity of  $K_{ir1.1}$  channels.

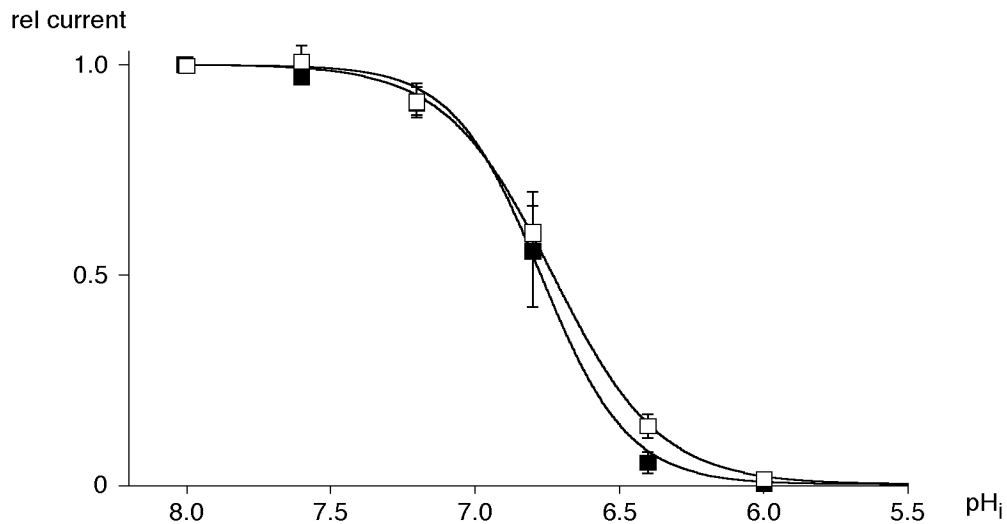


**Fig. 20.**  $pH_i$  concentration-response curves of  $K_{ir1.1}$ . Each data point represents the mean of steady-state activities in  $n$  experiments at the respective  $pH_i$  like in Fig. 19. Fits with a logistic function yielded  $pK_{app}=6.8$  and Hill coefficient=2.9 ( $n=11$ ) before (closed squares), and  $pK_{app}=6.7$  and Hill coefficient=2.4 ( $n=6$ ) after (open squares) application of PIP2 (10  $\mu$ M, 30 s). For details of data evaluation see "Materials and Methods".

Besides  $K_{ir1.1}$ , sensitivity to intracellular pH has also been reported for a strong inward-rectifier expressed in skeletal muscle (Blatz, 1984).  $K_{ir4.1}$  (BIR10) is assumed to underly this conductance and was therefore tested in inside-out patches from *Xenopus* oocytes.

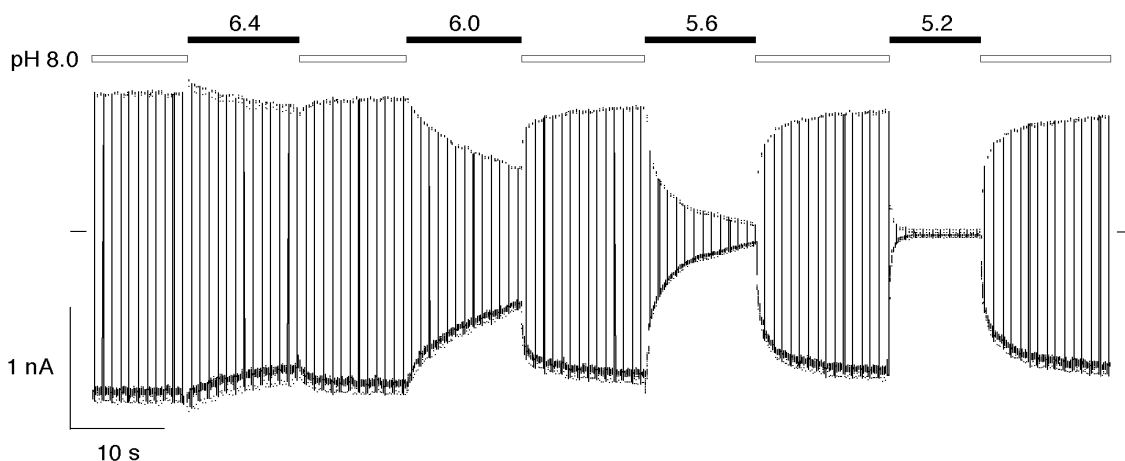


**Fig. 21.** pH titration of  $K_{ir4.1}$  currents. Experimental conditions as in Fig. 19.

For  $K_{ir}4.1$  the current- $pH_i$  relation was of similar steepness as for  $K_{ir}1.1$  (Hill coefficient 2.3), but shifted towards more acidic  $pH_i$  values (halfmaximal inhibition at  $pH$  6.1, see Fig. 28).

### 2.2.2 pH sensitivity of other $K_{ir}$ channels

Comparison of pH-gated versus pH-insensitive  $K_{ir}$  channels by primary sequence alignment should allow identification of molecular determinants required for pH-gating. Therefore, members of other  $K_{ir}$  subfamilies were tested for their sensitivity to  $pH_i$ .  $K_{ir}2.1$  (IRK1), a representative of the subfamily  $K_{ir}2$ , did not show inhibition upon intracellular acidification in whole-cell experiments (Doi et al., 1996). Accordingly,  $K_{ir}2.1$  channels remained active at low  $pH_i$  when examined in giant inside-out patches (Fig. 22).

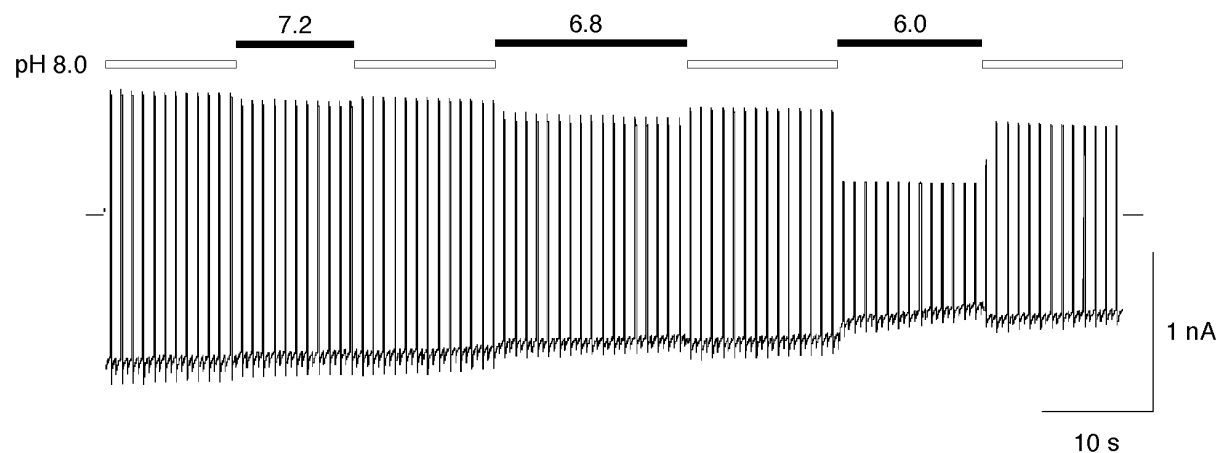


**Fig. 22.** pH sensitivity of  $K_{ir}2.1$  currents in excised inside-out patches. Intracellular solutions (without DTT) were applied as indicated by the bars. Note that inward-rectification is lost in the absence of intracellular spermine and  $Mg^{2+}$ . The partial decrease of outward current at  $pH$  6.0 was due to voltage-dependent block of the channel pore by intracellular protons.

Channels formed by  $K_{ir}6.2 + SUR1$  are characterized by their high sensitivity towards intracellular ATP (therefore referred to as  $K_{ATP}$  channels) and serve to couple cellular excitability to metabolism (Ashcroft, 1988; Cameron and Baghdady, 1994). A possible modulatory role of intracellular pH in this process has been discussed (Misler et al., 1989; Bond et al., 1991; Proks et al., 1994). In whole *Xenopus* oocytes, changes in  $pH_i$  had complex effects on  $K_{ATP}$  currents (experiments not shown). Thus,  $pH_i$ -sensitivity of  $K_{ir}6.2/SUR1$  currents was measured in excised inside-out patches in order to exclude any indirect influences of  $pH_i$  mediated by intracellular soluble factors. Prior to these experiments, 10  $\mu M$  PIP2 was applied to the patch for 20 s in order to prevent channel 'rundown'. Under these experimental conditions  $K_{ir}6.2/SUR1$  currents were insensitive to intracellular acidification (Fig. 23).

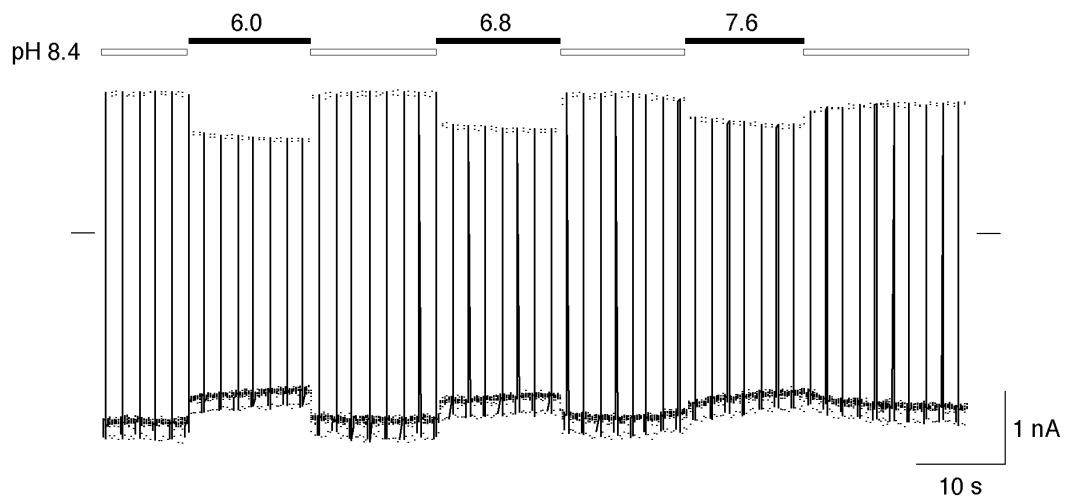


**Fig. 23.** pH sensitivity of  $K_{ir6.2}/SUR1$  currents after application of PIP2 (10  $\mu$ M, 20 s) in excised inside-out patches. Other experimental conditions as in Fig. 19.

Finally, members of the  $K_{ir3}$  subfamily were tested in whole-cell experiments using the two-electrode-voltage-clamp technique (Fig. 24).  $pH_i$  was monitored by a third microelectrode filled with a proton-selective polymer (Tsai et al., 1995). Intracellular acidification was achieved through application of an extracellular bicarbonate solution (90 mM  $KHCO_3$  pH 7.2; (Doi et al., 1996)). Uncharged  $H_2CO_3$  and  $CO_2$  molecules rapidly diffuse through the membrane and re-equilibrate with the cytoplasm.

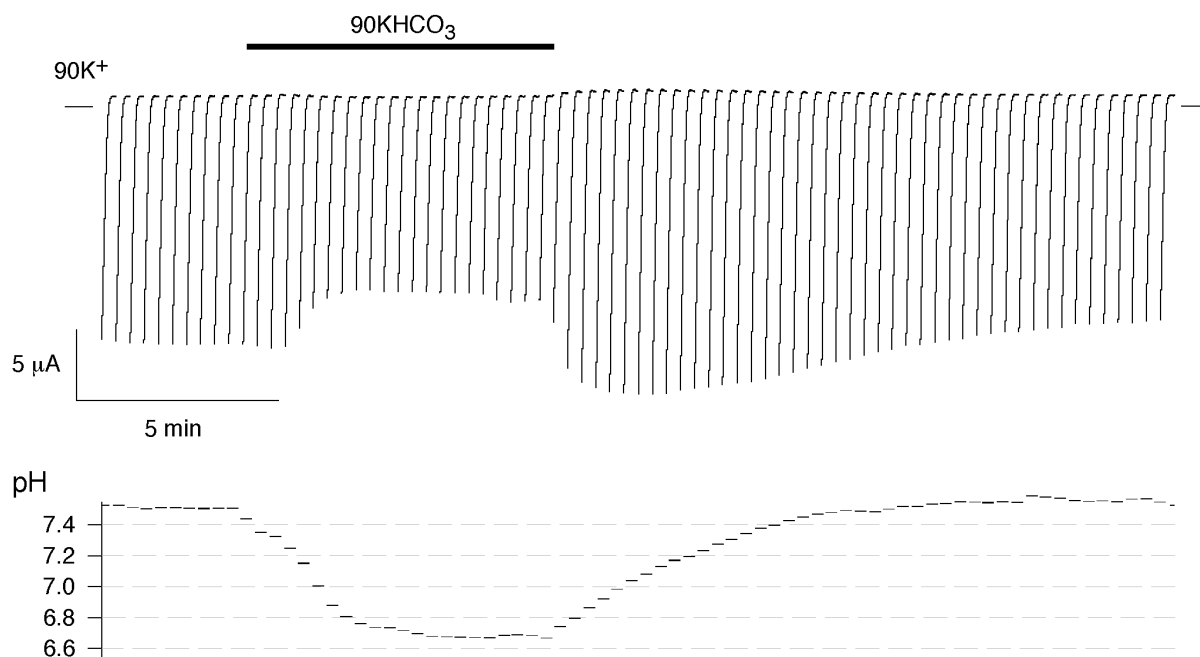


**Fig. 24.** Sensitivity of  $K_{ir3.1}/K_{ir3.4}$  homomeric channels to intracellular acidification in whole *Xenopus* oocytes. Upper trace: currents in response to voltage-ramps (-120 to +50 mV, 20 s) showing strong inward-rectification. Lower trace: intracellular pH as recorded with a pH-sensitive microelectrode (see "Materials and Methods").

With switching to extracellular  $90\text{KHCO}_3$ , the resting  $\text{pH}_i$  ( $\approx 7.5$ ) decreased to more acidic values ( $< 6.7$ ) and reversed upon withdrawal of external  $\text{HCO}_3^-$  with a tendency to overshoot re-alkalinization to values around 7.6. As can be seen in Fig. 24,  $\text{K}_{ir}3.1/\text{K}_{ir}3.4$ -mediated currents decreased only partially during acidification and recovered with a transient maximum upon re-alkalinization.  $\text{K}_{ir}3.2$  (data not shown) exhibited a similar behavior in this type of experiments. Further investigations with excised inside-out patches could not be carried out since G-protein coupled  $\text{K}_{ir}$  channels quickly lost activity upon patch excision (fast "rundown", also reported by Ruppertsberg et al. (1999)). From all  $\text{K}_{ir}$  channels tested, only  $\text{K}_{ir}1.1$  and  $\text{K}_{ir}4.1$  exhibited gating by intracellular protons.

### 2.2.3 Substitution of K80 by non-basic amino acids eliminates $\text{pH}$ -gating of $\text{K}_{ir}1.1$ channels

In experiments with chimeric  $\text{K}_{ir}$  constructs,  $\text{pH}_i$  sensitivity could be conferred to  $\text{K}_{ir}2.1$  by the N-terminus of  $\text{K}_{ir}1.1$  (Fakler et al., 1996b). Consequently, N-terminal amino acid sequences of the  $\text{K}_{ir}$  channels tested above were compared and analyzed for titratable amino acid residues. By site-directed mutagenesis, lysine 80 (K80) was found to be a crucial determinant for  $\text{pH}$ -gating (Fakler et al., 1996b).  $\text{K}_{ir}1.1$  channels where K80 had been replaced by a non-titratable amino acid ( $\text{K}_{ir}1.1(\text{K80T})$  or  $\text{K}_{ir}1.1(\text{K80M})$ ) were no longer sensitive to  $\text{pH}_i$  (Fig. 25).

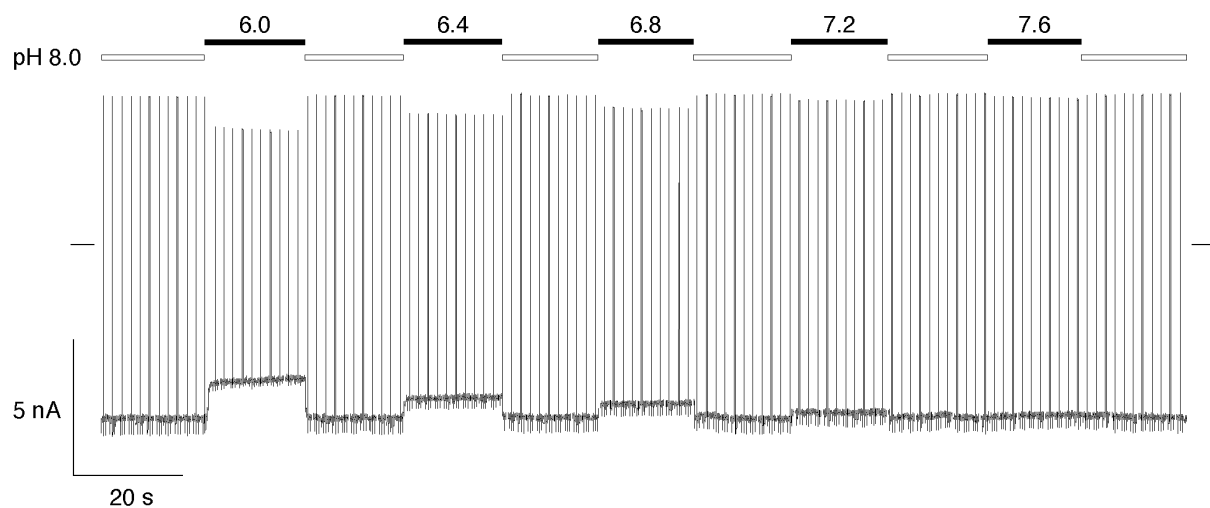


**Fig. 25.**  $\text{pH}$  titration of  $\text{K}_{ir}1.1(\text{K80M})$  currents in excised inside-out patches. Experimental conditions as in Fig. 19. Fits to the respective current- $\text{pH}_i$ -relation with a logistic function yielded a  $\text{pK}_{app}$  of 5.3 and a Hill coefficient of 0.5 ( $n=5$ ).

Thus, gating by  $\text{pH}_i$  and occurrence of a lysine residue at position 80 (or a homologous site) correlate well. All  $\text{K}_{ir}$  channels gated by  $\text{pH}_i$  exhibit a lysine residue at this site N-terminal to M1 (referred to as 'pre-M1 site'), all others show non-titratable amino acids at the homologous positions.

## 2.2.4 Chemical modification with amino-specific agents renders $K_{ir}1.1$ channels $pH_i$ -insensitive

The results presented above led to the hypothesis, that protonation of K80 might trigger  $pH$ -gating. However, this would require that the  $pK_a$  of the  $NH_2$ -group of this lysine residue is shifted by more than 3  $pH$  units compared to its standard value of 10.5 (Dawson et al., 1986). To verify this, the protonation state of K80 was investigated by application of FmocCl, a reagent that reacts rapidly and specifically with  $NH_2$ -groups but not with protonated  $NH_3^+$ -groups (Carpino and Han, 1970; Henczi and Weaver, 1994). Modification of unprotonated K80 would yield a urethane derivative which can no longer be protonated (Fig. 26 A).

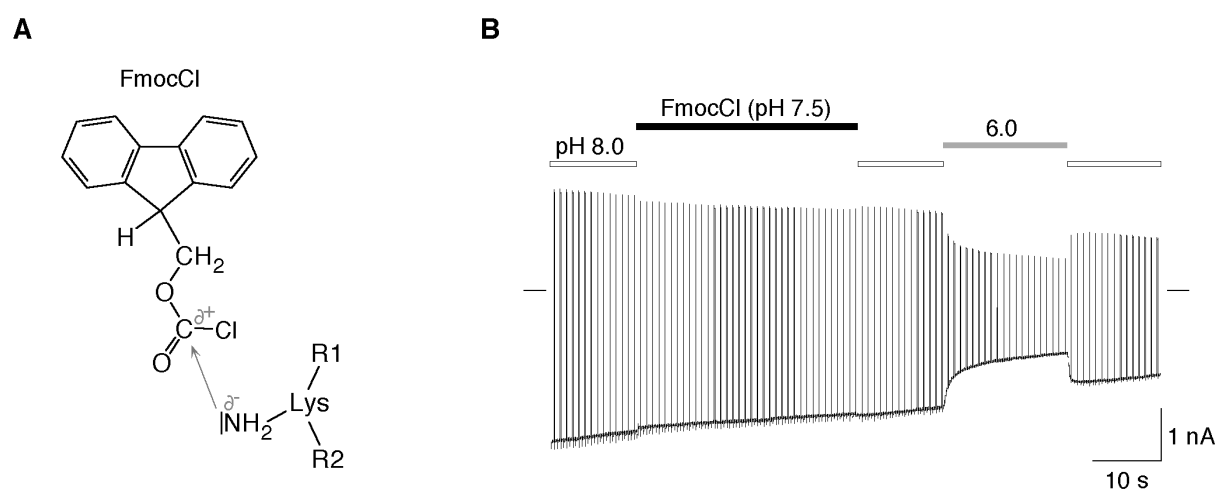


**Fig. 26.** (A) Reaction of FmocCl with  $NH_2$  of lysine. Nucleophilic addition and subsequent elimination of Cl yields a urethane derivative. (B) Chemical modification of  $K_{ir}1.1$  channels with FmocCl in an excised inside-out patch. FmocCl was freshly added to the modification buffer (MOD) from a stock solution (100 mM FmocCl in dioxane) for a final concentration of 0.1 mM. Solutions ( $K_{int}$  without DTT) were applied at the  $pH$  values indicated, other experimental conditions as before. Note that treatment of the patch with FmocCl did not alter channel activity.

As shown in Fig. 26 B,  $K_{ir}1.1$  channels which had been treated with FmocCl at  $pH_i$  7.5 prior to acidification were no longer inactivated at  $pH_i$  6.0. The partial decrease in current observed upon acidification was most likely due to channels not modified by FmocCl.

From this experiment it can be concluded that K80 is not protonated at  $pH_i > 7.5$ , and that protonation of this residue is a prerequisite for  $pH$ -gating.

## 2.2.5 Introduction of lysine at the pre-M1 site confers pH-gating to other $K_{ir}$ channels

Although K80 was necessary for pH-gating in  $K_{ir}1.1$ , it remained to be investigated if this determinant would be sufficient to induce pH-gating in other  $K_{ir}$  channels. Members of two  $K_{ir}$  subfamilies were mutated at the corresponding site ( $K_{ir}6.2(T71K)/SUR1$  and  $K_{ir}2.1(M84K)$ ), and the resulting channels were tested for sensitivity to  $pH_i$ .

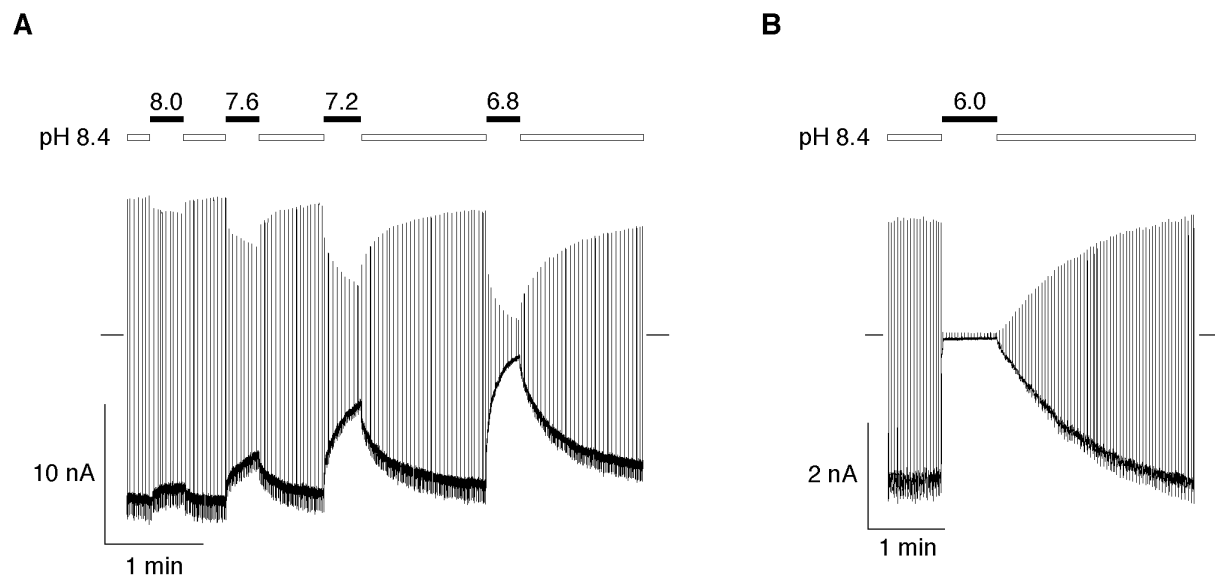


**Fig. 27.** pH sensitivity of (A)  $K_{ir}6.2(T71K)/SUR1$  channels (after application of 10  $\mu$ M PIP2 for 20 s) and (B)  $K_{ir}2.1(M84K)$  channels in excised inside-out patches. Experimental conditions as in Fig. 23. Note the time scales revealing slower kinetics of current recovery compared to Fig. 19.

As shown in Fig. 27,  $K_{ir}6.2(T71K)/SUR1$  channels (A) displayed a high sensitivity to  $pH_i$ , as did  $K_{ir}2.1(M84K)$  channels (B) (complete inhibition of channel activity at  $pH_i$  6.0). Compared to  $K_{ir}1.1$ , pH-gating had different kinetics and was less reversible at low  $pH_i$ .

The concentration-response curves from pH titration experiments with  $K_{ir}2.1(M84K)$  and  $K_{ir}6.2(T71K)/SUR1$  are plotted in Fig. 28 together with those obtained for  $K_{ir}1.1$  and  $K_{ir}4.1$ . All current- $pH_i$ -relations displayed positively cooperative pH-gating although there was some variability in  $pK_{app}$  and Hill coefficient (see legend Fig. 28). The finding that pH-gating could be conferred to members of different  $K_{ir}$  subfamilies via introduction of a lysine at the pre-M1 site allowed several conclusions:

- Lysine at this site is sufficient (in the sense of a subunit-specific determinant) for pH-gating.
- A gating machinery is present in all  $K_{ir}$  channels, which is coupled to the charge of the amino acid side chain at this site.
- A chemical environment is structurally conserved among  $K_{ir}$  subfamilies that leads to strong shifts in the apparent pK of lysine at this site (  $pK_{app}$  ranges from 3.1 to 4.4 pH units).

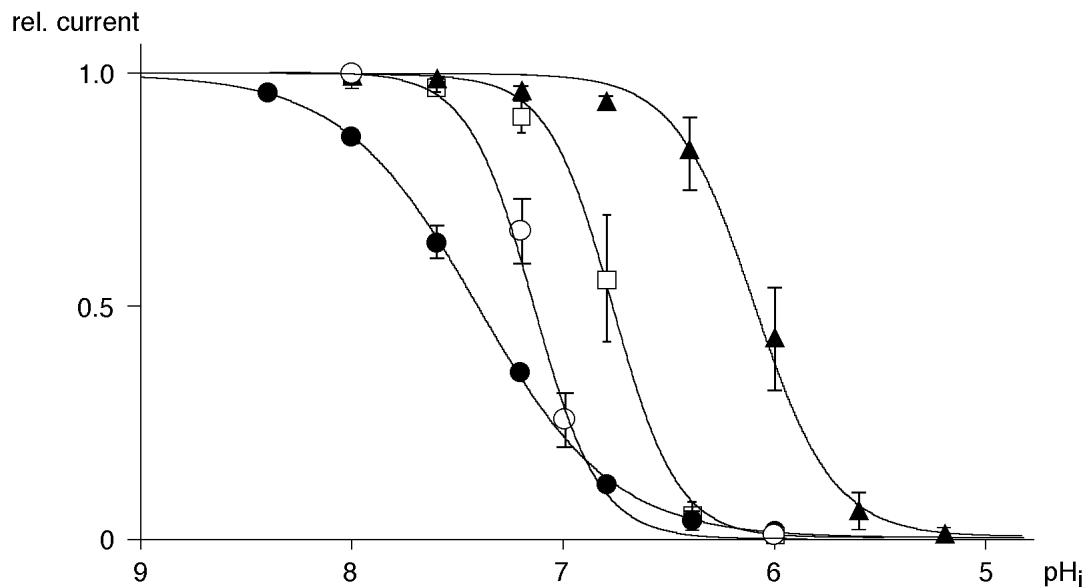


**Fig. 28.** pH concentration-response curves for pH-gated  $K_{ir}$  channels. Data points were obtained from pH titration experiments as in Fig. 19 as means of  $n$  steady-state values. Parameters of a logistic function fitted to the data were:  $pK_{app}=6.8$  and Hill coefficient= 2.9 ( $n=11$ ; taken from Fig. 20) for  $K_{ir}1.1$  (squares),  $pK_{app}=6.1$  and Hill coefficient=2.3 ( $n=6$ ) for  $K_{ir}4.1$  (triangles),  $pK_{app}=7.4$  and Hill coefficient=1.4 ( $n=4$ ) for  $K_{ir}6.2(T71K)/SUR1$  (closed circles) and  $pK_{app}=7.1$  and Hill coefficient=3.6 ( $n=5$ ) for  $K_{ir}2.1(M84K)$  (open circles).

## 2.3 Intrasubunit assembly of K80 with R41 and R311 causes the shift in $pK_{app}$

### 2.3.1 Substitution of some conserved positively charged amino acids leads to shifts in $pK_{app}$

In order to work as a sensor for  $pH_i$ , lysine 80 must bind a cytoplasmic proton. Accessibility of this site from the cytoplasm has been confirmed by cysteine modification experiments for  $K_{ir}2.1(M84C)$  (Fakler et al., 1996b). This evidence, together with the finding that the apparent affinity for  $H^+$  is more than 1000fold lower than the standard value, led to the assumption that in the context of the  $K_{ir}1.1$  protein K80 might be shielded by a positively charged environment repelling protons from its  $NH_2$ -group. Accordingly, neutralization of such an environment should shift titration of K80 back to its standard value and thus result in channels permanently inactivated in the neutral pH-range (depicted in Fig. 29 A). To test this hypothesis, all intracellular arginine and lysine residues conserved among the  $K_{ir}$  subfamilies analyzed in 2.2.2 were replaced by glutamine (Q). The gating parameters of the mutant channels were determined from pH concentration-response measurements.

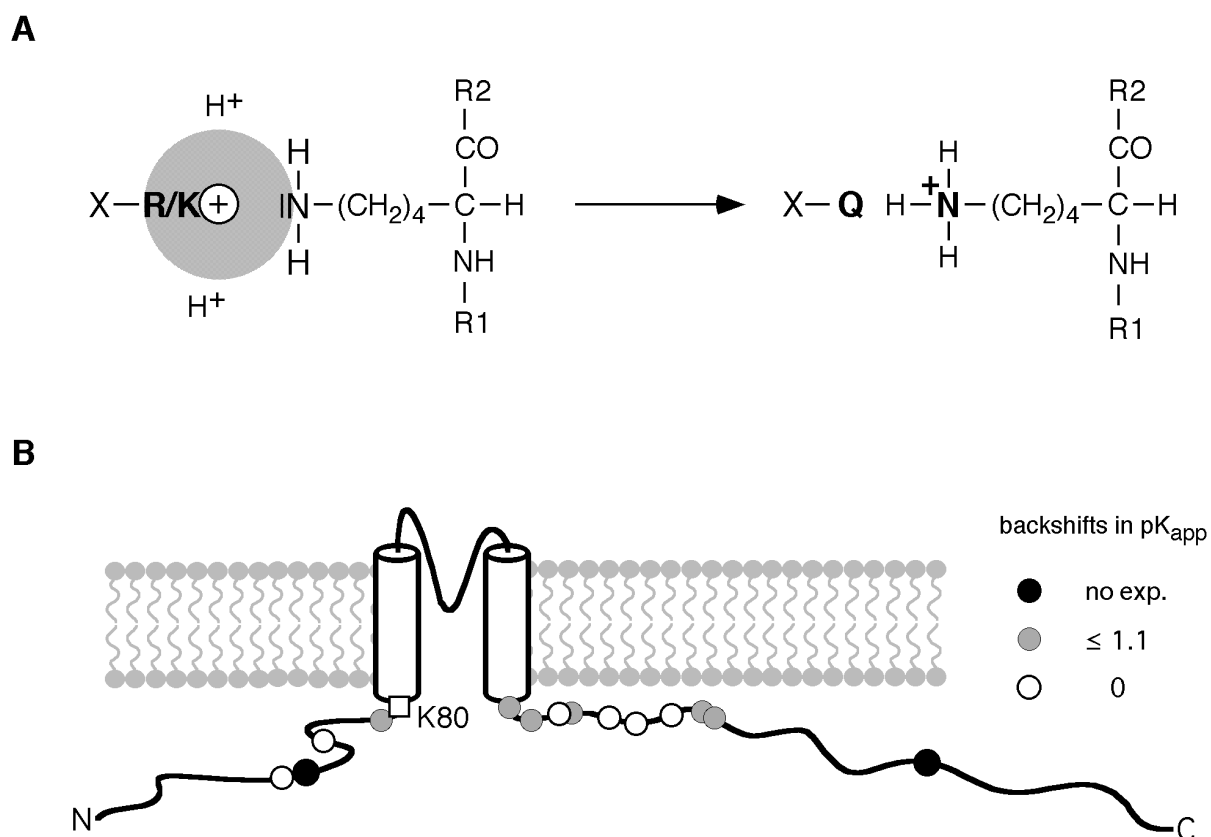


**Fig. 29.** (A) Electrostatic shielding of K80. X= backbone structure; grey zone: electrical field of the positive charge of R or K. When R or K are replaced by a neutral amino acid (Q), protons are no longer repelled from the  $\text{NH}_2$ -group of lysine (right). (B) Neutralization of conserved intracellular arginine and lysine residues in  $\text{K}_{\text{ir}}1.1$  (overview). Note that most mutations had no or only minor effects on  $\text{pK}_{\text{app}}$ .

As listed in Fig. 29 B and Table 1, most of the K/R → Q mutations resulted in channels with pH-gating either identical to  $\text{K}_{\text{ir}}1.1$  wildtype or with a minor backshift in the respective  $\text{pK}_{\text{app}}$ . The latter mutations were located in regions close to the membrane, either N-terminal to M1 or C-terminal to M2.

**Table 1.**  $\text{pK}_{\text{app}}$  values of  $\text{K}_{\text{ir}}1.1$  mutants. Concentration-response curves were obtained from at least 4 pH titration experiments and evaluated as described in Fig. 28. For  $\text{K}_{\text{ir}}1.1(\text{R41Q})$  and  $\text{K}_{\text{ir}}1.1(\text{R311Q})$  no channel activity could be detected.

| channel mutant | $\text{pK}_{\text{app}}$ | channel mutant | $\text{pK}_{\text{app}}$ | channel mutant | $\text{pK}_{\text{app}}$ |
|----------------|--------------------------|----------------|--------------------------|----------------|--------------------------|
| wildtype       | 6.8                      | K181→Q         | 7.5                      | K206→Q         | 6.8                      |
| R39→Q          | 6.9                      | R184→Q         | 7.1                      | R212→Q         | 6.7                      |
| <b>R41→Q</b>   | -                        | K187→Q         | 6.7                      | R217→Q         | 7.2                      |
| R61→Q          | 6.8                      | R188→Q         | 7.4                      | K218→Q         | 7.1                      |
| R78→Q          | 7.9                      | R203→Q         | 6.8                      | <b>R311→Q</b>  | -                        |



### 2.3.2 $K_{ir}1.1(R41Q)$ and $K_{ir}1.1(R311Q)$ form permanently pH-inactivated channels

Neutralization of either positive charge at position 41 (R41Q) in the N-terminus or at position 311 in the C-terminus (R311Q) led to a complete loss of channel activity up to a  $pH_i$  of 10.0 (Fig. 30). The small currents at extremely high pH values most likely resulted from endogenous *Xenopus* ion channels since they were also detectable in patches from control oocytes (data not shown).

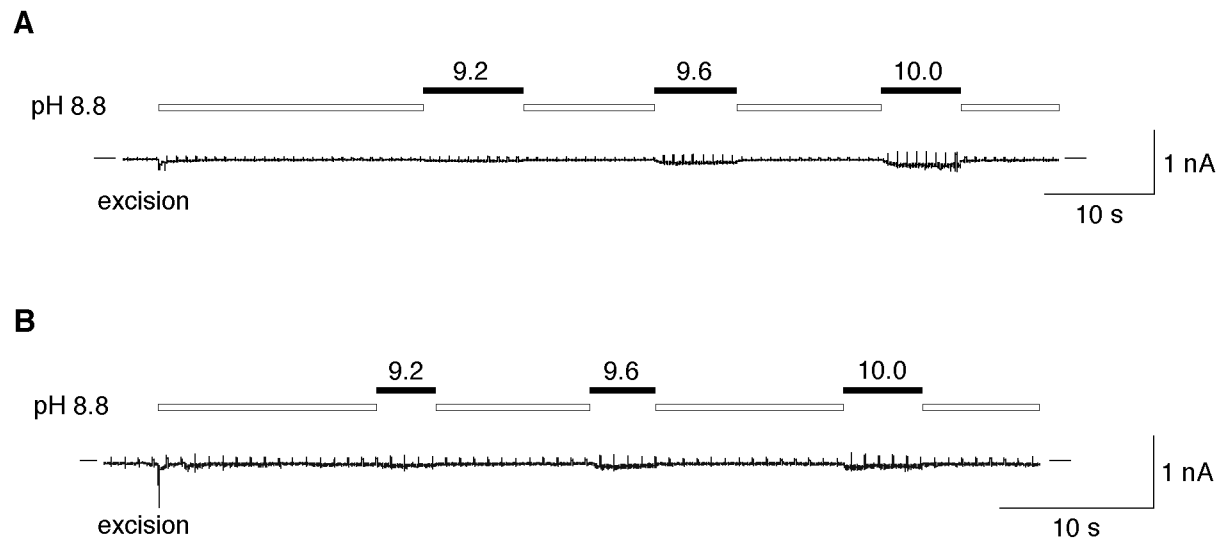


**Fig. 30.** Currents in excised inside-out patches from oocytes injected with (A)  $K_{ir}1.1(R41Q)$  cRNA or (B)  $K_{ir}1.1(R311Q)$  cRNA. Application of solutions ( $K_{int} + 0.1$  mM DTT) at alkaline pH as indicated by bars.

In order to verify that these mutants were actually translated and incorporated into the plasma membrane, they were tagged with a *flag* epitope (Wang et al., 1994) at their C-terminus and expressed in oocytes.

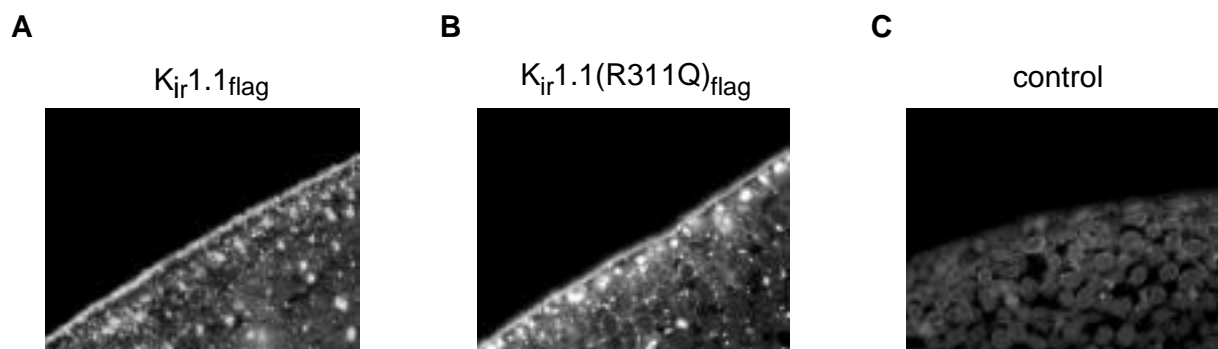


**Fig. 31.** Immunofluorescent staining of *Xenopus* oocytes injected with (A)  $K_{ir}1.1_{flag}$  cRNA or (B)  $K_{ir}1.1(R311Q)_{flag}$  cRNA; (C) a non-injected oocyte served as a negative control. Background fluorescence was negligible, whereas (A) and (B) showed strong fluorescence of the cell membrane and some intracellular vesicular structures. Slices (4  $\mu$ m) of fixed oocytes stained with anti-*flag* Cy3-labelled antibody were prepared as described in "Materials and Methods"; magnification approximately 200fold.

Immunostaining of slices from fixed oocytes with an anti-*flag* Cy3-labelled antibody showed that both mutants ( $K_{ir}1.1(R311Q)_{flag}$ ; data for  $K_{ir}1.1(R41Q)_{flag}$  not shown) were primarily localized in the plasma membrane (Fig. 31). Non-injected and  $K_{ir}1.1_{flag}$ -injected oocytes served as negative and positive controls, respectively.

If the loss of channel activity in these mutations was attributable to permanent pH-inactivation, an exchange of K80 in  $K_{ir}1.1(R311Q)$  or  $K_{ir}1.1(R41Q)$  by a non-titratable methionine would be expected to result in ‘recovery’ of channel function. Indeed, both  $K_{ir}1.1(R41Q,K80M)$  and  $K_{ir}1.1(K80M,R311Q)$  expressed functional channels which were insensitive to  $pH_i$  - very similar to  $K_{ir}1.1(K80M)$  (Fig. 32; compare to Fig. 25).

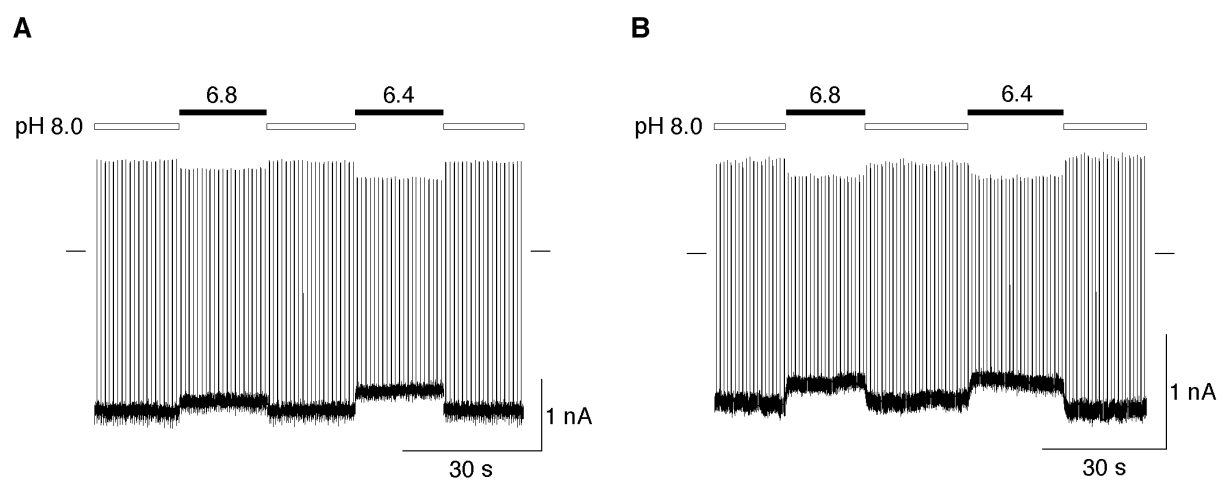


**Fig. 32.** pH sensitivity of (A)  $K_{ir}1.1(R41Q,K80M)$  and (B)  $K_{ir}1.1(R311Q,K80M)$  currents in excised inside-out patches. Experimental conditions like in the pH titration experiments before.

These results indicate that combined effects of arginines 41 and 311 are required to accomplish the anomalous titration of K80 in the  $K_{ir}1.1$  protein.

### 2.3.3 Titration of $K_{ir}4.1(R294Q)$ shows a $pK_{app}$ close to the standard pK of $NH_2$ -lysine

The experiments presented above suggested that neutralization of R41 and R311 resulted in closed channels due to permanent pH inactivation. However the possibility remained that these mutations affected the channel's gating machinery rather than shifting the  $pK_{app}$  of the  $pH_i$  sensor. Since this question could not be resolved with the  $K_{ir}1.1(R41Q)$  and  $K_{ir}1.1(R311Q)$  mutants, a homologous mutation was introduced in  $K_{ir}4.1$  ( $K_{ir}4.1(R294Q)$ ) and tested for channel activity at very alkaline pH.

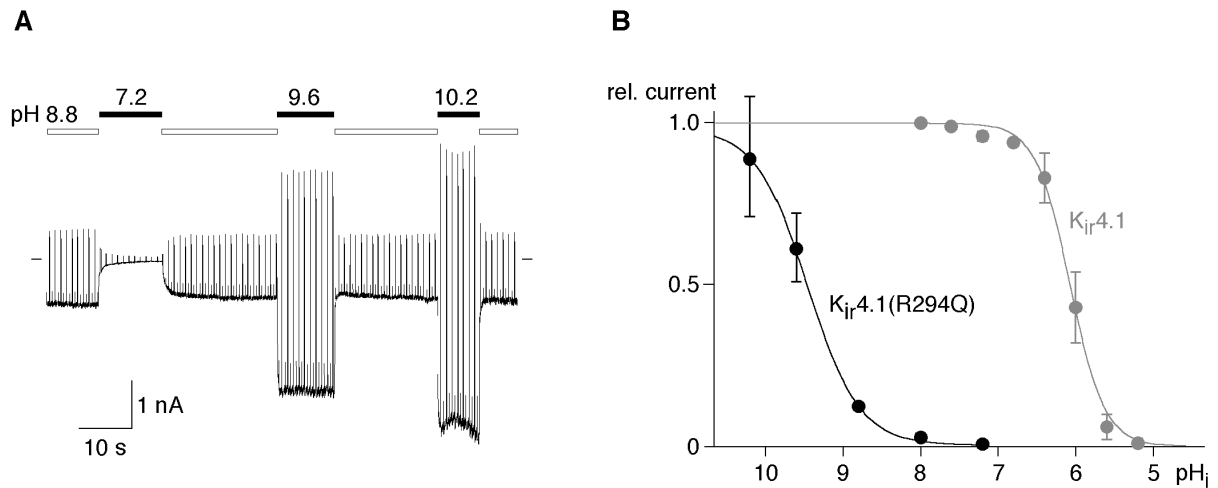


**Fig. 33.** (A) pH titration of  $K_{ir}4.1(R294Q)$  currents in excised inside-out patches at alkaline pH. Experimental conditions as in Fig. 19, scalings as indicated. (B) pH concentration-response curve for  $K_{ir}4.1(R294Q)$  as calculated from 5 experiments as in Fig. 33 A. Fit with a logistic function yielded  $pK_{app}=9.6$  (Hill coefficient=2.1) in comparison to  $pK_{app}=6.1$  (Hill coefficient=2.3) of  $K_{ir}4.1$  wildtype (grey curve, taken from Fig. 28).

As demonstrated in Fig. 33 A,  $K^+$  currents activated in excised inside-out patches and channels were still able to open and close at alkaline  $pH_i$ . Moreover, the resulting concentration-response curve (Fig. 33 B) showed that pH-gating was still positively cooperative, although it exhibited a  $pK_{app}$  (9.6) close to the standard value for lysine. These results indicate that neutralization of R41 or R311 specifically abolished the  $pK_{app}$ -shift of K80 but left the gating machinery intact.

#### 2.3.4 Evidence for electrostatic interaction of R41 and R311 with the sensor for $pH_i$

Changing arginines to glutamines could result in structural or electrostatic changes in the chemical environment of K80. Conservative substitutions by lysine ( $K_{ir}1.1(R41K)$ ,  $K_{ir}1.1(R311K)$  and  $K_{ir}1.1(R294K)$ ) were tested to elucidate the importance of positive charges at these sites. Fig. 34 shows that in  $K_{ir}1.1(R311K)$  channels pH-gating was shifted to more alkaline pH values by about 0.3 pH units, while in  $K_{ir}4.1$  the same mutation shifted pH-gating by 2 pH units. For  $K_{ir}1.1(R41K)$ , no channel activity could be observed up to a  $pH_i$  of 10.0. Thus, a positive charge at either determinant is not sufficient to explain the shift in  $pK_{app}$  observed for the gating-triggering lysine. Rather, they strongly suggest that lysine 80 and the two arginine residues are located in close proximity (an arrangement referred to as RKR triad (Schulte et al., 1999)), given that the mutagenesis effects illustrated in Fig. 34 were virtually caused by an exchange of a guanidino group versus an aminomethylene group.

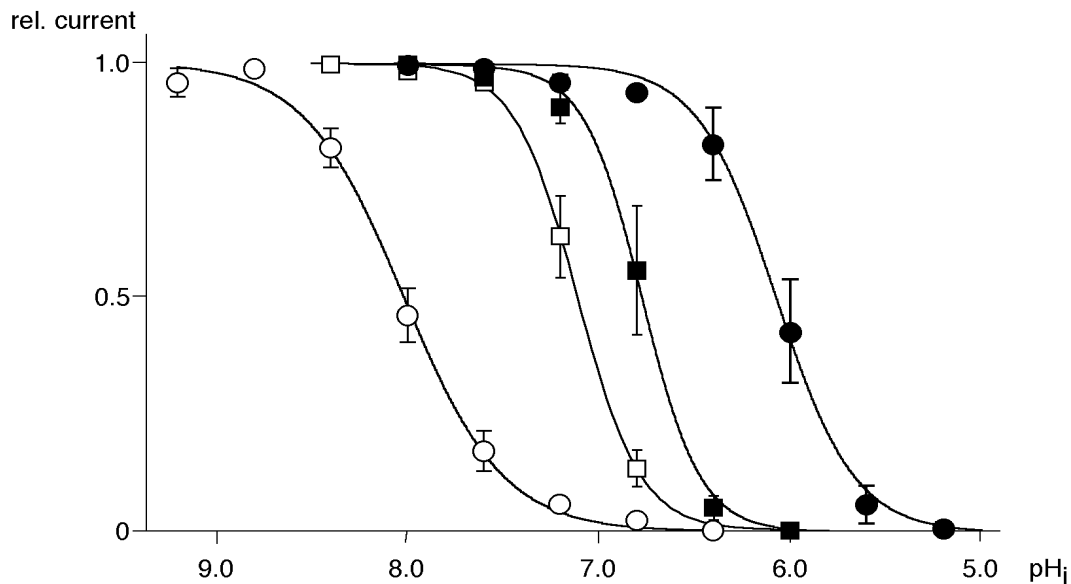


**Fig. 34.** pH concentration-response curves for  $K_{ir}1.1$ ,  $K_{ir}1.1(R311K)$ ,  $K_{ir}4.1$  and  $K_{ir}4.1(R294K)$  currents. pH titration experiments in excised inside-out patches were carried out as in Fig. 19. pH dose-responses were fitted with a logistic function to mean values of  $n$  experiments:  $pK_{app}=6.8$  and Hill coefficient=2.9 for  $K_{ir}1.1$  ( $n=11$ ; closed squares; taken from Fig. 20),  $pK_{app}=7.1$  and Hill coefficient=2.6 for  $K_{ir}1.1(R311K)$  ( $n=5$ ; open squares),  $pK_{app}=6.1$  and Hill coefficient=2.3 for  $K_{ir}4.1$  ( $n=6$ ; closed circles; taken from Fig. 28) and  $pK_{app}=8.0$  and Hill coefficient=1.7 for  $K_{ir}4.1(R294K)$  ( $n=5$ ; open circles).

### 2.3.5 The triad of K80, R41 and R311 is formed *within* an individual $K_{ir}$ subunit

The  $pH_i$ -sensing triad of K80, R41 and R311 could either be formed within a single  $K_{ir}1.1$  subunit or between N- and C-termini of different subunits. To resolve this question, the following coexpression strategy was used: cRNAs coding for a non-pH-gated (permanently open) subunit ( $K_{ir}1.1(K80M)$ ) and a non-functional (permanently pH-inactivated) subunit ( $K_{ir}1.1(R311Q)$  or  $K_{ir}1.1(R41Q)$  - not shown) were co-injected. The latter was additionally 'labelled' with a determinant for strong voltage-dependent pore block by the polyamine spermine (N171D; (Fakler et al., 1994b)). This method had been successfully used for the quantification of heteromultimeric channel populations (Glowatzki et al., 1995).

Four possible configurations could result from heterotetramer formation, two of which are depicted in Fig. 35. An intrasubunit interaction of R41, K80 and R311 would prevent the formation of functional triads. Consequently, all channel populations would be expected to be pH-insensitive, independent of the number of positive charges at K80 required to close the pore. Alternatively, if N- and C-terminal domains of neighbouring subunits interacted, neutralization of R311 in  $K_{ir}1.1(R311Q,N171D)$  would be compensated by R311 of  $K_{ir}1.1(K80M)$  to form a functional triad. In this case, at least one population should form, that is pH-gated and can be blocked by spermine (SPM) in a strongly voltage-dependent manner. For a detailed discussion of strategy and evaluation of the results see section 3.5.1.

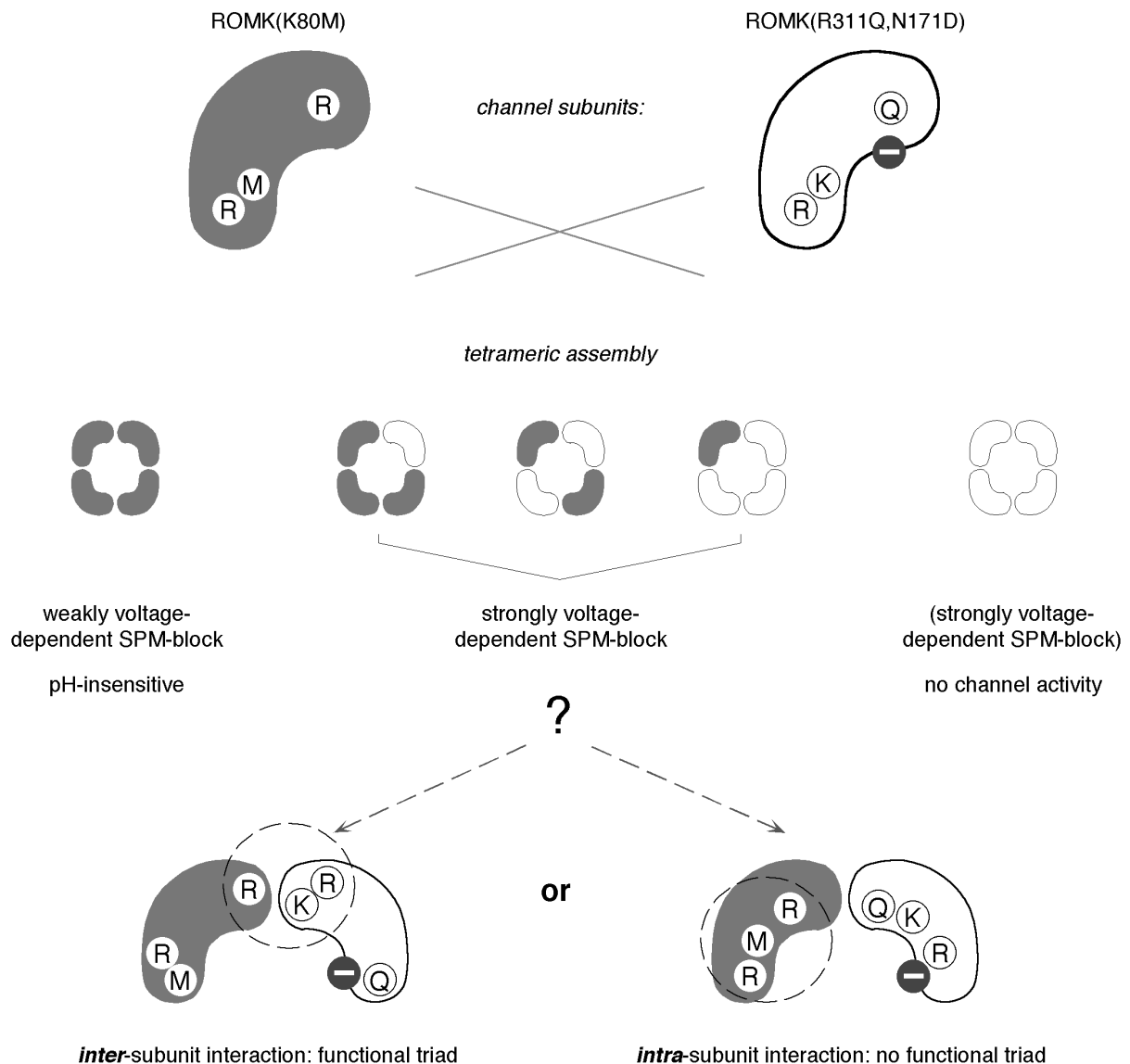


**Fig. 35.** Coexpression strategy to discriminate between *inter*- and *intrasubunit* RKR triad formation. In white:  $K_{ir}1.1(R311Q,N171D)$  subunits - permanently closed; in dark:  $K_{ir}1.1(K80M)$  subunits - permanently open. All heteromeric channels carry at least one negative charge in M2 and are therefore expected to be blocked by spermine with high voltage-dependence. Functional RKR triads only form upon intersubunit interactions. The sensitivity to  $pH_i$  of heteromeric channels could not be predicted.

Figs. 36 and 37 summarize the results of a series of coexpression experiments where a fixed amount of  $K_{ir}1.1(K80M)$  cRNA had been injected together with variable quantities of  $K_{ir}1.1(N171D,R311Q)$  cRNA in the ratios indicated. With increasing amounts of  $K_{ir}1.1(N171D,R311Q)$  cRNA, average current amplitudes decreased from about 12 nA to less than 300 pA per patch. No suppression of  $K_{ir}1.1(K80M)$  current was seen after co-injection of a control cRNA (coding for a non-functional channel) at a ratio of 1:10 (data not shown). Although the decrease did not reflect a binominal assembly, at least one non-functional heteromultimeric channel population must have formed. Similar results were obtained from coexpression experiments with  $K_{ir}1.1(K80M)$  and  $K_{ir}1.1(R41Q)$  (data not shown).

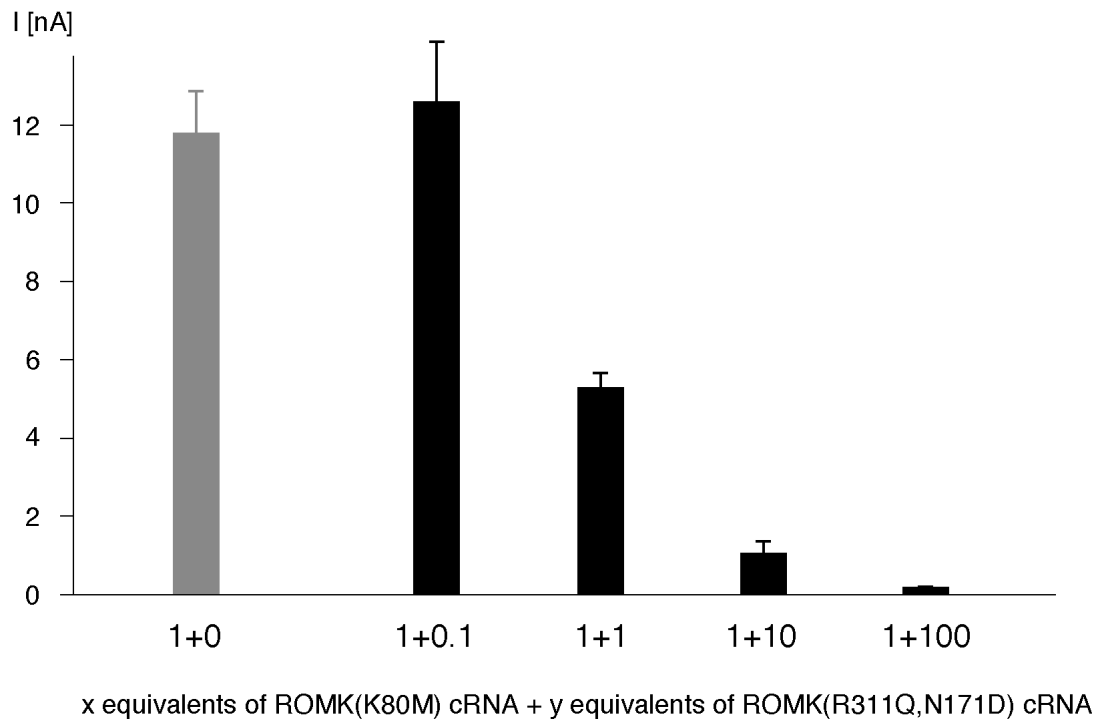


**Fig. 36.** Quantitative analysis of current amplitudes (at -80 mV,  $pH_i=8.0$ ) in excised inside-out patches resulting from coexpression of  $K_{ir}1.1(K80M)$  and  $K_{ir}1.1(R311Q,N171D)$  at the cRNA ratios indicated. Mean values of at least 3 oocytes (12 patches each) are presented.

The resulting currents were further analyzed for pH sensitivity and voltage-dependence of block by intracellular spermine.

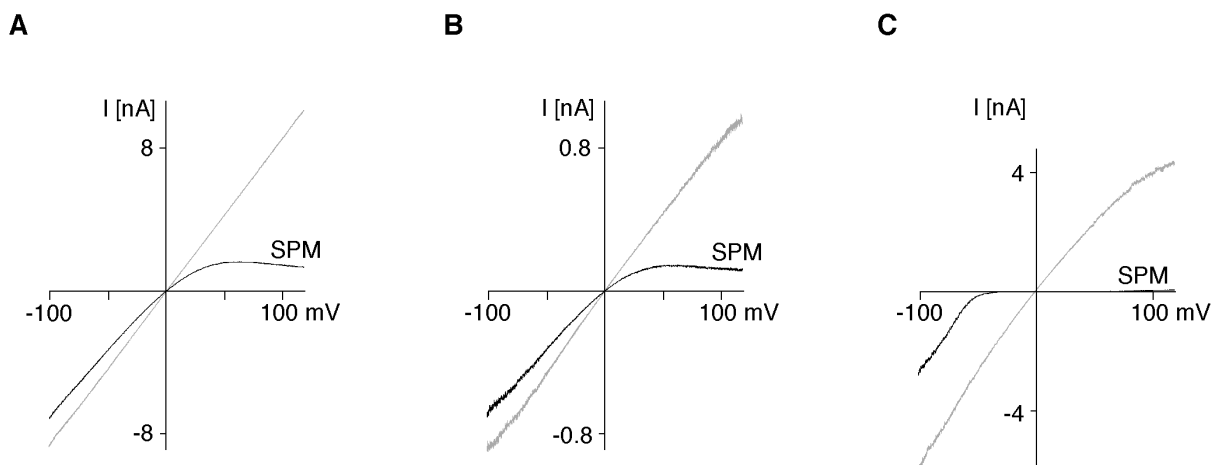


**Fig. 37.** Currents in response to voltage-ramps (-100 to +120 mV) measured in excised inside-out patches. In grey:  $K_{int}$  pH 8.0 - no inward-rectification; in black:  $K_{int}$  pH 8.0 + 1 mM SPM mediating voltage-dependent inward-rectification. (A)  $K_{ir}1.1(K80M)$  currents, (B) currents resulting from coexpression of  $K_{ir}1.1(K80M)$  and  $K_{ir}1.1(R311Q,N171D)$  cRNAs at a ratio of 1:10, (C)  $K_{ir}1.1(K80M,R311Q,N171D)$  currents as a positive control. Note the different current scales in (A) and (B).

Voltage-dependence of block was quantified by converting the current-voltage-recordings into conductance-voltage-plots and fitting them with Boltzmann functions as described in "Materials and Methods". Weakly voltage-dependent rectification mediated by 1 mM SPM could be seen with  $K_{ir}1.1(K80M)$  in accordance with published results (Glowatzki et al., 1995). However, currents from all coinjection ratios displayed the same weak voltage dependence as  $K_{ir}1.1(K80M)$  (shown for the example of the 1:10 cRNA ratio). The triple mutant  $K_{ir}1.1(K80M,N171D,R311Q)$  harbouring a negatively charged aspartate in M2 was blocked with high voltage-dependence (onset of block was already visible at voltages negative from  $E_{K^+}$ ) as expected and served as a positive control. Currents from all coexpressions displayed the same insensitivity to  $pH_i$  as  $K_{ir}1.1(K80M)$  currents in the range of pH 6.8-9.6. This was tested in excised inside-out patches (n=12 each) as described in Fig. 33 A (data not shown).

These findings indicate that all currents resulted from  $K_{ir}1.1(K80M)$  homotetramers and that all heteromultimeric channels formed were non-functional. This can only be explained by an intrasubunit assembly of the triad, as discussed in detail in section 3.1.5. In that case, any  $K_{ir}1.1(N171D,R311Q)$  subunit would carry a permanent positive charge which could lead to channel closure. For the case of an intersubunit interaction, one or two functional triads would have formed, so the resulting channels should have been sensitive to acidic  $pH_i$ .

In summary, K80 together with R41 and R311 forms a triad within individual  $K_{ir}$  subunits. As a consequence of this structural arrangement protons are repelled from the  $NH_2$ -group of K80 resulting in anomalous titration of this residue within the  $K_{ir}1.1$  protein.

## 2.4 Defective pH-gating as a molecular mechanism for the pathogenesis of aBS

Disruption of the RKR triad by the R41Q and R311Q mutations in  $K_{ir}1.1$  resulted in channel proteins that were incorporated into the plasma membrane, but were non-functional under physiological conditions (Fig. 30). Since such alterations in pH-gating might well explain impaired  $K_{ir}1.1$  channel function under physiological conditions, the effect of known mutations associated with aBS on pH-gating was investigated. It is noteworthy that most of these mutations are clustered around the RKR triad or in domains close to it when considered in the context of the tertiary folding for  $K_{ir}$  proteins deduced from the results above (Fig. 38).

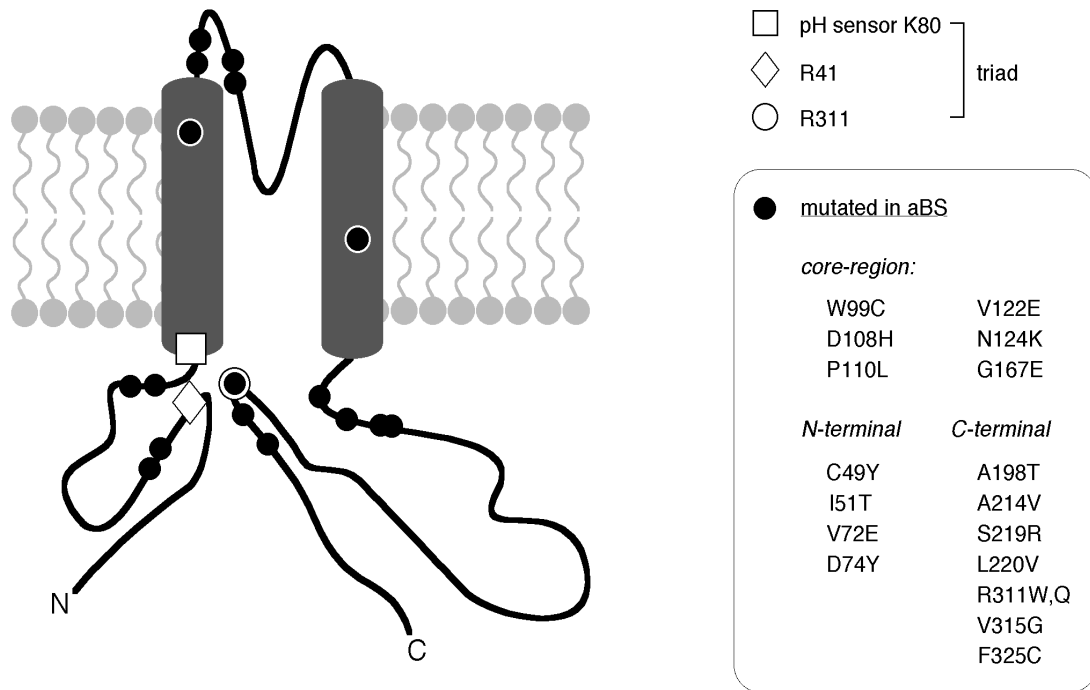


**Fig. 38.** Localization of known aBS mutations in a structural model of  $K_{ir}1.1$ . Determinants of the RKR triad (open symbols) are in close spatial proximity. Point mutations as taken from the literature: V72E, D74Y, W99C, D108H, P110L, V122E, G167E, A198T and V315G (Karolyi et al., 1997), N174K (Derst et al., 1998), A214V, S219R (Simon et al., 1996c); C49Y, I51T, L220V, R311W, R311Q and F325C (Schulte et al., 1999); see also "Materials and Methods" section 4.2.4.

Mutations in the intracellular N- and C-termini were expected to disturb the structural arrangement of the RKR triad, and in turn shift the pH-gating off the neutral range. This hypothesis was tested by heterologous expression of individual aBS mutant  $K_{ir}1.1$  channels in *Xenopus* oocytes. Indeed, the majority of these mutations led to shifts in pH-gating towards more alkaline pH values (Fig. 39). The backshifts ranged from 0.3 pH units to > 2 pH units, with the largest shifts observed for mutations of the triad residues themselves (for example  $K_{ir}1.1(R311W)$ ).  $K_{ir}1.1(R311Q)$  did not express functional channels (Fig. 30). The ability of the channels to open and close was not affected in either of the aBS mutations investigated, nor was the cooperativity of the gating process altered significantly (Fig. 39).

It should be emphasized that a shift in pH-gating of as small as 0.3 pH units was able to induce severe clinical symptoms. For example, one patient (see "Materials and Methods" section 4.2.4) combined mutations L220F (  $pH_{0.5}$ : 0.3) with R311W (  $pH_{0.5}$ : 2.2) and another one harbored mutations I51T (  $pH_{0.5}$ : 0.5) and C49Y (  $pH_{0.5}$ : 0.7). In both cases, none of the parents (heterozygous carriers of a mutated allele) had shown symptoms of aBS.



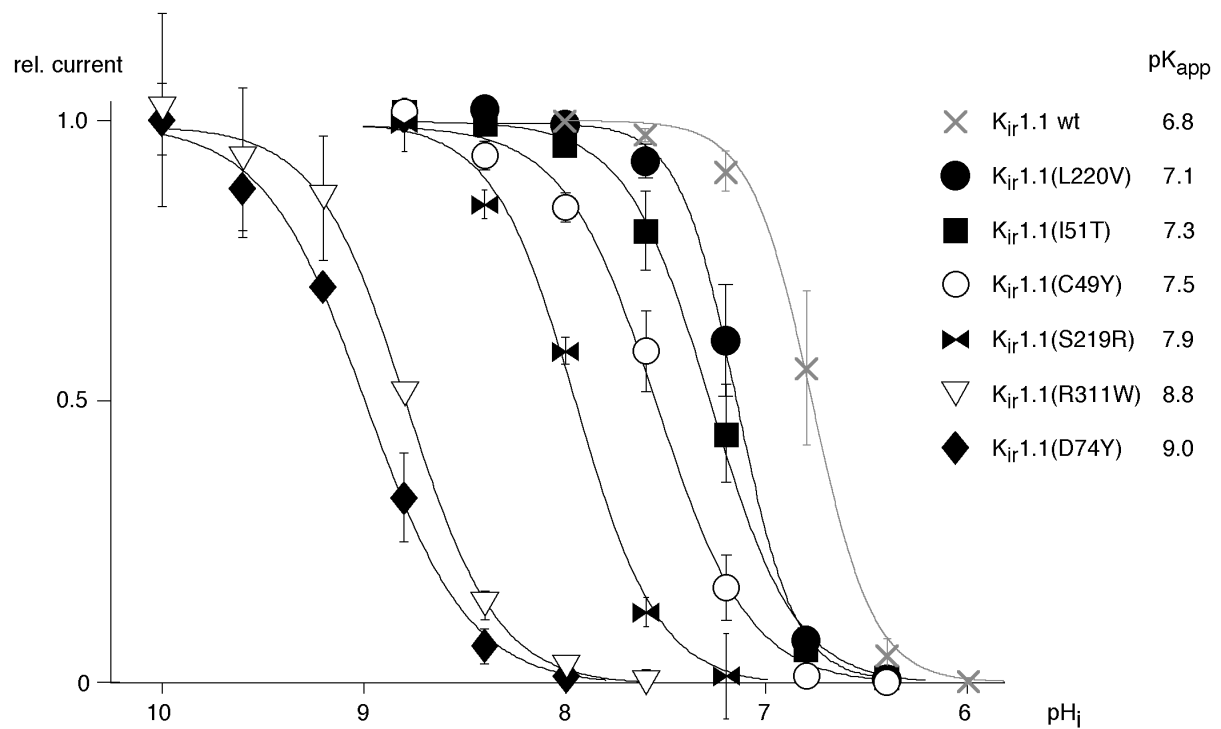


**Fig. 39.** pH concentration-response curves for currents of  $K_{ir}1.1$  mutants identified in patients with aBS. pH titration experiments, data evaluation and fitting with a logistic function as described before (e.g., in Fig. 23). Note the wide range of backshifts in  $pK$  ( $pK_{app} = 0.3$  to  $2.2$  pH units).

Taken together, these results suggest that structural disturbance of the RKR triad in  $K_{ir}1.1$  leading to defective pH-gating is a major molecular cause for the pathogenesis of aBS.

## 3 Discussion

### 3.1 pH-gating of $K_{ir}$ channels

#### 3.1.1 Comparison of whole cell and patch experiments with physiological data

$K_{ir1.1}$  channels display a high sensitivity to intracellular protons with acidification ( $pH_i$  6.0) leading to complete channel closure. Since the single channel conductance was not affected by  $pH_i$  in the range of 6.0 - 8.0, the pH dose-response curves determined for macroscopic currents quantitatively reflected the dependence of 'channel open probability' on  $pH_i$ , referred to as pH-gating. Experiments with giant inside-out patches yielded titration curves with an apparent pK value of 6.8 and a Hill coefficient of 3.1 for  $K_{ir1.1}$  (Fig. 20). The values for  $K_{ir1.1a}$  were not significantly different from those for the splice variant  $K_{ir1.1b}$  as confirmed by several groups (Fakler et al., 1996b; Choe et al., 1997; McNicholas et al., 1998). The  $pK_{app}$  values showed very little variation ( $\approx 0.1$  pH units) when experiments were repeated with different batches of oocytes (5 series of titration experiments). The Hill coefficient ranged from 2.7 to 3.5 which may in part result from irreversible components of pH-induced channel inactivation. Therefore, only experiments showing more than 90% reversibility were considered for final evaluation. In these cases, the current inactivation time courses could be well fitted with a monoexponential function to determine steady-state inhibition (as described in section 4.5.4).

$pH_i$ -induced inactivation measured in whole oocytes was completely reversible in 90 mM  $K^+$  extracellular solution (Fakler et al., 1996b). More than 90%  $K_{ir1.1}$  current inhibition was observed at  $pH_i = 6.6$ , which was monitored with a pH-sensitive microelectrode (as described in section 4.4.2). This value is higher than the 80% inhibition expected from the concentration-response curve at the same  $pH_i$ . It has to be considered, however, that the sensor for  $pH_i$  (lysine 80) is located at the intracellular surface of the plasma membrane and that the microelectrode can not sense the actual pH at that site. pH sensitivity of cloned  $K_{ir1.1}$  has also been measured by others (Tsai et al., 1995; Choe et al., 1997; McNicholas et al., 1998) with very similar results. Thus, pH-gating is an intrinsic property of  $K_{ir1.1}$  channels and is independent from intracellular factors.

$K^+$  secretion channels in the apical membrane of tubular kidney cells have been shown to be particularly sensitive to intracellular acidification. In excised patches from rat principal cells (Wang et al., 1990), 'channel open probability' decreased from 0.96 at  $pH_i$  7.4 to 0.15 at

pH<sub>i</sub> 7.0. In another study with inside-out patches from opossum kidney cells, K<sub>ir</sub> currents displayed a pH<sub>i</sub>-concentration-response with a pK<sub>app</sub> of 7.5 (Ohno-Shosaku et al., 1990). These pK<sub>app</sub> values are somewhat higher than those reported for cloned K<sub>ir</sub>1.1 channels, but the significance of these differences remains unclear.

So far, gating properties of K<sub>ir</sub>4.1 channels have been poorly described in the literature. This study probably delivers a first quantitative description of gating by pH<sub>i</sub> for this inward-rectifier K<sup>+</sup> channel. K<sub>ir</sub>4.1 is expressed in a variety of tissues including skeletal muscle cells (Bond et al., 1994), for which a pH<sub>i</sub>-sensitive inwardly rectifying K<sup>+</sup> current has been described (pK<sub>app</sub> = 6.1, Hill coefficient = 3; (Blatz, 1984)). These results are in good agreement with the findings for cloned K<sub>ir</sub>4.1 channels in the present study (pK<sub>app</sub> = 6.1 and Hill coefficient = 2.3).

### 3.1.2 The role of K80 as a determinant for pH-gating

The results presented here establish that pH-gating of K<sub>ir</sub>1.1 channels is determined by protonation of lysine 80. Replacement of this residue by a neutral amino acid (for example in K<sub>ir</sub>1.1(K80M) or K<sub>ir</sub>1.1(K80T)) resulted in channels which were no longer gated by pH<sub>i</sub>. Moreover, pH<sub>i</sub>-sensitivity could be conferred on other members of the inward-rectifier family by changing the amino acid at the site homologous to lysine 80 (referred to as pre-M1 site). This was shown for K<sub>ir</sub>2.1 and K<sub>ir</sub>6.2 which are pH-insensitive. Of all K<sub>ir</sub> subunits known to date, only members of the subfamilies 1 and 4 carry a lysine at this position. This correlates well with the pH sensitivity of these channels as described in sections 2.1.1 and 2.1.2. A minor pH<sub>i</sub>-effect with negative cooperativity was found in some pH-insensitive K<sub>ir</sub> channels like K<sub>ir</sub>2.1 or K<sub>ir</sub>1.1(K80M). The nature of this effect most likely is a pore block by protons, which are present in micromolar concentrations at pH<sub>i</sub> values < 6.0. These less pronounced effects of pH<sub>i</sub> coincide with the presence of non-titratable amino acids at the homologous positions: asparagine (in K<sub>ir</sub>3.1, K<sub>ir</sub>3.2 and K<sub>ir</sub>3.4), threonine (in K<sub>ir</sub>6), arginine (in K<sub>ir</sub>3.3) and methionine (in K<sub>ir</sub>2, K<sub>ir</sub>5.1 and K<sub>ir</sub>7.1).

The role of lysine 80 as a pH<sub>i</sub> sensor could be verified in a number of further experiments. Since protonation at this site induced channel closure (Figs. 7, 26), introduction of a "permanent" positive charge would be expected to result in closed channels. Indeed, when K80 in K<sub>ir</sub>1.1 was replaced by arginine (K<sub>ir</sub>1.1(K80R)), only minimal currents could be detected (<2 μA at -100 mV and 90 mM extracellular K<sup>+</sup> in whole oocytes; data not shown). Correspondingly, K<sub>ir</sub>2.1(M84R) did not express functional channels, but K<sub>ir</sub>2.1(M84K) and K<sub>ir</sub>2.1(M84H) exhibited pH-gating in the neutral and acidic range, respectively (Fakler et al., 1996b). Replacement of this methionine 84 by any non-basic amino acid yielded functional K<sub>ir</sub>2.1 channels which were insensitive to pH<sub>i</sub>. Finally, the mutagenesis results were confirmed

by lysine modification experiments. FmocCl is known to selectively react with unprotonated amino groups and is therefore widely used in solid phase peptide synthesis as a protective group (Carpino and Han, 1970).  $\alpha$ -Amino-groups of lysine are effectively modified only if pH is kept above pH 9 (Henczi and Weaver, 1994). After FmocCl (0.1 mM) had been applied to excised inside-out patches for 30 s at pH 7.5,  $K_{ir}1.1$  channels (which remained fully active under these conditions) were found to be insensitive against intracellular acidification (Fig. 26). The remaining partial reduction in current amplitude was probably due to incomplete modification which is not surprising as modification of lysine 80 in all four  $K_{ir}1.1$  subunits is expected to be necessary to abolish pH-gating (see sections 3.1.4 and 3.1.5). In summary, protonation of lysine 80 is both required and sufficient to induce pH-inactivation in  $K_{ir}$  channels tested.

### 3.1.3 Mechanisms for shifts in $pK_{app}$ as found for titratable residues within proteins

The finding that a lysine residue is titratable in the neutral pH range implies a shift in  $pK_{app}$  by more than 3 pH units ( $pK_{app} = -4.4$  for  $K_{ir}4.1$ ) compared to the standard value of 10.5 for  $NH_2$ -lysine. In general,  $pK_{app}$ -shifts of titratable groups are thought to occur when amino acid side chains are placed in particular chemical environments within a protein, such as hydrophobic pockets, interact with other charges, or form hydrogen bonds. In this context, a decrease in  $pK_i$  by almost 4 pH units was assumed for either one or both of two lysine residues interacting via hydrogen bonds in ovotransferrin (Dewan et al., 1993), and an increase by about 3 pH units was reported for a histidine residue embedded in a highly positively charged environment within the FK506 binding protein (Yu and Fesik, 1994).

In  $K_{ir}$  proteins, the side chain of the amino acid at the pre-M1 site should be readily accessible from the cytoplasm, since lysine 80 in  $K_{ir}1.1$  channels binds intracellular protons and cysteine 84 in  $K_{ir}2.1$ (M84C) channels could be chemically modified by MTSEA (Akabas et al., 1992; Fakler et al., 1996b). Therefore, hydrophobic shielding of lysine 80 appears to be rather unlikely. Instead, the mutagenesis experiments performed in this study strongly suggest, that this lysine residue is embedded in a positively charged environment formed by arginines 41 and 311. These arginines are assumed to be permanently charged under physiological conditions, since their guanidino-groups have a standard  $pK_a$  value of 12.5 (Dawson et al., 1986). Conservative mutations (R  $\rightarrow$  K) introduced at positions 41 and 311 in  $K_{ir}1.1$  and at position 294 in  $K_{ir}4.1$  had very different effects.  $K_{ir}1.1$ (R311K) channels displayed only a small backshift in  $pK_{app}$  (-0.3 pH units), but the homologous mutation in  $K_{ir}4.1$  ( $K_{ir}4.1$ (R294K)) had a more dramatic effect, as the apparent pK was shifted back by about 2 pH units. And for  $K_{ir}1.1$ (R41K) no functional expression was found up to a  $pH_i$  of 10 (data not shown). This indicated that not only the charge of these side chains is critical for the protonation behaviour of

K80 but also their location relative to the  $\text{NH}_2$ -group of lysine 80. Based on these results, it is concluded that K80, R41 and R311 are located in close proximity - an arrangement referred to as RKR triad (Schulte et al., 1999) - where the positively charged arginines establish a local field repelling protons from the lysine amino group. This field does not interfere with the transmembrane electrical field, since pH-gating was not voltage-dependent. Another position in the primary sequence was identified, from which charges exerted an electrostatic effect on pH-gating. Introduction of a lysine or glutamate at position 51 in  $\text{K}_{\text{ir}}1.1\text{b}$  (equivalent to residue 70 in  $\text{K}_{\text{ir}}1.1\text{a}$ ) shifted pH-gating by about 0.5 pH units to more acidic or alkaline  $\text{pK}_{\text{app}}$  values, respectively (Choe et al., 1997). Alternatively to electrostatic interactions, the arginine and lysine residues in the RKR triad might form hydrogen bonds similar to what has been reported for two lysines and a tyrosine residue in ovotransferrin (Dewan et al., 1993).

### 3.1.4 Positive cooperativity and stoichiometry of pH-gating

The mutagenesis results suggest a common molecular basis of pH-gating for all  $\text{K}_{\text{ir}}$  channels as further discussed in section 3.2. Key characteristics of pH-gating are a Hill coefficient  $> 2$  indicating positive cooperativity and pH-dependent inactivation kinetics pointing to a complex gating reaction.

In general, positive cooperativity serves to increase the sensitivity of a stimulus-response coupled system within a narrow range of stimulus intensity. For  $\text{K}_{\text{ir}}1.1$  the Hill coefficient was determined to be close to 3. Although this coefficient does not necessarily reflect positive cooperativity in the sense of conformational changes of proteins (Forsen and Linse, 1995), there are several lines of evidence that in the case of pH-gating of  $\text{K}_{\text{ir}}$  channels, the Hill coefficient indeed arises from cooperative interaction of the four subunits. Firstly, when pH-gated  $\text{K}_{\text{ir}}1.1$  and non-gated  $\text{K}_{\text{ir}}1.1(\text{K80M})$  subunits were coexpressed, the measured  $\text{pH}_i$  dose-response curves displayed a lower Hill coefficient (around 1.5) without a significant shift in  $\text{pK}_{\text{app}}$  (data not shown). Secondly, one of the  $\text{K}_{\text{ir}}1.1$  mutants where a conserved lysine residue had been replaced by glutamine ( $\text{K}_{\text{ir}}1.1(\text{K181Q})$ ; see Fig. 29) was pH-gated with a  $\text{pK}_{\text{app}}$  of 7.4 and a Hill coefficient close to 1. The inactivation kinetics of this mutant were very fast and independent of  $\text{pH}_i$ . It is tempting to speculate that in this mutant conformational transitions of individual subunit gates were uncoupled. This could explain the accelerated inactivation kinetics and may also account for the observed increase in  $\text{pK}_{\text{app}}$ . If this was indeed the case, it would imply that a single subunit gate in a closed conformation was sufficient to occlude the pore. Coexpression experiments with non-pH-gated  $\text{K}_{\text{ir}}1.1(\text{K80M})$  and permanently pH-inactivated  $\text{K}_{\text{ir}}1.1(\text{R311Q},\text{N171D})$  subunits confirmed this "one gate" hypothesis. Firstly,  $\text{K}_{\text{ir}}1.1(\text{R311Q},\text{N171D})$  cRNA had an inhibitory effect on the expression of functional  $\text{K}_{\text{ir}}1.1$  channels (Fig. 36), which means that inactive heterotetramers must have formed. Secondly,

since no channel populations with a strongly voltage-dependent block by spermine were detectable, all heterotetramers formed must have been inactive (Fig. 36).

How do these results match with established concepts explaining cooperativity in multimeric proteins? According to the sequential model proposed by Koshland et al. (1966), all subunits would be in an active (open) conformation in the absence of ligands. Binding of  $H^+$  induced an inactive (closed) conformation of the respective subunit and increased the  $H^+$ -affinity of associated subunits. The "one gate hypothesis", however, is conflicting with the sequential model. Opening and closing (but not the protonation) of  $K_{ir}1.1$  channels could be monitored electrophysiologically as an "all or none" transition - subconductance states were only rarely detectable in single channel experiments (compare the results of Choe et al. (1997) with those of Wang et al. (1990)). Since protonation of the first subunit can not be cooperative but would already close the channel, the resulting titration curve would be strongly distorted (not following a logistic function).

Alternatively, a model has been established in which only symmetrical transitions of subunit conformations are allowed to occur (Monod et al., 1965). The open conformation does not bind the ligand but participates in an equilibrium with a closed conformation in which the single subunits independently bind ligands. Such an "all or none" transition could explain some of the characteristics of pH-gating but this model also causes problems. With respect to the "one gate hypothesis" one could argue, that a permanently inactivated subunit couples to the conformations of other subunits in a way that forces the whole tetramer into a closed conformation. This would still be compatible with the finding that cooperativity is lost in  $K_{ir}1.1(K181Q)$ , where conformations of subunits may not be strongly coupled any more. Moreover, this model would explain why assembly of permanently pH-inactivated and pH-insensitive channels (as tested for  $K_{ir}1.1(K80M)$  coexpressed with  $K_{ir}1.1(R311Q,N171D)$  or  $K_{ir}1.1(R41Q)$ ; see section 2.3.5) did not follow a binominal distribution. Assembly of subunits in closed and open conformations into  $K_{ir}$  channels would be energetically unfavourable. That would not be a problem in the sequential model. However, the symmetry model must also meet the kinetic aspects of pH-induced inactivation. If only subunits in the closed state bind intracellular protons, then the spontaneous transition open  $\rightarrow$  closed should become rate-limiting at low  $pH_i$ . In fast application experiments, which allow exchange of intracellular solutions at giant inside-out patches within a few milliseconds, the time constant of current inactivation did not saturate at low  $pH_i$  ( $\tau_{inact} = 580$  ms at  $pH_i$  6.0 and  $246$  ms at  $pH_i$  5.0; B. Fakler, personal communication). A time constant lower than 200 ms for a symmetrical transition would be compatible with the finding that renal  $K^+$  secretion channels display one open state with a mean lifetime of 18.6 ms and one closed state with a mean lifetime of 0.7 ms at  $pH_i$  7.4 (Wang et al., 1990).

Apart from these considerations it should be kept in mind, that both theories on cooperativity had been developed for the case of multimeric proteins in which each subunit represents a functional unit. This is definitely not the case for  $K_{ir}$  channels, in which all *four* subunits are required for formation of *one* functional channel. Therefore, more detailed experiments combined with a different theoretical concept may be required to explain cooperativity of ion channel gating.

### 3.1.5 *Intra-* versus *inter-*subunit interaction

The identification of conserved arginines 41 and 311 closely interacting with lysine 80 in  $K_{ir}1.1$  channels raised the question, how this arrangement is formed in the quarternary structure. Theoretically, there may be four possibilities to form an RKR triad, involving one, two or three subunits: (a) all residues within a single subunit interact, (b) K80 and R41 from subunit I interact with R311 from an adjacent subunit II, (c) K80 and R311 from subunit I interact with R41 from an adjacent subunit II, and (d) K80 from subunit I interacts with R41 from an adjacent subunit II and R311 from another adjacent subunit III. A strategy was designed to address this problem consisting of two series of coexpressions: non-pH-gated  $K_{ir}1.1(K80M)$  together with permanently pH-inactivated (i)  $K_{ir}1.1(R311Q)$  or (ii)  $K_{ir}1.1(R41Q)$ . As already discussed in section 3.1.4, only currents indistinguishable from  $K_{ir}1.1(K80M)$  could be detected in these coexpression experiments indicating that all heterotetramers formed were non-functional in the  $pH_i$  range of 6.4 to 9.6. This means that at least one subunit in the heterotetramers must be permanently pH-inactivated. Only assembly (a) full-fills this condition for both coexpression series. In the case of (i), R311Q would be compensated by the corresponding R311 of  $K_{ir}1.1(K80M)$  yielding a functional triad (not permanently pH-inactivated; see Fig. 35) according to the assembly models (c) or (d). Correspondingly, R41Q (ii) would be compensated by R41 of  $K_{ir}1.1(K80M)$  as a result of an assembly like in (b) or (d). Thus, K80, R41 and R311 form triads underlying pH-gating in the physiological range *within* individual  $K_{ir}$  subunits. This may have important consequences for possible compensation of mutations affecting pH-gating and for the understanding of subunit assembly.

Nevertheless it is expected that also N- and C-termini of *adjacent* subunits interact with each other. Several approaches have been taken to identify the sites responsible for subunit assembly into functional  $K_{ir}$  tetramers (Tinker et al., 1996; Woodward et al., 1997). In addition, open and closed subunit conformations must somehow interact to explain the positive cooperativity observed for pH-gating.

### 3.1.6 A model for pH-gating of $K_{ir}1.1$ channels

Altogether, at least one open and two closed conformational states of  $K_{ir}1.1$  have been characterized in this study. In  $Mg^{2+}$ -free alkaline (pH 8.0) solution  $K^+$  currents remained constant reflecting a stable open conformation of the  $K_{ir}1.1$  protein. Protonation induced a conformational change that led to channel closure (Fig. 6). This reaction was very slow, and the rate of inactivation was strongly dependent on  $pH_i$  (see Fig. 19) as already discussed in section 3.1.4. But protonation-deprotonation reactions are the fastest diffusion-controlled reactions known in solutions, their rate constants ranging below 10 ns. Thus the kinetic behaviour could not be explained by a simple one-step reaction. It rather pointed towards a reaction sequence involving multiple conformational transitions. In fact, there must be at least two closed states as revealed by patch clamp experiments on the interaction of  $K^+$  regulation and  $pH_i$ -gating of  $K_{ir}1.1$  (see section 2.1.2). When channels were inactivated by application of pH 6.0 for a few seconds, a significant fraction recovered instantaneously in the absence of extracellular  $K^+$  (Fig. 9 A). Thus a closed state must exist with  $K^+$  still bound to an extracellular part of the pore. Recovery from pH-induced inactivation failed with increased periods of inactivation. From such experiments, the time constant for  $K^+$  dissociation from pH-inactivated  $K_{ir}1.1$  channels could be estimated to be somewhat less than 10 s. It seems unlikely, however, that dissociation of  $K^+$  is responsible for the slow inactivation kinetics, since pH-gating of  $K^+$ -independent  $K_{ir}1.1(K_{ir}2.1p)$  channels displayed very similar pH-dependent inactivation kinetics (with a  $pK_{app}$  of 6.6) as  $K_{ir}1.1$  wildtype (data not shown). A preliminary reaction sequence is proposed on the basis of these results, which could deliver an alternative explanation for the positive cooperativity of pH-gating (compared with the sequential or the symmetric model discussed in section 3.1.4):

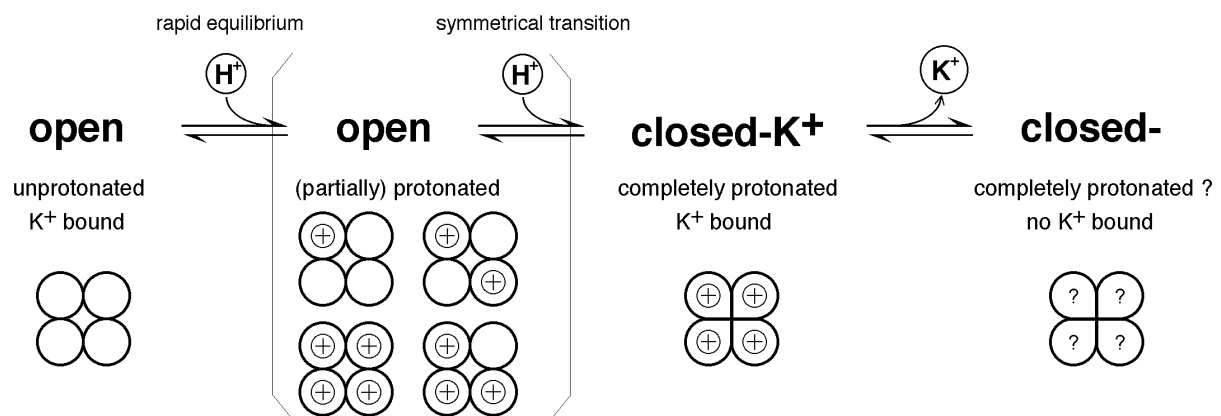


**Fig. 40.** Kinetic model of pH-gating of  $K_{ir}1.1$  channels. In brackets: hypothetical channel states. Protonation is indicated by "H". Note that only the second transition (open  $\rightarrow$  closed) can be monitored directly. The protonation state of the  $K^+$ -depleted closed state could not be determined.



The majority of open channels is unprotonated but participates in a rapid protonation-deprotonation equilibrium. Partially protonated channels would still be open for a short period of time before they are either deprotonated or undergo a symmetrical conformational change into a closed state. Positive charges at K80 in the open conformation are energetically unfavourable. Therefore, an increase in the number of positive charges would accelerate the transition into a closed state. The closed state must have a higher affinity for protons, since protonation of K80 is the source of energy for the gating reaction. Because of that, the closed state is believed to be highly protonated (indicated above by 4 positive charges). This would explain both the positive cooperativity and the pH-dependent inactivation kinetics of pH-gating. Evidently this reaction sequence combines aspects of both allosteric models discussed in chapter 3.1.4.

In its closed conformation,  $K_{ir}1.1$  has a lower affinity for  $K^+$  bound to an extracellular domain. As demonstrated in giant-inside-out patch experiments (see Figs. 9 and 10) this may be due to an increased off-rate for  $K^+$  binding. The closed,  $K^+$ -depleted channel can only be reopened if  $K^+$  is present extracellularly and the cytosol is alkalinized subsequently. Structural aspects of these transitions are discussed further in section 3.2.1.

## 3.2 Structural implications for gating of $K_{ir}$ channels

### 3.2.1 Conformational changes in $K_{ir}1.1$ induced by protonation

$K_{ir}$  channels are presently conceived as ion-selective pores mainly controlled by intracellular blocking cations such as polyamines,  $Mg^{2+}$  or protons, but not undergoing significant conformational changes. In the present study two interdependent regulatory mechanisms are analyzed which imply conformational changes of the channel protein. pH-dependent opening and closing of  $K_{ir}1.1$  channels is accompanied by conformational changes involving movement of the intracellular N- and C-termini. This was visualized by state-dependent modification of cysteines 49 and 308, which were susceptible to reaction with DTNB in the pH-inactivated state, while no modification was observed for open channels. It should be pointed out that these residues are close to the two conserved arginines that were found to underly the large pK-shift of K80. As concluded from a putative gating model (Fig. 40),  $K_{ir}1.1$  channels should have a higher affinity for protons in the open than in the closed state. This could be achieved by movements of structural determinants of the RKR triad (as depicted in Fig. 41), which is in agreement with the finding that C49 and C308 move during gating. Conversely, mutations at these two sites and closeby (as found in aBS patients, for example; see section 3.3.3) display

slight shifts of  $pK_{app}$  to alkaline values, emphasizing the coupling of structural changes in these regions to the titration properties of K80.

Besides modification by DTNB or MTSES, channels were also oxidized in a state-dependent manner. Cu-Phen applied at  $pH_i$  6.0 prevented that channels recovered from inactivation - an effect that could be fully reversed by application of the reducing agent DTT (Schulte et al., 1998). But although oxidation and reduction were induced by agents specific for formation and cleavage of disulfide bonds, no significant alteration of the redox-sensitivity was observed in either of the C A/S mutations. Moreover, oxidation was also observed in the double-mutant  $K_{ir}1.1(C49,308A)$  which completely abolished state-dependent modification by DTNB (Fig. 18) as well as in the triple mutants  $K_{ir}1.1(C308,355,358A)$  and  $K_{ir}1.1(C49,175,308A)$  (data not shown). When all cysteines outside the 'core-region' were replaced by alanine, no channel activity could be detected. Thus, it was not possible to identify the cysteine residues involved in oxidation or to exclude a role of proteins closely associated with  $K_{ir}1.1$ .

$K_{ir}1.1$  and  $K_{ir}4.1$  channels are unique among inward-rectifiers in that they are dependent on extracellular ions like  $K^+$ ,  $NH_4^+$ ,  $Rb^+$  or  $Cs^+$  (but not  $Li^+$  and  $Na^+$ ), previously described as  $K^+$ -regulation (Doi et al., 1996; Pearson et al., 1999). The requirement of extracellular  $K^+$  for channel activity was found to be dependent on the conformational state. At  $pH_i$  8.0,  $K_{ir}1.1$  channels showed no inactivation even in the complete absence of intra- and extracellular  $K^+$  (see Fig. 10). In contrast, pH-inactivated channels ( $pH_i$  6.0) could not be recovered in the absence of extracellular  $K^+$  (as a function of time spent in the closed state; see Fig. 9). Thus, pH-induced inactivation either alters the affinity of an extracellular  $K^+$  binding site or leads to a pore conformation that is then dependent on extracellular  $K^+$  (not shown in Fig. 41). Further experiments will be needed to discriminate between these possibilities. In line with these findings, the non-pH-gated mutant  $K_{ir}1.1(K80M)$  did not display any dependence on extracellular  $K^+$  (Fig. 12). Taken together, these results provide a molecular explanation for the allosteric interaction of  $K^+$ -regulation with  $pH_i$ -gating described for  $K_{ir}1.1$  (Doi et al., 1996) as summarized in the structural model of Fig. 41.

So far, the extracellular binding site for  $K^+$  could not be identified. The selectivity pattern for alkali ions raises the possibility, that the binding site may be located in a restrictive structure of the pore, possibly close to or in the selectivity filter. Consequently, replacing the pore-forming loop of  $K_{ir}1.1$  by that of  $K_{ir}2.1$  in a chimeric construct ( $K_{ir}1.1(K_{ir}2.1p)$ ) abolished dependence on extracellular  $K^+$  without affecting gating by  $pH_i$  significantly (Fig. 11). Furthermore it remains to be elucidated in which way the conformational changes resulting from pH-dependent gating may be linked to other processes reported to affect channel activity such as phosphorylation by protein kinase A (Xu et al., 1996) or interaction with anionic phospholipids (Huang et al., 1998).

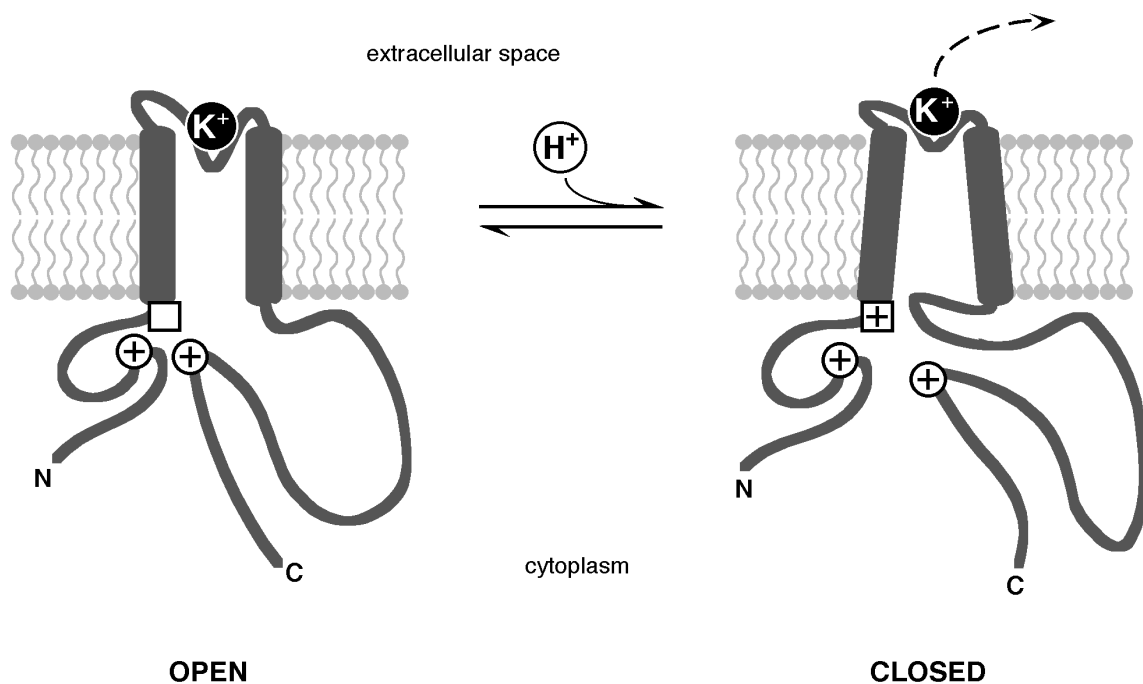


**Fig. 41.** Structural model of pH-gating of  $K_{ir}1.1$  channels. Circles: arginines 41 and 311 (permanently positively charged); squares: lysine 80 (pre-M1 site). Conformational changes during pH-gating may rearrange the RKR triad and affect the interaction of extracellular  $K^+$  with the P-loop.

### 3.2.2 Comparison of pH-gating with gating mechanisms in other $K_{ir}$ channels

pH-gating could be introduced into members of different  $K_{ir}$  subfamilies by mutating the pre-M1 site to a lysine residue (Fig. 27). Although the respective  $pK_{app}$  values displayed some variability, titration of the  $NH_2$ -group in all these subtypes was shifted down by more than 3 pH units compared to its standard value. Thus, all  $K_{ir}$  proteins basically offered the structural context necessary for formation of the RKR triad and the associated gating machinery. Regarding the primary structure this may not be too surprising, since both arginine residues are conserved throughout the  $K_{ir}$  family and reside within the region where  $K_{ir}$  proteins show a very high degree of homology. Taking into account the sensitivity to minor side chain variations (Fig. 34), this result points to a significant conservation among  $K_{ir}$  subunits also on the level of their tertiary structure. Although deduced from functional analysis, these results suggest a first rough framework for the folding of  $K_{ir}$  proteins, in that N- and distal C-termini are backfolded to the pre-M1 region (Fig. 41). In line with such an interpretation, some studies reported involvement of both N- and C-termini in G protein-dependent gating of  $K_{ir}3$  channels (Huang et al., 1997) or inhibition of  $K_{ATP}$  channels by ATP (Tucker et al., 1998).

$K_{ir}$  channels may possess different trigger mechanisms linked to the same or structurally separate "gates". For example,  $K_{ir}6.2(T71K)/SUR1$  channels are pH<sub>i</sub>-gated (Fig. 28) and completely inhibited by ATP at intracellular concentrations of 1 mM (Ruppertsberg et al., 1999).

Application of 10  $\mu$ M PIP2 (20 s) strongly reduced the sensitivity to intracellular ATP (data not shown) but did not abolish gating by pH<sub>i</sub>. For K<sub>ir</sub>1.1 it was demonstrated that protonation and 'inactivation-gating' are actually mediated by separate determinants. In K<sub>ir</sub>1.1(R311W) and K<sub>ir</sub>4.1(R294Q) mutant channels the working range of the 'pH-sensor' was shifted back closely towards the standard value of NH<sub>2</sub>-lysine with the gating machinery left intact (Figs. 33 and 39). Thus, the RKR triad presented here explains the molecular mechanism underlying the 'driving-force' of pH-gating, but the localization of the gate remains open.

Recently, gating induced by changes in extracellular pH (pK<sub>app</sub> around 2.5) has been related to conformational changes in the two segment-type K<sup>+</sup> channel from *Streptomyces lividans* (Perozo et al., 1998). Using EPR-spectroscopy, Perozo and coworkers uncovered structural rearrangements at the C-terminal end of the second transmembrane helix which were hypothesized to change the width of the inner vestibule and to thereby control ion permeation. Whether such a mechanism also underlies pH-gating in K<sub>ir</sub>1.1 remains to be elucidated. Alternatively, the gate may be formed by protein domains neighbouring the RKR triad, since these domains including cysteines 49 and 308 were shown to move during pH-gating.

Activation of K<sub>ir</sub>3 channels by G proteins as well as regulation of K<sub>ATP</sub> channels by sulfonyl-ureas and channel openers are mediated by accessory proteins interacting with the K<sub>ir</sub> subunits. Consequently, these gating mechanisms can be classified as being *extrinsic* with respect to the channels. In contrast to that, pH-gating is *intrinsic* to the K<sub>ir</sub>1.1 and K<sub>ir</sub>4.1 proteins, i.e. it does not require any accessory  $\beta$ -subunit or cofactors such as anionic phospholipids. As shown in Figs. 8 and 20, K<sub>ir</sub>1.1 channels did not display 'run-down' in these experiments, nor did application of PIP2 change steady-state parameters of pH-gating significantly. Furthermore, pH-gating was also observed in K<sub>ir</sub>1.1(R188Q) mutant channels, which were reported to have reduced binding affinity for PIP2 (Huang et al., 1998). The mild shift in pK<sub>app</sub> found for this mutant was similar to that seen in other N- and C-terminal mutations (see Fig. 29).

### 3.3 Physiological importance

#### 3.3.1 Redox sensitivity of K<sub>ir</sub>1.1 channels

The presence of reducing agents like DTT (0.1mM) and GSH (5 mM) was required for complete recovery from pH-induced inactivation in excised inside-out patches. In living cells, however, the redox-sensitivity most likely is not of physiological importance, since reduced glutathione should be available in millimolar concentrations. Nitric oxide has been reported to act as a physiological modifying agent of thiol groups. For example, NO could be replaced by

DTNB in activation of cyclic nucleotide-gated channels (Broillet and Firestein, 1996, 1997). However, in inside-out patch experiments nitric oxide donors (SIN-1 and S-nitrosocysteine, see "Materials and Methods") did not reveal any effect on pH-gating of  $K_{ir}1.1$  channels (data not shown). Thus it remains unclear if state-dependent reactivity of these conserved cysteines has functional consequences *in vivo*.

### 3.3.2 $K^+$ secretion in the kidney

Only 1-2 % of total body  $K^+$  is located in the extracellular fluid, the vast majority is contained by cells (Stanton and Giebisch, 1992). As a consequence, extracellular  $K^+$  levels can be strongly increased by dietary intake and internal redistribution. Under normal conditions, rapid changes of extracellular  $K^+$  levels are effectively buffered by cellular uptake and secretion of  $K^+$ . Long-term  $K^+$  homeostasis is achieved by regulation of renal  $K^+$  secretion (Giebisch, 1998). A major source of disturbance is the acid-base status in the body, since pH and extracellular  $K^+$  levels are tightly coupled. During acidosis, for example,  $Na^+/H^+$ -antiport in cells is activated and the depletion of intracellular  $Na^+$  impairs  $Na^+/K^+$ -ATPase leading to extracellular accumulation of  $K^+$  (Lang and Rehwald, 1992; Giebisch, 1998). Disturbance of  $K^+$  blood plasma levels can be life-threatening, mainly because of evoked cardiac arrhythmias. Other common symptoms of hyperkalemia are muscular weakness, impaired peristaltic movements of the gut and metabolic alkalosis (Thier, 1986).

The interdependence of  $K^+$  and pH requires a complex regulation of kidney function. Renal  $K^+$  secretion is enhanced during metabolic alkalosis and inhibited during metabolic acidosis. The latter is an important mechanism to prevent excessive loss of  $K^+$  during acidosis (Wang, 1995). pH-gating of  $K_{ir}1.1$  channels represents a molecular mechanism linking both  $K^+$  and pH:

- Since  $K_{ir}1.1$  channels are responsible for  $K^+$  recycling into the lumen of the thick ascending loop of Henle (Fig. 5 A), their inhibition by acidic  $pH_i$  would lead to enhanced  $K^+$  reabsorption. The same effect would result from inhibition of  $K^+$  secretion in principal cells of the cortical collecting duct (Fig. 5 B) by intracellular acidification (Wang et al., 1992; Tsai et al., 1995).
- As described in section 1.2.3, aldosterone stimulates reabsorption of  $Na^+$  and secretion of  $K^+$  in the cortical collecting duct. Elevation of this hormone during high  $K^+$  diet was hypothesized to increase  $K_{ir}1.1$  activity, at least in part, by increasing the intracellular pH via stimulation of  $Na^+/H^+$ -antiport (Oberleithner et al., 1987).
- For effective  $K^+$  secretion in principal cells the activity of basolateral  $Na^+/K^+$ -ATPase must be coupled to the apical  $K^+$  conductance. As an alternative to the mechanism proposed by Wang et al. (1993), activation of  $Na^+/K^+$ -ATPase could enhance  $Na^+/H^+$ -antiport, thereby increasing  $pH_i$  and apical  $K_{ir}1.1$  channel activity.

- As a more general mechanism, pH-gating of  $K_{ir}$  channels could play a protective role in secretory epithelia. To maintain cation balance during  $K^+$  secretion, epithelial cells exchange  $K^+$  with  $Na^+$  or  $H^+$  (Lang and Rehwald, 1992). Inactivation of  $K_{ir}$  channels as a result of excessive uptake of protons would prevent further acidification of these cells.

Although an increase of  $K^+$  secretion at higher luminal  $K^+$  concentrations has been described (Giebisch, 1998), a direct activation of  $K_{ir}1.1$  channels by luminal  $K^+$  ions has not yet been taken into account. The discovery of  $K^+$  regulation and its allosteric interaction with pH-gating of  $K_{ir}1.1$  channels delivers a molecular explanation for this phenomenon and opens some interesting perspectives.  $K^+$  secretion increases the tubular  $K^+$  concentration, which would activate apical  $K_{ir}1.1$  channels. This mechanism therefore might represent a positive feedback control of the  $K^+$  secretion process which would otherwise be negatively affected by the decreased electrochemical driving force that accompanies increased luminal  $K^+$  concentrations. Since the  $K^+$  level in the blood plasma is very stable, the control circuit of  $K^+$  homeostasis must have a high gain. A positive feedback, such as the direct  $K^+$  regulation described here, might increase the overall gain of  $K^+$  control and contribute to the stability of the blood plasma  $K^+$  concentration.

In kidney epithelial cells a drop in intracellular pH induces formation and subsequent elimination of  $NH_4^+$  which helps to control  $pH_i$  in these cells (Knepper et al., 1989). However this would require the presence of  $NH_4^+$ -conducting channels which are active at acidic  $pH_i$  in the apical membrane.  $K_{ir}1.1$  channels were found to conduct  $NH_4^+$  and to be effectively up-regulated not only by  $K^+$  but also by  $NH_4^+$  at slightly acidic  $pH_i$  (Doi et al., 1996). The idea, that allosteric regulation of  $K_{ir}1.1$  channels could affect  $pH_i$  or  $NH_4^+$  excretion needs to be investigated in a physiological system.

### 3.3.3 Differential diagnosis and possible treatment of aBS

$K_{ir}1.1$  point mutations identified in aBS patients to date are scattered throughout the amino acid sequence. However, when considering the tertiary folding of N- and C-termini as deduced in section 2.3.5, most aBS mutations were found to fall into two categories: (i) mutations in the inner core-region formed by the highly conserved P-loop and (ii) mutations in or close to the determinants of the RKR triad (Fig. 38). In heterologous expression experiments, category (i) mutants did not lead to channel activity (Derst et al., 1997), while most of the category (ii) mutants tested to date encoded functional channels. pH-gating of the latter, however, was shifted to more alkaline pH values compared to  $K_{ir}1.1$  wildtype, with backshifts in  $pK_{app}$  ranging from about 0.3 pH units ( $K_{ir}1.1(L220F)$ ) to more than 2 pH units ( $K_{ir}1.1(R311W)$ ,  $K_{ir}1.1(R311Q)$ ; see Fig. 39). On the molecular level, these shifts in pH-gating either result from disruption of the RKR triad or may be a consequence of mutation-induced structural

disturbances of this arrangement. Such minor shifts in  $pK_{app}$  have been observed for quite a number of amino acid exchanges (see Figs. 29 and 39).

In coexpression experiments  $K_{ir}1.1(R311Q)$  behaved as a dominant-negative subunit (Fig. 36). Therefore the corresponding allele should be dominant in terms of the development of aBS. Surprisingly, the carrier of  $K_{ir}1.1(R311Q)$  did not show clinical symptoms. It remains to be elucidated if this discrepancy results from non-binominal subunit assembly (compare the relative currents in Fig. 36 resulting from a 1:1 cRNA coexpression with functional  $K_{ir}1.1(K80M)$ ) or overexpression of the functional allele in the kidney.

Under physiological conditions, the mild shift in  $pK_{app}$  caused by the  $K_{ir}1.1(L220F)$  mutation in one patient was enough to develop the complete clinical phenotype of aBS. The non-functional allele  $K_{ir}1.1(R311W)$  he carried on the other chromosome was not sufficient by itself to cause aBS since his mother - the carrier of this allele - was healthy (see "Materials and Methods" section 4.2.4). For this patient, a mild alkalization of epithelial cells in the distal nephron should be able to restore functional activity of homomeric  $K_{ir}1.1(L220F)$  channels and thereby bring this patient close to his mother. Currently such an approach is under clinical trial for a subset of aBS patients with  $K_{ir}1.1$  mutations leading to smaller backshifts in  $pK_{app}$ .

Taken together, these results suggest that defective pH-gating is a major molecular cause for the pathogenesis of aBS. This may open up a new perspective for differential diagnosis and treatment of at least some of the aBS patients.

### 3.4 Research perspectives

Several properties reported for  $K_{ir}1.1$  channels in kidney cells could not be reproduced for cloned  $K_{ir}1.1$  expressed in *Xenopus* oocytes, such as block by intracellular ATP and regulation by PKA (Wang and Giebisch, 1991a, b). In a recent publication it was suggested that  $K_{ir}1.1$  couples functionally with CFTR, a chloride channel of the ABC protein family (Ruknudin et al., 1998). Upon coexpression,  $K^+$  currents showed ATP-dependent gating and became sensitive to glibenclamide. Whether  $K_{ir}1.1$  channels directly associate with CFTR or other ABC proteins and what the functional consequences of such an interaction may be needs to be investigated in more detail. Apart from the properties described above, direct interaction of  $K_{ir}1.1$  with membrane proteins could also be involved in state-dependent oxidation of  $K_{ir}1.1$  channels in excised inside-out patches. As a future approach, intracellular portions of  $K_{ir}1.1$  subunits (expressed in bacteria and purified) could be used to identify possible binding partners (when coupled to a chromatography column, in a blot overlay assay or using the yeast two-hybrid system).

After the structure of the KcsA core region has been resolved by x-ray crystallography, attention is now focused on the structure of intracellular domains of channel proteins and on rearrangements involved in gating. Clearly these goals are beyond the limitations of site-directed mutagenesis. A first step may be structural analysis of purified N- and C-termini of  $K_{ir}$  proteins with multidimensional NMR spectroscopy.

Some aspects of the pathophysiology of aBS remain puzzling. For example, why are carriers of a single dominant-negative  $K_{ir}1.1$  allele apparently healthy? Are there compensatory mechanisms at the level of  $K_{ir}1.1$  or other ion channels or transporters in the nephron? Coexpression experiments with  $K_{ir}1.1$  mutants in the same combinations as found in compound heterozygous patients may help to answer these questions. After all it would also be important to actually measure the intracellular pH (below the apical membrane) in renal epithelial cells under various physiological conditions. Perhaps  $K_{ir}1.1$  channels themselves could be used to monitor changes in intracellular pH.



## 4 Materials and Methods

### 4.1 Equipment and materials

#### 4.1.1 Laboratory equipment

##### Molecular biology:

|                             |   |
|-----------------------------|---|
| centrifuge                  | Microfuge and Centrifuge 5417C, Eppendorf, Hamburg, Germany   |
| DNA sequencing              | ALF express sequencing system, Pharmacia Biotech, Uppsala, Sweden   |
| film processing             | Fuji RGII X-ray Film Processor, Fuji Photo Film (Europe) GmbH, Düsseldorf, Germany  |
| gel documentation system    | UV lamp: Vilber Lourmat 302 nm, Bachofer, Reutlingen, Germany; camera E.A.S.Y. 429K and personal computer, Herolab, Wiesloch, Germany |
| gel electrophoresis         | Horizon 58, Life Technologies, Gaithersburg MD, USA; power supply EPS 600, Pharmacia Biotech, Uppsala, Sweden                         |
| PCR machine                 | DNA Thermal Cycler, Perkin Elmer, Norwalk CT, USA   |
| pipettes                    | Pipetman P2 / P20 / P200 / P1000, Gilson Medical Electronics, Villiers-le-Bel, France   |
| shakers                     | MS1 IKA Works Inc., Wilmington NC, USA, and Thermomixer 5436 Eppendorf, Hamburg, Germany  |
| temperature-controlled bath | GFL 1003, Gesellschaft für Labortechnik mbH, Burgwedel, Germany   |

##### Electrophysiology:

|                      |  |
|----------------------|--|
| acquisition software | Pulse++ (non-commercial software), developed by U. Rexhausen, Department of Physiology II, University of Tübingen, Germany |
| balance              | Mettler AE 163, Mettler Waagen, Giessen, Switzerland   |
| binocular            | Wild M3C, Leica, Bensheim, Germany; light source: Leica IL 1500 electronic, Schott-Geräte, Germany                         |

|                                       |   |
|---------------------------------------|---|
| chart recorder                        | Kipp&Zonen BD 41, Kipp&Zonen, Netherlands   |
| computational software                | IgorPro, Wavemetrics, USA   |
| computer                              | Macintosh PowerPC 8500/120, Tübingen, Germany                                       |
| digitization board                    | ITC16, HEKA electronics, Lamprecht, Germany   |
| electrode puller                      | DMZ-Universal Puller, Zeitz-Instrumente, Augsburg, Germany                          |
| incubator                             | WTB Binder, Tuttlingen, Germany   |
| inverted microscope                   | Axioskop, Zeiss, Germany  |
| magnetic stirrer                      | IKA Combimag RET, Janke&Kunkel, Staufen, Germany                                    |
| microforge                            | microscope ID 03 Carl Zeiss, Germany; power supply Luigs&Neumann, Ratingen, Germany |
| micromanipulator, manual              | Leitz, Wetzlar, Germany   |
| micromanipulator, programmable        | Eppendorf, Hamburg, Germany   |
| oscilloscope                          | HM 1007, Hameg, Frankfurt, Germany  |
| patch clamp amplifier                 | EPC9 amplifier, HEKA electronics, Lamprecht, Germany                                |
| pH meter                              | pH-Meter CG 840, Schott-Geräte, Hofheim, Germany                                    |
| pH microelectrode amplifier           | built by U. Schüler, Department of Physiology II, University of Tübingen, Germany   |
| precision forceps (size 3 and size 5) | Dumont, Basel, Switzerland  |
| pump                                  | WISA, Wuppertal, Germany  |
| two-electrode voltage-clamp amplifier | TurboTec 01C amplifier, npi electronic GmbH, Tamm, Germany                          |
| ultrasonic bath                       | Transsonic T420, Elma, Singen, Germany  |

#### Immunocytochemistry:

|                               |                                     |
|-------------------------------|-------------------------------------|
| an epifluorescence microscope | Zeiss Axioskop FS, Jena, Germany    |
| CCD camera                    | Princeton Instruments, Trenton, USA |
| microtome                     | Leica, Wetzlar, Germany             |

#### 4.1.2 Materials

##### Molecular biology:

|                        |  |
|------------------------|--|
| filter tips            | SafeSeal Tips, Biozym Diagnostic, Oldendorf, Germany |
| glass wool             | Supelco, Bellefonte PA, USA                          |
| petri dishes (sterile) | Greiner, Frickenhausen, Germany                      |
| x-ray films            | Biomax MR, Eastman Kodak Company, Rochester NY, USA  |

##### Electrophysiology:

|                                |  |
|--------------------------------|--|
| filter holders                 | FP 030/3 0.2 µm, Renner, Dannstadt, Germany            |
| borosilicate glass capillaries | Zinsstag Glasbläserei, Stuttgart, Germany              |
| capillaries with filament      | GB 200F-8P, Science Products, Hofheim, Germany         |
| loading capillaries            | transferpettor cups (orange) 10 µl, Brand, Deutschland |
| microloaders                   | Eppendorf, Hamburg, Germany                            |

##### Immunocytochemistry:

|                   |   |
|-------------------|---|
| embedding polymer | Technovit 7100, Heraeus Kulzer, Wehrheim, Germany                     |
| glass slides      | Superior, Germany; sealed with Entellan, E. Merck, Darmstadt, Germany |

#### 4.1.3 Chemicals and reagents

##### Molecular biology:

|                         |   |
|-------------------------|---|
| 5'-Cy5 labelled primers | Gibco BRL, Life Technologies, Karlsruhe, Germany            |
| agar                    | Roth, Karlsruhe, Germany                                    |
| agarose                 | electrophoresis grade, Life Technologies, Paisley, Scotland |
| ampicillin              | Sigma, St. Louis, USA                                       |

|                            |   |
|----------------------------|---|
| cRNA synthesis and DNase I | mMessage-mMachine kit, Ambion, Austin, USA                        |
| DNA sequencing             | DNA Sequencing Kit, Amersham, Cleveland, USA                      |
| ethidium bromide           | Sigma, St. Louis, USA   |
| gel electrophoresis        | CleanGel DNA Analysis Kit, Pharmacia Biotech, Uppsala, Sweden     |
| LB medium                  | Luria Broth base, Gibco BRL, Life Technologies, Paisley, Scotland |
| mineral oil                | Sigma, St. Louis, USA   |
| nucleotides                | nucleotide mix, Stratagene Europe, Amsterdam, Netherlands         |
| oocyte expression vector   | pBF (B. Fakler, unpublished)                                      |
| PCR buffer                 | Gibco BRL, Life Technologies, Karlsruhe, Germany                  |
| plasmid preparation        | Midi Prep Kit, Quiagen, Hilden, Germany                           |
| restriction enzymes        | Boehringer Mannheim, Germany                                      |
| RNA standards              | 0.24-9.5 kb RNA Ladder, Life Technologies, Karlsruhe, Germany     |
| Taq polymerase             | Gibco BRL, Life Technologies, Karlsruhe, Germany                  |

### Electrophysiology

|                                   |   |
|-----------------------------------|---|
| antibiotics                       | stock solution (10.000 U penicillin and 10 mg streptomycin per ml), Sigma, St. Louis, USA |
| collagenase type II               | clostridiopeptidase A, EC 3.4.24.3, Sigma, St. Louis, USA                                 |
| Cu-phenanthroline                 | Aldrich-Chemie, Steinheim, Germany  |
| DTT, DTNB                         | Sigma, St. Louis, USA   |
| FmocCl                            | Sigma, St. Louis, USA   |
| GSH                               | Sigma, St. Louis, USA   |
| H <sup>+</sup> -selective polymer | pH ionophore II, Fluka Chemie, Germany  |
| hexamethyl-disilazane             | Fluka Chemie, Germany   |
| MgATP, K <sub>2</sub> ATP         | Sigma, St. Louis, USA   |
| MTSES                             | Toronto Research Chemicals, North York, Canada  |
| PIP2                              | Boehringer Mannheim, Germany  |
| SIN-1                             | Calbiochem, San Diego, USA  |
| Spermine                          | Sigma, St. Louis, USA   |

## Immunocytochemistry

|                    |  |
|--------------------|--|
| goat serum         | Gibco BRL, Life Technologies, Karlsruhe, Germany       |
| paraformaldehyde   | Sigma, St. Louis, USA                                  |
| primary antibody   | mouse anti-flag antibody M2, Sigma Kodak, USA          |
| secondary antibody | goat anti-mouse Cy3-coupled, Dianova, Hamburg, Germany |

## 4.2 Heterologous expression in *Xenopus* oocytes

### 4.2.1 cRNA synthesis

Site-directed mutagenesis and construction of  $K_{ir}$  chimeras was performed with standard techniques (described in (Fakler et al., 1995)) by Dr. J. Ludwig, Dr. H. Hahn, and S. Weidemann (Department of Physiology II, Eberhard-Karls-University of Tübingen, Germany) and Dr. C. Derst (Institute for Physiology, Philipps-University of Marburg, Germany).  $K_{ir}$  mutants were verified by sequencing and subcloned into pBF expression vector. Linearized template DNA was kindly provided for *in-vitro* synthesis of capped cRNA using the mMessage-mMachine kit. RNase-free water (DEPC-water) was prepared as follows: 50 ml  $H_2O_{bidest}$  + 50  $\mu$ l diethyl-pyrocabonate were mixed, incubated overnight at 37°C and autoclaved. Transcription was carried out according to the manufacturer's instructions:

- 6  $\mu$ l template DNA
- 2  $\mu$ l 10x transcription buffer
- 10  $\mu$ l 2x ribonucleotide mix
- 2  $\mu$ l SP6 polymerase (premix)

were mixed and incubated for 1.5 h at 37°C. After that, 1  $\mu$ l DNase I (RNase free, 2 U/ $\mu$ l) was added and the mixture was incubated for 15 min at 37°C. Finally, 80  $\mu$ l RNase free water was added and proteins were extracted with phenol / chloroform (mixture + 1 volume of phenol + 1 volume of chloroform upper aqueous phase washed again with 1 volume of chloroform).

RNA was precipitated from the aqueous phase with ethanol: 3 volumes ethanol and 0.1 volumes 3 M sodium acetate pH 4.8 were mixed and incubated on ice for at least 5 min. After centrifugation (5 min at 14000 rpm, Microfuge) the pellet was washed with 70% ethanol, lyophilized and dissolved in DEPC-water. Aliquots were tested on denaturing agarose gels,

fluorescence signals were quantified using RNA standards (0.24-9.5 kb RNA Ladder) and the RNA concentration was finally adjusted to 0.5  $\mu\text{g}/\mu\text{l}$  after repeated precipitation.

#### 4.2.2 Preparation and injection of oocytes

*Xenopus* oocytes were surgically removed from adult females and manually dissected. About 50 nl of a solution containing cRNA (concentration 50  $\mu\text{g}/\mu\text{l}$  or less, diluted with RNase-free water) was injected into Dumont stage VI oocytes. Two days later, oocytes were treated 15 min with collagenase type II (Clostridiopeptidase A), washed several times and incubated at 19 °C for at least 2 more days. Through all these procedures, oocytes were kept in OR-2 culture medium.

For two-electrode voltage-clamp experiments only the follicular cell layer was removed using precision forceps. For patch-clamp experiments, the respective oocyte was placed in hypertonic solution (200 mM  $\text{K}^+$  aspartate, pH 7.2 adjusted with KOH), allowed to shrink and all extracellular layers were removed with precision forceps. Oocytes were then placed in the bath chamber and allowed to adhere to the glass bottom (at least 5 min).

#### 4.2.3 Culture media

##### OR-2 (oocyte culture medium):

|                           |         |
|---------------------------|---------|
| NaCl                      | 82.5 mM |
| KCl                       | 2.5 mM  |
| $\text{Na}_2\text{HPO}_4$ | 1.0 mM  |
| HEPES                     | 5.0 mM  |
| PVP                       | 0.5 g/l |
| $\text{MgCl}_2$           | 1.0 mM  |
| $\text{CaCl}_2$           | 1.0 mM  |

pH 7.3 was adjusted with NaOH, and antibiotics (premixed stock solution containing 10.000 U penicillin and 10 mg streptomycin per ml) were added (10 ml per liter OR-2) to prevent bacterial contamination.

#### 4.2.4 $K_{ir}1.1$ mutations identified in aBS patients

Apart from the  $K_{ir}1.1$ -aBS mutations published, six missense mutations were tested which had only recently been identified in three (compound heterozygous) patients (Jeck, N., and Konrad, M., Department of Pediatrics, Philipps-University Marburg, Germany):

- patient 1:  $K_{ir}1.1$ (R311W) and  $K_{ir}1.1$ (L220F)
- patient 2:  $K_{ir}1.1$ (R311Q) and  $K_{ir}1.1$ (F325C)
- patient 3:  $K_{ir}1.1$ (C49Y) and  $K_{ir}1.1$ (I51T)

All these patients displayed a clinical course indicative of defective ROMK function including marked polyhydramnios with premature birth, marked hyperkalemia in the postnatal period and hypokalemia later on, severe salt wasting and hyperreninemic hyperaldosteronism.

Mutation analysis was performed as follows (Derst et al., 1998; Konrad et al., 1999). Genomic DNA was extracted from peripheral leukocytes isolated from the patients' blood. Aberrant band patterns for the *romk* gene were sought by means of single-strand conformation polymorphism analysis (SSCP) using primers described previously (Károlyi et al., 1997). PCR was performed in a 20  $\mu$ l volume containing 50 ng of genomic DNA, 1.5 mM  $MgCl_2$ , 5 mM Tris (pH 8.3), 50 mM KCl, 10 pmol of each primer and 1.0 U of Taq polymerase. After an initial step at 94 °C for 5 min, PCR was conducted for 30 cycles with denaturation at 94 °C for 45 s, annealing at 55 °C for 30 s and extension at 72 °C for 45 s. The reaction was completed with a final elongation step at 72 °C for 10 min. Amplified products were separated using the CleanGel DNA Analysis Kit with the Multiphor II electrophoresis system. Migration was performed at 18 W constant power at 15 °C for 1 h. The band patterns were visualized by silver staining (Derst et al., 1998). Direct sequencing was performed after reamplification of the remaining PCR product using 5'-Cy5 labelled primers on an ALF express sequencing system following the protocols provided by the manufacturer.

### 4.3 Immunocytochemistry

Immunostainings were performed in collaboration with Dr. K. Wild using the following procedure (Wild, 1999). After removal of the vitelline membrane oocytes were fixed overnight at -20 °C in fixative (Dent et al., 1989). The fixation reagent was washed out with PBS (137 mM NaCl, 2.7 mM KCl, 8.4 mM  $Na_2HPO_4 \cdot 2H_2O$ , pH 7.2 adjusted with HCl). Then oocytes were incubated with a mouse anti-flag antibody (dilution 1:1000 in PBS + 10% goat serum) at room temperature for 3 h. After washing with PBS, incubation with the secondary

antibody (goat anti-mouse Cy3-coupled, dilution 1:200) was performed either overnight at 4 °C or at room temperature for one hour. Stained oocytes were washed 8 times in PBS (for increasing periods of time, 5 min to 1 hour) and post-fixed with 3.7% paraformaldehyde in PBS for one hour. Embedding in Technovit 7100 was carried out according to the manufacturer's instructions. Embedded oocytes were cut to 4 µm sections, covered on glass slides and analyzed with an epifluorescence microscope. Photos were taken with a CCD camera and stored on harddisk.

## 4.4 Whole-cell recording

### 4.4.1 Two-electrode voltage-clamp

Electrophysiological recordings were performed 3 to 7 days after injection. For two-microelectrode recordings current and voltage electrodes were pulled from thick-walled borosilicate glass, had resistances between 0.1 and 0.5 MΩ and were filled with 3 M KCl. Currents were recorded with a TurboTec 01C amplifier, digitized at 0.1 kHz and stored on harddisk. The bath chamber was designed as a narrow canal to achieve complete solution exchange in less than 10 s.

**Table 2.** Composition of bath solutions used for two-electrode voltage-clamp experiments; all concentrations are given in mM. Intracellular acidification was achieved by replacing KCl in 90K with equimolar concentrations of KHCO<sub>3</sub> (90KHCO<sub>3</sub>). The pH value was adjusted to 7.2 by titration with HCl.

| Bath solution     | 2.5K | 0K    | 20K  | 90K  |
|-------------------|------|-------|------|------|
| NaCl              | 115  | 117.5 | 97.5 | 27.5 |
| KCl               | 2.5  | -     | 20   | 90   |
| HEPES             | 10   | 10    | 10   | 10   |
| CaCl <sub>2</sub> | 1.8  | 1.8   | 1.8  | 1.8  |



#### 4.4.2 Recording of intracellular pH (pH<sub>i</sub>)

pH-sensitive electrodes were made and calibrated as described (Tsai et al., 1995). Micro-electrodes were filled with hexamethyl-disilazane and baked for 10 min at 200 °C. Tips of the silanized electrodes were filled with a H<sup>+</sup>-selective polymer (pH ionophore II). The rest of the electrode was filled with K<sub>int</sub> pH 7.0. Calibration was carried out in pH 6.5 and pH 7.5 solutions and only electrodes with linear slopes of > 50 mV/pH unit were used for experiments. The intracellular pH was determined during voltage-clamp experiments by measuring the potential of the pH electrode relative to the command voltage. The measured potential was low-pass filtered (cut-off frequency of 0.1 Hz) and stored on harddisk. In pH<sub>i</sub> traces such as in Fig. 24 only a single data point per voltage ramp (at 0 mV) is shown.

#### 4.4.3 Voltage protocols and data evaluation

The voltage-command protocol used for all whole-cell measurements consisted of repetitive voltage ramps: hyperpolarization at -120 mV for one second followed by a linear ramp up to +50 mV in 20 s. For the recording in Fig. 2, short voltage ramps (from -100 mV to +100 mV in 5 s) were used. Stored data were analyzed with commercial software on a Macintosh PowerPC. Activation and deactivation time courses were fitted with monoexponential functions to the current amplitudes at -80 mV:

$$I(t) = I_{\max} \cdot e^{-(t/\tau)} + I_0 \quad (\text{with } I_{\max} = \text{maximal current, } I_0 = \text{steady-state current, } \tau = (\text{in})\text{activation time constant})$$

All mean values are given as mean ± standard deviation of n experiments.

### 4.5 Patch-clamp experiments

#### 4.5.1 Giant inside-out patch-clamp technique

Giant patch-clamp recordings were performed as described previously (Fakler et al., 1995). Briefly, pipettes were made from thick-walled borosilicate glass and had resistances of 0.3 - 0.6 MΩ (tip diameter of 20 - 30 μm). Currents were sampled at 1 kHz (unless stated otherwise) and corrected for capacitive transients with an EPC9 amplifier, with analog filter set to 3 kHz (-3 dB). Solutions were applied to the cytoplasmic side of the excised patches via a multi-barrel pipette.

**Table 3.** Solutions used in giant inside-out patch-clamp experiments. All concentrations are given in mM. pH of bath and pipette solutions were adjusted to pH 7.2 with KOH (NaOH in the case for Na<sub>pipette</sub>). K<sub>int</sub> was first adjusted to pH 8.0 with KOH and then titrated with KOH or HCl to the pH values indicated.

| Solutions           | bath | K <sub>pipette</sub> | Na <sub>pipette</sub> | K <sub>int</sub> | NMDG <sub>int</sub> |
|---------------------|------|----------------------|-----------------------|------------------|---------------------|
| NaCl                | -    | -                    | 120                   | -                | -                   |
| KCl                 | 100  | 120                  | -                     | 120              | -                   |
| NMDG                | -    | -                    | -                     | -                | 120                 |
| HEPES               | 10   | 10                   | 10                    | 10               | 10                  |
| K <sub>2</sub> EGTA | 10   | -                    | -                     | 10               | 10                  |
| MgCl <sub>2</sub>   | 1.44 | -                    | -                     | -                | -                   |
| CaCl <sub>2</sub>   | -    | 1.8                  | 1.8                   | -                | -                   |

DTT (100 mM stock solution, pH 7.2 adjusted with KOH) was added to all K<sub>int</sub> solutions at a final concentration of 0.1 mM prior to the experiments unless stated otherwise. All other compounds were prepared as stock solutions and applied in the concentrations indicated.

- Spermine: Stock solution of 100 mM, stored at -20°C
- MgATP, K<sub>2</sub>ATP: Stock solution of 0.5 M K<sub>2</sub>ATP (pH 6.0 adjusted with KOH). Added together with MgCl<sub>2</sub> to the applied K<sub>int</sub> solutions to yield the free concentrations indicated. Total and free concentrations of Mg<sup>2+</sup> and ATP were calculated using the Fabiato program (Fabiato, 1988).
- PIP2: added to solutions at the final concentration and sonified for at least 30 min. These solutions were used for one day.

All experiments were performed at room temperature (approximately 23 °C).

#### 4.5.2 Chemical modification of cysteine

For DTT and DTNB, stock solutions (100 mM) were made and stored at -20 °C; the final dilutions were used for about 8 hours. MTSES was freshly prepared at the final concentration (100 μM) prior to each experiment and used within 20 min. Glutathione was dissolved in K<sub>int</sub> solution at a concentration of 5 mM. The NO-donor SIN-1 was prepared as a 100 mM stock solution on ice and used for 4 hours. S-Nitrosocysteine was freshly prepared according to Broillet and Firestein (1997) from equimolar amounts of NaNO<sub>2</sub> and cysteine. Stock solutions (100 mM) were kept on ice and used for 1 hour.

### 4.5.3 Chemical modification of lysine

FmocCl was chosen due to its high reactivity and selectivity for unprotonated amino groups. Water-free dioxane was used as solvent for the stock solution (100 mM). Three microliters were added to 3 ml of modification buffer no later than 1 min prior to each experiment to yield a final concentration of 0.1 mM FmocCl and 0.1% dioxane.

Modification buffer (MOD):

|                                |        |
|--------------------------------|--------|
| KCl                            | 100 mM |
| H <sub>3</sub> PO <sub>4</sub> | 10 mM  |

pH was adjusted to 7.5 with KOH.

### 4.5.4 Voltage protocols and data evaluation

For evaluation of pH dependence, the steady-state value for relative inhibition ( $I_{rel}$ ) at a given  $pH_i$  was determined by monoexponential fits to the time course of  $pH_i$ -induced current inhibition. This value was normalized to the maximum current, which was reached at  $pH_i = pK_{app} + 1$  pH unit in the case of most pH-gated  $K_{ir}$  channels. When the apparent pK was higher than 8.0, the current amplitude at  $pH_i$  8.8 was chosen as reference value because of the limited patch stability at higher  $pH_i$ .

To obtain  $pK_{app}$  and the Hill coefficient for the pH dependence,  $I(X)$  was fitted to a modified Hill equation:

$$I_{rel} / I_0 = 1 / \{ 1 + (X / K_{0.5})^N \} ; \text{ with } K_D = K_{0.5}^N$$

( $X$  = concentration of intracellular  $H^+$  ions ( $[H^+]_i$ ),  $K_{0.5}$  is  $[H^+]_i$  at half maximal inhibition (=  $10^{-pK_{app}}$ ),  $N$  = Hill coefficient and  $I_0$  is the asymptotic value of  $I_{rel}$ ).

Fractional recovery of oxidized channels by DTT (rel. recovery) was calculated as follows:

$$\text{rel. recovery} = [ I_{pH_{8.0}}(+\text{DTT}) - I_{pH_{8.0}}(\text{after}) ] / [ I_{pH_{8.0}}(\text{before}) - I_{pH_{8.0}}(\text{after}) ]$$

with  $I_{pH_{8.0}}(+\text{DTT})$  steady-state current amplitude at  $pH_i$  8.0 in the presence of DTT,  $I_{pH_{8.0}}(\text{after})$  current amplitude at  $pH_i$  8.0 after acidification,  $I_{pH_{8.0}}(\text{before})$  current amplitude at  $pH_i$  8.0 before acidification.

## 5 References

- Aguilar-Bryan, L., Nichols, C. G., Wechsler, S. W., Clement IV, J. P., Boyd III, A. E., Gonzalez, G., Herrera-Sosa, H., Nguy, K., Bryan, J., and Nelson, D. A. (1995) Cloning of the cell high-affinity sulfonylurea receptor: a regulator of insulin secretion. *Science* **268**, 423-426.
- Akabas, M. H., Stauffer, D. A., Xu, M., and Karlin, A. (1992) Acetylcholine receptor channel structure probed in cysteine-substitution mutants. *Science* **258**, 307-310.
- Ashcroft, F. M. (1988) Adenosine 5'-triphosphate-sensitive potassium channels. *Ann. Rev. Neurosci.* **11**, 97-118.
- Ashford, M. L., Bond, C. T., Blair, T. A., and Adelman, J. P. (1994) Cloning and functional expression of a rat heart KATP channel. *Nature* **370**, 456-459.
- Bartter, F. C., Pronove, P., Gill, J. R., and MacCardle, R. C. (1962) Hyperplasia of the juxtaglomerular complex with hyperaldosteronism and hypokalemic alkalosis. A new syndrome. *Am. J. Med.* **33**, 811-828.
- Baukrowitz, T., Schulte, U., Oliver, D., Herlitze, S., Krauter, T., Tucker, S. J., Ruppersberg, J. P., and Fakler, B. (1998) PIP2 and PIP as determinants for ATP inhibition of KATP channels. *Science* **282**, 1141-1144.
- Baukrowitz, T., Tucker, S. J., Schulte, U., Benndorf, K., Ruppersberg, J. P., and Fakler, B. (1999) Inward rectification in K<sub>ATP</sub> channels: a pH switch in the pore. *EMBO J.* **18**, 847-853.
- Blatz, A. L. (1984) Asymmetric proton block of inward rectifier K channels in skeletal muscle. *Pflügers Arch. (Eur. J. Physiol.)* **401**, 402-407.
- Bleich, M., Schlatter, E., and Greger, R. (1990) The luminal K<sup>+</sup> channel of the thick ascending limb of Henle's loop. *Pflügers Arch. (Eur. J. Physiol.)* **415**, 449-460.
- Boim, M. A., Ho, K., Shuck, M. E., Bienkowski, M. J., Block, J. H., Slightom, J. L., Yang, Y., Brenner, B. M., and Hebert, S. C. (1995) ROMK inwardly rectifying ATP-sensitive K<sup>+</sup> channel: II. Cloning and distribution of alternative forms. *Am. J. Physiol.* **268**, F1132-F1140.
- Bond, C. T., Pessia, M., Xia, X. M., Lagrutta, A., Kavanaugh, M. P., and Adelman, J. P. (1994) Cloning and expression of a family of inward rectifier potassium channels. *Recept. Channel* **2**, 183-191.
- Bond, J. M., Herman, B., and Lemasters, J. J. (1991) Protection by acidotic pH against anoxia/reoxygenation injury to rat neonatal cardiac myocytes. *Biochem. Biophys. Res. Commun.* **179**, 798-803.
- Broillet, M. C., and Firestein, S. (1996) Direct activation of the olfactory cyclic nucleotide-gated channel through modification of sulfhydryl groups by NO compounds. *Neuron* **16**, 377-385.
- Broillet, M. C., and Firestein, S. (1997)  $\beta$  subunits of the olfactory cyclic nucleotide-gated channel form a nitric oxide activated Ca<sup>2+</sup> channel. *Neuron* **18**, 951-958.

- Cameron, J. S., and Baghdady, R. (1994) Role of ATP sensitive potassium channels in long term adaptation to metabolic stress. *Cardiovasc. Res.* **28**, 788-796.
- Carpino, L. A., and Han, G. Y. (1970) The 9-fluorenylmethoxy-carbonyl function, a new base sensitive amino protecting group. *J. Am. Chem. Soc.* **92**, 5748-5794.
- Chang, S. S., Grunder, S., and Hanukoglu (1996) Mutations in the subunits of the epithelial sodium channel cause salt wasting with hyperkalaemic acidosis, pseudohypoaldosteronism type 1. *Nature Genet.* **12**, 248-253.
- Choe, H., Zhou, H., Palmer, L. G., and Sackin, H. (1997) A conserved cytoplasmic region of ROMK modulates pH sensitivity, conductance, and gating. *Am. J. Physiol.* **273**, F516-F529.
- Cohen, I. S., DiFrancesco, D., Mulrine, N. K., and Pennefather, P. (1989) Internal and external K<sup>+</sup> help gate the inward rectifier. *Biophys. J.* **55**, 197-202.
- Dascal, N., Schreibmayer, W., Lim, N. F., Wang, W., Chavkin, C., DiMagno, L., Labarca, C., Kieffer, B. L., Gaveriaux-Ruff, C., D., T., and Lester, H. (1993) Atrial G protein-activated K<sup>+</sup> channel: expression cloning and molecular properties. *Proc. Natl. Acad. Sci. USA* **90**, 10235-10239.
- Dawson, R. M. C., Elliot, D. C., Elliot, W. H., and Jones, K. M. (1986) Data for Biochemical Research, 3rd Edition (Oxford University Press, London).
- Dent, J., Polson, A., and Klymkowsky, M. (1989) A whole-mount immunocytochemical analysis of the expression of the intermediate filament protein vimentin in *Xenopus*. *Development* **105**, 61-74.
- Derst, C., Konrad, M., and Köckerling, A. (1997) Mutations in the ROMK gene in antenatal Bartter syndrome are associated with impaired K<sup>+</sup> channel function. *Biochem. Biophys. Res. Commun.* **203**, 641-645.
- Derst, C., Wischmeyer, E., Preisig-Muller, R., Spauschus, A., Konrad, M., Hensen, P., Jeck, N., Seyberth, H. W., Daut, J., and Karschin, A. (1998) A hyperprostaglandin E syndrome mutation in K<sub>ir</sub>1.1 (renal outer medullary potassium) channels reveals a crucial residue for channel function in K<sub>ir</sub>1.3 channels. *J. Biol. Chem.* **273**, 23884-23891.
- Dewan, J. C., Mikami, B., Hirose, M., and Sacchettini, J. C. (1993) Structural evidence for a pH-sensitive dilysine trigger in the hen ovotransferrin N-lobe: implications for transferrin iron release. *Biochemistry* **16**, 11963-11968.
- Doi, T., Fakler, B., Schultz, J. H., Schulte, U., Brändle, U., Weidemann, S., Zenner, H. P., Lang, F., and Ruppersberg, J. P. (1996) Extracellular K<sup>+</sup> and intracellular pH allosterically regulate renal K<sub>ir</sub>1.1 channels. *J. Biol. Chem.* **271**, 17261-17266.
- Doupnik, C. A., Davidson, N., and Lester, H. A. (1995) The inward rectifier potassium channel family. *Curr. Opin. Neurobiol.* **5**, 268-277.
- Doyle, D. A., Cabral, J. M., Pfuetzner, R. A., Kuo, A., Gulbis, J. M., Cohen, S. L., Chait, B. T., and MacKinnon, R. (1998) The structure of the potassium channel: molecular basis of K<sup>+</sup> conductivity and selectivity. *Science* **280**, 69-77.
- Fabiato, A. (1988) Computer programs for calculating total from specified free or free from specified total concentrations in aqueous solutions containing multiple metals and ligands. *Methods Enzymol.* **157**, 378-417.

- Fakler, B., and Ruppertsberg, J. P. (1996) Functional and molecular diversity classifies the family of inward-rectifier K<sup>+</sup> channels. *Cell. Physiol. Biochem.* **6**, 195-209.
- Fakler, B., Brändle, U., Glowatzki, E., Zenner, H.-P., and Ruppertsberg, J. P. (1994a) K<sub>ir</sub>2.1 inward rectifier K<sup>+</sup> channels are independently regulated by protein kinases and ATP hydrolysis. *Neuron* **13**, 1413-1420.
- Fakler, B., Brändle, U., Glowatzki, E., König, C., Bond, C., Adelman, J. P., Zenner, H.-P., and Ruppertsberg, J. P. (1994b) A structural determinant of differential sensitivity of cloned inward rectifier channels to intracellular spermine. *FEBS Lett.* **356**, 199-203.
- Fakler, B., Brändle, U., Glowatzki, E., Weidemann, S., Zenner, H.-P., and Ruppertsberg, J. P. (1995) Strong voltage-dependent inward-rectification of inward rectifier K<sup>+</sup> channels is caused by intracellular spermine. *Cell* **80**, 149-154.
- Fakler, B., Bond, C. T., Adelman, J. P., and Ruppertsberg, J. P. (1996a) Heterooligomeric assembly of inward-rectifier K<sup>+</sup> channels from subunits of different subfamilies: K<sub>ir</sub>2.1 (IRK1) and K<sub>ir</sub>4.1 (BIR10). *Pflügers Arch. (Eur. J. Physiol.)* **433**, 77-83.
- Fakler, B., Schultz, J. H., Yang, J., Schulte, U., Brändle, U., Zenner, H. P., Jan, L. Y., and Ruppertsberg, J. P. (1996b) Identification of a titratable lysine residue that determines sensitivity of kidney potassium channels (ROMK) to intracellular pH. *EMBO J.* **16**, 4093-4099.
- Fanconi, A., Schachenmann, G., Nüssli, R., and Prader, A. (1971) Chronic hypokalaemia with growth retardation, normotensive hyperrenin-hyperaldosteronism ("Bartter's syndrome"), and hypercalciuria. Report of two cases with emphasis on natural history and on catch-up growth during treatment. *Helv. Paed. Acta* **2**, 144-163.
- Ficker, E., Tagliatela, M., Wible, B. A., Henley, C. M., and Brown, A. M. (1994). Spermine and spermidine as gating molecules for inward rectifier K<sup>+</sup> channels. *Science* **266**, 1068-1072.
- Forsen, S., and Linse, S. (1995) Cooperativity: over the Hill. *TIBS* **20**, 495-497.
- Giebisch, G. (1998) Renal potassium transport: mechanism and regulation. *Am. J. Physiol.* **274**, F817-F833.
- Gitelman, H. J., Graham, J. B., and Welt, L. G. (1966) A new familial disorder characterized by hypokalemia and hypomagnesemia. *Trans. Assoc. Am. Physiol.* **79**, 221-235.
- Glowatzki, E., Fakler, G., Brändle, U., Rexhausen, U., Zenner, H.-P., Ruppertsberg, J. P., and Fakler, B. (1995) Subunit-dependent assembly of inward-rectifier K<sup>+</sup> channels. *Proc. R. Soc. Ser. B.* **261**, 251-261.
- Graber, M., and Pastoriza-Munoz, E. (1993) Regulation of cell pH by K<sup>+</sup>/H<sup>+</sup> antiport in renal epithelial cells. *Am. J. Physiol.* **265**, F773-F783.
- Hagiwara, S., Miyazaki, S., and Rosenthal, N. P. (1976) Potassium current and the effect of caesium on this current during anomalous rectification of the egg cell membrane of a starfish. *J. Gen. Physiol.* **67**, 621-638.
- Hebert, S. C. (1998) Roles of Na-K-2Cl and NaCl cotransporters and ROMK potassium channels in urinary concentration mechanism. *Am. J. Physiol.* **275**, F325-F327.
- Hein, J. (1989) Unified approach to alignments and phylogenies. *Meth. Enzymol.* **1989**, 624-645.

- Henczi, M., and Weaver, D. F. (1994) An improved synthesis of N -Fmoc-L-lysine and N -Fmoc-L-ornithine. *Org. Prep. Proced. Int.* **26**, 578-580.
- Hilgemann, D. W., and Ball, R. (1996) Regulation of cardiac Na<sup>+</sup>,Ca<sup>2+</sup> exchange and KATP potassium channels by PIP2. *Science* **273**, 956-959.
- Hille, B. (1992); in: Ionic channels in excitable membranes, 2nd ed. Sinauer Sutherland (Massachusetts, USA), pp. 127-130.
- Ho, K., Nichols, C. G., Lederer, W. J., Lytton, J., Vassilev, P. M., Kanazirska, M. V., and Hebert, S. C. (1993) Cloning and expression of an inwardly rectifying ATP-regulated potassium channel. *Nature* **362**, 31-38.
- Huang, C.-L., Slesinger, P. A., Casey, P. J., Jan, Y. N., and Jan, L. Y. (1995) Evidence that direct binding of G<sub>β</sub> to the GIRK1 G protein-gated inwardly rectifying K<sup>+</sup> channel is important for channel activation. *Neuron* **15**, 1133-1143.
- Huang, C.-L., Jan, Y. N., and Jan, L. Y. (1997) Binding of the G protein  $\beta$  subunit to multiple regions of G protein-gated inward-rectifying K<sup>+</sup> channels. *FEBS Lett.* **405**, 291-298.
- Huang, C.-L., Feng, S., and Hilgemann, D. W. (1998) Direct activation of inward rectifier potassium channels by PIP2 and its stabilization by G<sub>β</sub>. *Nature* **391**, 803-806.
- Inagaki, N., Gono, T., Clement, J. P., Namba, N., Inazawa, J., Gonzales, G., Aguilar-Bryan, L., Seino, S., and Bryan, J. (1995a) Reconstitution of IKATP: An inward rectifier subunit plus the sulfonylurea receptor. *Science* **270**, 1166-1169.
- Inagaki, N., Tsuura, Y., Namba, N., Masuda, K., Gono, T., Horie, M., Seino, Y., Mizuta, M., and Seino, S. (1995b) Cloning and functional characterization of a novel ATP-sensitive potassium channel ubiquitously expressed in rat tissues, including pancreatic islets, pituitary, skeletal muscle, and heart. *J. Biol. Chem.* **270**, 5691-5694.
- Inagaki, N., Gono, T., Clement, J. P., Wang, C. Z., Aguilar-Bryan, L., Bryan, J., and Seino, S. (1996) A family of sulfonylurea receptors determines the pharmacological properties of ATP-sensitive K<sup>+</sup> channels. *Neuron* **16**, 1011-1017.
- Isomoto, S., Kondo, C., Yamada, M., Matsumoto, S., Higashiguchi, O., Horio, Y., Matsuzawa, Y., and Kurachi, Y. (1996) A novel sulfonylurea receptor forms with BIR (Kir6.2) a smooth muscle type ATP-sensitive K<sup>+</sup> channel. *J. Biol. Chem.* **271**, 24321-24324.
- Karolyi, L., Konrad, M., Köckerling, A., Ziegler, A., Zimmermann, D. K., Roth, B., Wieg, C., Grzeschik, K., Koch, M., Seyberth, H. W., Vargas, R., Forestier, L., Jean, G., Deschaux, M., Rizzoni, G. F., Niaudet, P., Antignac, C., Feldmann, D., Lorrison, F., Cougoureux, E., Laroze, F., Alessandri, J., David, L., Saunier, P., Deschenes, G., Hildebrandt, F., Vollmer, M., Proesmans, W., Brandis, M., van den Heuvel, L., Lemmink, H. H., Nillesen, W., Monnens, L. A. H., Knoers, N., Woodford, L. M., Wright, C. J., Madrigal, G., and Hebert, S. C. (1997) Mutations in the gene encoding the inwardly-rectifying renal potassium channel, ROMK, cause the antenatal variant of Bartter syndrome: evidence for genetic heterogeneity. *Hum. Mol. Genet.* **6**, 17-26.
- Kelly, M. E., Dixon, S. J., and Sims, S. M. (1992) Inwardly rectifying potassium current in rabbit osteoclasts: a whole-cell and single-channel study. *J. Membr. Biol.* **126**, 171-181.
- Knepper, M. A., Packer, R., and Good, D. W. (1989) Ammonium transport in the kidney. *Physiol. Rev.* **69**, 179-249.

- Kobashi, K. (1968) Catalytic oxidation of sulfhydryl groups by o-phenanthroline copper complexes. *Biochim. Biophys. Acta* **158**, 239-245.
- Köckerling, A., Konrad, M., and Seyberth, H. W. (1998) Hereditäre Tubulopathien mit Diuretika-ähnlichem Salzverlust. *Dt. Ärztebl.* **95**, 1841-1846.
- Kondo, C., Isomoto, S., Matsumoto, S., Yamada, M., Horio, Y., Yamashita, S., Takemura-Kameda, K., Matsuzawa, Y., and Kurachi, Y. (1996) Cloning and functional expression of a novel isoform of ROMK inwardly rectifying ATP-dependent K<sup>+</sup> channel, ROMK6 (K<sub>r</sub>1.1f). *FEBS Lett.* **399**, 122-126.
- Konrad, M., Leonhardt, A., Hensen, P., Seyberth, H. W., and Kockerling, A. (1999) Prenatal and postnatal management of hyperprostaglandin E syndrome after genetic diagnosis from amniocytes. *Pediatrics* **103**, 678-683.
- Koshland, D. L., Nemethy, G., and Filmer, D. (1966) Comparison of experimental binding data and theoretical models in proteins containing subunits. *Biochemistry* **5**, 365-385.
- Krapivinsky, G., Krapivinsky, L., Wickman, K., and Clapham, D. E. (1995a) G binds directly to the G protein-gated K<sup>+</sup> channel, I<sub>KACH</sub>. *J. Biol. Chem.* **270**, 29059-29062.
- Krapivinsky, G., Gordon, E. A., Wickman, K., Velimirovic, B., Krapivinsky, L., and Clapham, D. E. (1995b) The G-protein-gated atrial K<sup>+</sup> channel IKACH is a heteromultimer of two inwardly rectifying K<sup>+</sup>-channel proteins. *Nature* **374**, 135-141.
- Krapivinsky, G., Medina, I., Eng, L., Krapivinsky, L., Yang, Y., and Clapham, D. E. (1998) A novel inward rectifier K<sup>+</sup> channel with unique pore properties. *Neuron* **20**, 995-1005.
- Kubo, Y., Baldwin, T. J., Jan, Y. N., and Jan, L. Y. (1993) Expression cloning of inward rectifier K<sup>+</sup> channel cDNA from j774 macrophage cell-line. *Biophys. J.* **64**, A 341-341.
- Kurachi, Y. (1985) Voltage-dependent activation of the inward-rectifier potassium channel in the ventricular cell membrane of guinea-pig heart. *J. Physiol. (Lond.)* **366**, 365-385.
- Lang, F., and Rehwald, W. (1992) Potassium channels in renal epithelial transport regulation. *Physiol. Rev.* **72**, 1-31.
- Lee, W.-S., and Hebert, S. (1995) ROMK inwardly rectifying ATP-sensitive K<sup>+</sup> channel: I. expression in rat distal nephron segments. *Am. J. Physiol.* **268**, F1124-F1131.
- Leech, C. A., and Stanfield, P. R. (1981) Inward rectification in frog skeletal muscle fibres and its dependence on membrane potential and external potassium. *J. Physiol. (Lond.)* **319**, 295-309.
- Lesage, F., Duprat, F., Fink, M., Giullemare, E., Coppola, T., Lazdunski, M., and Hugnot, J.-P. (1994) Cloning provides evidence for a family of inward rectifier and G-protein coupled K<sup>+</sup> channels in the brain. *FEBS Lett.* **353**, 37-42.
- Lopatin, A. N., Makhina, E. H., and Nichols, C. G. (1994) Potassium channel block by cytoplasmic polyamines as the mechanism of intrinsic rectification. *Nature* **372**, 366-369.
- Lopatin, A. N., Makhina, E. N., and Nichols, C. G. (1995) The mechanism of inward rectification of potassium channels: "long-pore plugging" by cytoplasmic polyamines. *J. Gen. Physiol.* **106**, 923-955.
- Lu, Z., and MacKinnon, R. (1994) Electrostatic tuning of Mg<sup>2+</sup> affinity in an inward-rectifier K<sup>+</sup> channel. *Nature* **371**, 243-246.



- MacKinnon, R. (1991) Determination of the subunit stoichiometry of a voltage-activated potassium channel. *Nature* **350**, 232-235.
- Martin, R. S., Panese, S., Virginillo, M., Gimenez, M., Litardo, M., Arrizurieta, E., and Hayslett, J. P. (1986) Increased secretion of potassium in the rectum of humans with chronic renal failure. *Am. J. Kidney Dis.* **8**, 105-110.
- Matsuda, H. (1991) Effects of external and internal K<sup>+</sup> ions on magnesium block of inwardly rectifying K<sup>+</sup> channels in guinea-pig heart cells. *J. Physiol. (Lond.)* **435**, 83-99.
- McNicholas, C. M., Wang, W.-H., Ho, K., Hebert, S. C., and Giebisch, G. (1994) Regulation of ROMK1 K<sup>+</sup> channel activity involves phosphorylation processes. *Proc. Natl. Acad. Sci. USA* **91**, 8077-8081.
- McNicholas, C. M., MacGregor, G. G., Islas, L. D., Yang, Y., Hebert, S. C., and Giebisch, G. (1998) pH-dependent modulation of the cloned renal K<sup>+</sup> channel, ROMK. *Am. J. Physiol.* **275**, F972-F981.
- Misler, S., Gillis, K., and Tabacharani, J. (1989) Modulation of gating of a metabolically regulated potassium channel by intracellular pH of the pancreatic islet. *J. Membr. Biol.* **109**, 135-143.
- Monod, J., Wyman, J., and Changeux, J.-P. (1965) On the nature of allosteric transitions: a plausible model. *J. Mol. Biol.* **12**, 88-118.
- Nichols, C. G., and Lopatin, A. N. (1997) Inward rectifier potassium channels. *Annu. Rev. Physiol.* **59**, 171-191.
- O'Neil, R. G. (1990) Aldosterone regulation of sodium and potassium transport in the cortical collecting duct. *Semin. Nephrol.* **10**, 365-374.
- Oberleithner, H., Weigt, M., Westphale, H. J., and Wang, W.-H. (1987) Aldosterone activates Na<sup>+</sup>/H<sup>+</sup> exchange and raises cytoplasmic pH in target cells of the amphibian kidney. *Proc. Natl. Acad. Sci. USA* **84**, 1464-1468.
- Ohno-Shosaku, T., Kubota, T., Yamaguchi, J., and Fujimoto, M. (1990) Regulation of inwardly rectifying K<sup>+</sup> channels by intracellular pH in opossum kidney cells. *Pflügers Arch. (Eur. J. Physiol.)* **416**, 138-143.
- Partiseti, M., Collura, V., Agnel, M., Culouscou, J.-M., and Graham, D. (1998) Cloning and characterization of a novel human inwardly rectifying potassium channel predominantly expressed in small intestine. *FEBS Lett.* **434**, 171-176.
- Pearson, W. L., Dourado, M., Schreiber, M., Salkoff, L., and Nichols, C. G. (1999) Expression of a functional K<sub>ir</sub>4 family inward rectifier K<sup>+</sup> channel from a gene cloned from mouse liver. *J. Physiol. (Lond.)* **514**, 639-653.
- Perozo, E., Cortes, D. M., and Cuello, L. G. (1998) Three-dimensional architecture and gating mechanism of a K<sup>+</sup> channel studied by EPR spectroscopy. *Nature Struc. Biol.* **5**, 459-469.
- Proks, P., Takano, M., and Ashcroft, F. M. (1994) Effects of intracellular pH on ATP-sensitive K<sup>+</sup> channels in mouse pancreatic  $\beta$ -cells. *J. Physiol. (Lond.)* **475**, 33-44.
- Riddles, P. W., Blakeley, R. L., and Zerner, B. (1979) Ellman's reagent: 5,5'-dithiobis(2-nitrobenzoic acid)--a reexamination. *Anal. Biochem.* **94**, 75-81.

- Ruknudin, A., Schulze, D. H., Sullivan, S. K., Lederer, W. J., and Welling, P. A. (1998) Novel subunit composition of a renal epithelial  $K_{ATP}$  channel. *J. Biol. Chem.* **273**, 14165-14171.
- Ruppersberg, J. P., Schultz, J., Brändle, U., Fakler, B., and Schulte, U. (1999) Intracellular regulation of inwardly rectifying potassium channels. In: *Current Topics in Membranes* **46** (Y. Kurachi., L.E. Jan und M. Lasdunski eds.), Academic Press, San Diego (USA), pp. 223-241.
- Schrempf, H., Schmidt, O., Kümmerlen, R., Hinnah, S., Müller, D., Betzler, M., Seinkamp, T., and Wagner, R. (1995) A prokaryotic potassium ion channel with two predicted transmembrane segments from *Streptomyces lividans*. *EMBO J.* **14**, 5170-5178.
- Schulte, U., Hahn, H., Wiesinger, H., Ruppersberg, J. P., and Fakler, B. (1998) pH-dependent gating of ROMK ( $K_{ir}1.1$ ) channels involves conformational changes in both N and C termini. *J. Biol. Chem.* **273**, 34575-34579.
- Schulte, U., Hahn, H., Konrad, M., Jeck, N., Derst, C., Wild, K., Weidemann, S., Ruppersberg, J. P., Fakler, B., and Ludwig, J. (1999) pH-gating of ROMK ( $K_{ir}1.1$ ) channels: Control by an Arg-Lys-Arg-triad disrupted in antenatal Bartter syndrome. *Proc. Natl. Acad. Sci. USA*, in press.
- Seyberth, H. W., Rascher, W., Schweer, H., Kühl, P. G., Mehls, O., and Schärer, K. (1985) Congenital hypokalemia with hypercalciuria in preterm infants: a hyperprostaglandinuric tubular syndrome different from Bartter syndrome. *J. Pediatr.* **107**, 694-701.
- Seyberth, H. W., Soergel, M., and Köckerling, A. (1997) The hyperprostaglandin E syndrome and Gitelman-Bartter syndrome. In: *Hypokalemic Tubular Disorders*, 2nd Edition, (A. M. Davison, J. S. Cameron, J. P. Grünfeld, D. N. Kerr and E. Ritz, eds.), Oxford University Press, London.
- Shuck, M. E., Bock, J. H., Benjamin, C. W., Tsai, T. D., Lee, K. S., Slightom, J. L., and Bienkowski, M. J. (1994) Cloning and characterization of multiple forms of the human kidney ROMK potassium channel. *J. Biol. Chem.* **269**, 24261-24270.
- Shuck, M. E., Piser, T. M., Bock, J. H., Slightom, J. L., Lee, K. S., and Bienkowski, M. J. (1997) Cloning and characterization of two  $K^+$  inward rectifier ( $K_{ir}$ ) 1.1 potassium channels homologs from human kidney ( $K_{ir}1.2$  and  $K_{ir}1.3$ ). *J. Biol. Chem.* **272**, 586-593.
- Shyng, S. L., and Nichols, C. G. (1998) Membrane phospholipid control of nucleotide sensitivity of KATP channels. *Science* **282**, 1138-1141.
- Silver, M. R., and DeCoursey, T. E. (1990) Intrinsic gating of inward rectifier in bovine pulmonary artery endothelial cells in the presence or absence of internal  $Mg^{2+}$ . *J. Gen. Physiol.* **96**, 109-133.
- Simon, D. B., Nelson-Williams, C., Bia, M. J., Ellison, D., Karet, F. E., Molina, A. M., Vaara, I., Iwata, F., Cushner, H. M., Koolen, M., Gainza, F. J., Gitelman, H. J., and Lifton, R. P. (1996a) Gitelman's variant of Bartter's syndrome, inherited hypokalemic alkalosis, is caused by mutations in the thiazide-sensitive Na-Cl-cotransporter. *Nature Genet.* **12**, 24-30.
- Simon, D. B., Karet, F. E., Hamdan, J. M., DiPietro, A., Sanjad, S. A., and Lifton, R. P. (1996b) Bartter's syndrome, hypokalaemic alkalosis with hypercalciuria, is caused by mutations in the Na-K-2Cl cotransporter NKCC2. *Nature Genet.* **13**, 183-188.

- Simon, D. B., Karet, F. E., Rodriguez-Soriano, J., Hamdan, J. H., DiPietro, A., Trachtman, H., Sanjad, S. A., and Lifton, R. P. (1996c) Genetic heterogeneity of Bartter's syndrome revealed by mutations in the K<sup>+</sup> channel, ROMK. *Nature Genet.* **14**, 152-156.
- Stanfield, P. R., Davies, N. W., Shelton, I. A., Sutcliffe, M. J., Khan, I. A., Brammar, W. J., and Conley, E. C. (1994) A single aspartate residue is involved in both intrinsic gating and blockade by Mg<sup>2+</sup> of the inward rectifier, IRK1. *J. Physiol. (Lond.)* **478**, 1-6.
- Stanton, B. A. (1989) Renal potassium transport: morphological and functional adaptations. *Am. J. Physiol.* **257**, F989-F997.
- Stanton, B. A., and Giebisch, G. (1992) Renal potassium transport. In: Handbook of Physiology: Renal Physiology **1**(19), Am. Physiol. Soc., Bethesda (USA), pp. 813-874
- Tagliatela, M., Wible, B. A., Caporaso, R., and Brown, A. M. (1994) Specification of pore properties by the carboxyl terminus of inwardly rectifying K<sup>+</sup> channels. *Science* **264**, 844-847.
- Tagliatela, M., Ficker, E., Wible, B. A., and Brown, A. M. (1995) C-terminus determinant for Mg<sup>2+</sup> and polyamine block of the inward rectifier K<sup>+</sup> channel IRK1. *EMBO J.* **14**, 5532-5541.
- Takahashi, N., Morishige, K. I., Jahangir, A., Yamada, M., Findlay, I., Koyama, H., and Kurachi, Y. (1994) Molecular cloning and functional expression of cDNA encoding a second class of inward rectifier potassium channels in the mouse brain. *J. Biol. Chem.* **269**, 23274-23279.
- Thier, S. O. (1986) Potassium physiology. *Am. J. Med.* **80**, 3-7.
- Tinker, A., Jan, Y. N., and Jan, L. Y. (1996) Regions responsible for the assembly of inwardly rectifying potassium channels. *Cell* **87**, 857-868.
- Tsai, T. D., Shuck, M. E., Thompson, D. P., Bienkowski, M. J., and Lee, K. S. (1995) Intracellular H<sup>+</sup> inhibits a cloned rat kidney outer medulla K<sup>+</sup> channel expressed in *Xenopus* oocytes. *Am. J. Physiol.* **37**, C1173-C1178.
- Tucker, S. J., Gribble, F. M., Proks, P., Trapp, S., Ryder, T. J., Haug, T., Reimann, F., and Ashcroft, F. M. (1998) Molecular determinants of K<sub>ATP</sub> channel inhibition by ATP. *EMBO J.* **17**, 3290-3296.
- Vandenberg, C. A. (1987) Inward rectification of a potassium channel in cardiac ventricular cells depends on internal magnesium ions. *Proc. Natl. Acad. Sci. USA* **84**, 2560-2566.
- Wang, N., Maurizi, M. R., Emmert-Buck, L., and Gottesman, M. M. (1994) Synthesis, processing, and localization of human Lon protease. *J. Biol. Chem.* **269**, 29308-29313.
- Wang, W.-H. (1995) View of K<sup>+</sup> secretion through the apical K channel of the cortical collecting duct. *Kidney Int.* **48**, 1024-1030.
- Wang, W.-H., and Giebisch, G. (1991a) Dual effect of adenosine triphosphate on the apical small conductance K<sup>+</sup> channels of rat cortical collecting duct. *J. Gen. Physiol.* **98**, 35-61.
- Wang, W.-H., and Giebisch, G. (1991b) Dual modulation of renal ATP-sensitive K<sup>+</sup> channel by protein kinases A and C. *Proc. Natl. Acad. Sci. USA* **88**, 9722-9725.

- Wang, W.-H., Schwab, A., and Giebisch, G. (1990) Regulation of small-conductance K<sup>+</sup> channel in apical membrane of rat cortical collecting tubule. *Am. J. Physiol.* **259**, F494-F502.
- Wang, W.-H., Sackin, H., and Giebisch, G. (1992) Renal potassium channels and their regulation. *Annu. Rev. Physiol.* **54**, 81-96.
- Wang, W.-H., Geibel, J., and Giebisch, G. (1993) Mechanism of apical K<sup>+</sup> channel modulation in principal renal tubule cells. Effect of inhibition of basolateral Na<sup>+</sup>-K<sup>+</sup>-ATPase. *J. Gen. Physiol.* **101**, 673-694.
- Wei, A., Jegla, T., and Salkoff, L. (1996) Eight potassium channel families revealed by the *C. elegans* genome project. *Neuropharmacology* **35**, 805-829.
- Wible, B. A., Tagliatela, M., Ficker, E., and Brown, A. M. (1994) Gating of inwardly rectifying K<sup>+</sup> channels localized to a single negatively charged residue. *Nature* **371**, 246-249.
- Wild, K. (1999) Subzelluläre Verteilung und Nachweis von Ionenkanälen in epithelial strukturierten Zellen. Dissertation at the Faculty of Biology, University of Tübingen, Germany.
- Woodhull, A. (1973) Ionic blockage of sodium channels in nerve. *J. Gen. Physiol.* **61**, 687-708.
- Woodward, R., Stevens, E. B., and Murrell-Lagnado, R. D. (1997) Molecular determinants for assembly of G-protein-activated inwardly rectifying K<sup>+</sup> channels. *J. Biol. Chem.* **272**, 10823-10830.
- Xu, Z. C., Yang, Y., and Hebert, S. C. (1996) Phosphorylation of the ATP-sensitive, inwardly rectifying K<sup>+</sup> channel, ROMK, by cyclic AMP-dependent protein kinase. *J. Biol. Chem.* **271**, 9313-9319.
- Xu, J. Z., Hall, A. E., Peterson, L. N., Bienkowski, M. J., Eessalu, T. E., and Hebert, S. C. (1997) Localization of the ROMK protein on apical membranes of rat kidney nephron segments. *Am. J. Physiol.* **273**, F739-F748.
- Yang, J., Jan, Y. N., and Jan, L. Y. (1995a) Control of rectification and permeation by residues in two distinct domains in an inward rectifier K<sup>+</sup> channel. *Neuron* **14**, 1047-1054.
- Yang, J., Jan, Y. N., and Jan, L. Y. (1995b) Determination of the subunit stoichiometry of an inwardly rectifying potassium channel. *Neuron* **15**, 1441-1447.
- Yano, H., Philipson, L. H., Kugler, J. L., Tokuyama, Y., Davis, E. M., Le Beau, M., Nelson, D. J., Bell, G. I., and Takeda, J. (1994) Alternative splicing of human inwardly rectifying K<sup>+</sup> channel ROMK1 mRNA. *Mol. Pharmacol.* **45**, 854-860.
- Yu, L., and Fesik, S. W. (1994) pH titration of the histidine residues of cyclophilin and FK506 binding protein in the absence and presence of immunosuppressant ligands. *Biochim. Biophys. Acta* **1209**, 24-32.

## 6 Summary

ROMK ( $K_{ir}1.1$ ), a member of the family of inwardly rectifying ( $K_{ir}$ ) potassium channels, forms the channel responsible for  $K^+$  secretion in the distal tubulus of the kidney.  $K^+$  homeostasis is strictly controlled by the intracellular pH in a way that  $K_{ir}1.1$  channels close in response to a decrease in  $pH_i$ . In this study it was shown that pH-gating is associated with conformational changes in the  $K_{ir}1.1$  protein. Firstly, conformational states of open and closed  $K_{ir}1.1$  channels were probed intracellularly by cysteine modification. Irreversible modification by sulfhydryl reagents was observed for  $K_{ir}1.1$  channels only in the closed but not in the open state. Mutagenesis of intracellular cysteines revealed cysteine 49 in the N- and cysteine 308 in the C-terminus as targets for state-dependent modification. Secondly,  $K_{ir}1.1$  channels have been shown to be allosterically regulated by extracellular  $K^+$  and intracellular pH. At alkaline  $pH_i$ ,  $K_{ir}1.1$  channels remained active in the absence of extracellular  $K^+$  but failed to recover from pH-induced inactivation. Dependence on extracellular  $K^+$  was abolished in a pH-gated  $K_{ir}1.1$  chimera ( $K_{ir}1.1(K_{ir}2.1p)$ ), where the P-loop had been replaced by the corresponding sequence of  $K_{ir}2.1$ . These results indicate that pH-gating of  $K_{ir}1.1$  channels involves conformational changes in both N- and C-termini as well as in extracellular parts of the pore.

Among all inward-rectifiers tested, only  $K_{ir}1.1$  and  $K_{ir}4.1$  displayed sensitivity to  $pH_i$  in the physiological range ( $pK_{app} = 6.8$  / Hill coefficient of 2.9 and  $pK_{app} = 6.1$  / Hill coefficient of 2.3, respectively). By sequence alignment and site-directed mutagenesis a lysine residue N-terminal to M1 (K80) was identified as the  $pH_i$  sensor for pH-gating. Replacing lysine 80 by a neutral amino acid like methionine or modification with an aminogroup-specific agent removed pH-gating of  $K_{ir}1.1$  channels. Conversely, introduction of lysine at the pre-M1 site conferred pH-gating to other  $K_{ir}$  channels. These results implied that titration of lysine 80 was shifted by more than 3 pH units compared to the free amino acid in all  $K_{ir}1.1$  channels tested. By neutralization of conserved positive charges in  $K_{ir}1.1$  it was found that the anomalous titration was due to electrostatic interactions within an intrasubunit triad of basic amino acid residues formed by lysine 80, arginine 41 in the N- and arginine 311 in the C-terminus of  $K_{ir}1.1$ . These results provided the first rough network for the tertiary folding of intracellular domains of  $K_{ir}$  channels.

Disruption of the RKR triad resulted in defective ROMK function and is found in families with antenatal Bartter-syndrome (aBS). Moreover, the majority of known  $K_{ir}1.1$ -aBS missense mutations is found to be located close to the triad in a structural model deduced from the findings reported here. Analysis of these mutants revealed titration shifts ranging from +0.3 to +2.2 pH units compared to  $K_{ir}1.1$  wildtype. This suggests that structural disturbance of the triad in  $K_{ir}1.1$  is a major molecular cause for the pathogenesis of aBS.



## *Acknowledgements*

This work would not be complete without acknowledging the contributions of my helpful colleagues and friends. Not only did they add to the scientific excitement I experienced but also made this time a very enjoyable one.

In the first place I want to thank my supervisor Priv. Doz. Dr. B. Fakler for providing well organized projects, for the time he spent with me discussing experiments and for his constructive criticism. From different perspectives, Prof. Dr. J. P. Ruppertsberg and Prof. Dr. B. Hamprecht watched over the progress of my work, combining encouragement with many helpful corrections.

I feel especially indebted to Dr. J. Ludwig, Dr. H. Hahn and Dr. C. Derst, who generously provided the DNA clones and constructs needed for my experiments. In addition, I want to thank S. Weidemann, B. Blickle and K. Geckle for their help with cRNA synthesis.

I am also grateful to Dr. K. Wild for her diligent support with immunocytochemical studies.

Among the external collaborators I want to mention Prof. Dr. H. W. Seyberth, Dr. M. Konrad and Dr. N. Jeck who added exciting clinical aspects to this work. With the help of Prof. Dr. H. Wiesinger and Dr. B. Müller I managed to keep some of my roots in biochemistry.

Last but not least I wish to thank Dr. T. Baukowitz and D. Oliver for their proof-reading of my manuscripts, the stimulating discussions we had, and the good sense of humor we shared.

Meine akademischen Lehrer waren:

An der Universität Stuttgart:

Prof. Dr. W. Becker  
Prof. emer. Dr. W. Eisenmenger  
Priv. Doz. H. D. Hausen  
Prof. Dr. W. Kaim  
Prof. Dr. J. Weidlein

An der University of California at Riverside:

Prof. Dr. J. H. Ashe  
Prof. Dr. M. A. Baker  
Prof. Dr. C. V. Byus  
Prof. Dr. B. N. Cohen  
Prof. Dr. S. N. Currie  
Prof. Dr. A. Dugaiczky  
Prof. Dr. M. F. Dunn  
Prof. Dr. D. R. Gallie  
Prof. Dr. A. Grosovsky  
Prof. emer. Dr. D. Holten  
Prof. Dr. D. A. Johnson  
Prof. Dr. C. Nelson  
Prof. Dr. M. L. Oster-Granite  
Prof. Dr. S. R. Spindler  
Prof. Dr. B. G. Stanley  
Prof. Dr. J. A. Traugh  
Prof. Dr. A. M. Walker  
Prof. Dr. C. Webster

An der Universität Tübingen:

Prof. emer. Dr. E. Bayer  
Prof. Dr. H. Bisswanger  
Prof. Dr. P. Bohley  
Prof. Dr. V. Braun  
Prof. Dr. Dr. U. Breyer-Pfaff  
Hochschul-Doz. Dr. K.-U. Fröhlich  
Prof. Dr. K. Eisele  
Prof. Dr. G. Gauglitz  
Prof. Dr. R. Gebhardt



Prof. Dr. F. Götz  
Prof. Dr. J. Guglielmi  
Prof. Dr. H. Hagenmaier  
Prof. Dr. B. Hamprecht  
Prof. Dr. Dr. h.c. M. Hanack  
Prof. Dr. V. Hoffmann  
Prof. Dr. G. Jung  
Prof. Dr. F. Lang  
Prof. Dr. E. Lindner  
Prof. Dr. M. Mathieu  
Prof. Dr. D. Mecke  
Prof. Dr. Dr. h.c. H. Metzner  
Prof. Dr. W. Nakel  
Prof. Dr. D. Oelkrug  
Prof. Dr. H. Oberhammer  
Prof. Dr. E. Pfaff  
Prof. Dr. W. Pfeiffer  
Priv. Doz. H. Pommer  
Prof. Dr. K. Poralla  
Prof. Dr. H. Probst  
Prof. Dr. K. Reutter  
Prof. Dr. J. P. Ruppertsberg  
Prof. Dr. J. Strähle  
Prof. Dr. Dr. h.c. W. Voelter  
Prof. Dr. Dr. h.c. K. Wegmann  
Prof. Dr. J. Werringloer  
Prof. Dr. U. Weser  
Prof. Dr. H. Wiesinger

# Lebenslauf

- 16.07.1970 Geboren in München-Gräfelfing als Sohn von Knud Schulte und Uta Schulte, geb. Hamel.
- 1976 - 1980 Besuch der Grundschule (Schlehengäu-Schule) in Gechingen (Kreis Calw).
- 1980 - 1989 Hermann-Hesse-Gymnasium Calw, mit Abitur am 24.04.89 abgeschlossen.
- 22.02.1989 Dienst im Katastrophenschutz für 10 Jahre beim Technischen Hilfswerk OV Calw; Ausbildung zum „ABC-Helfer aller Fachdienste“.
- 01.06.-15.10.89 Aushilfstätigkeit bei Hewlett-Packard GmbH Böblingen in der R&D-Abteilung für Medizinelektronik.
- WS 1989/90 Studium der Chemie (Diplom) an der Universität Stuttgart.
- SS 1990 bis SS 1995 Studium der Biochemie an der Eberhard-Karls-Universität Tübingen. Vordiplomsprüfungen abgeschlossen am 12.10.1992.
- Sommer 1991 und 1993 SEED-Praktikant bei Hewlett Packard Laboratories in Palo Alto (Californien, USA) in der Abteilung „Chemische Analytik“.
- September 1993 bis Juni 1994 Auslandsstudium an der University of California / Riverside als „graduate student“ in Biochemie, abgeschlossen mit einem „Master of Science“.
- 15.05.1995 Abschluß der Diplom-Hauptprüfung (Biochemie).
- 03.07.95 - 11.03.96 Diplomarbeit in der klinischen Forschergruppe "Sensorische Biophysik" der HNO-Klinik Tübingen bei Herrn Prof. Dr. J. P. Ruppertsberg zum Thema "Regulation von einwärtsgerichtenden  $K^+$ -Kanälen durch extrazelluläres  $K^+$  und intrazellulären pH".
- April 1996- Mai 1999 Anfertigung der Doktorarbeit mit dem Titel "Molekularer Mechanismus und strukturelle Implikationen des pH-Gatings einwärtsgerichtender  $K^+$ -Kanäle ( $K_{ir}$ )" (englischer Titel: "pH-Gating of Inward-Rectifier  $K^+$  Channels ( $K_{ir}$ ): Molecular Mechanism and Structural Implications") am Lehrstuhl für Physiologie II der Universität Tübingen unter Anleitung von Priv. Doz. Dr. B. Fakler und Prof. Dr. B. Hamprecht.

Tübingen, den 28.10.99